

2014

The Role of Histone Methyltransferases in Determining Developmental Potential of Bovine Oocytes

Jairo Alberto Sarmiento

Louisiana State University and Agricultural and Mechanical College

Follow this and additional works at: https://digitalcommons.lsu.edu/gradschool_dissertations



Part of the [Animal Sciences Commons](#)

Recommended Citation

Sarmiento, Jairo Alberto, "The Role of Histone Methyltransferases in Determining Developmental Potential of Bovine Oocytes" (2014). *LSU Doctoral Dissertations*. 3275.

https://digitalcommons.lsu.edu/gradschool_dissertations/3275

This Dissertation is brought to you for free and open access by the Graduate School at LSU Digital Commons. It has been accepted for inclusion in LSU Doctoral Dissertations by an authorized graduate school editor of LSU Digital Commons. For more information, please contact gradetd@lsu.edu.

THE ROLE OF HISTONE METHYLTRANSFERASES IN DETERMINING DEVELOPMENTAL POTENTIAL OF BOVINE OOCYTES

A Dissertation

Submitted to the Graduate Faculty of the
Louisiana State University and
Agricultural and Mechanical College
in partial fulfillment of the
requirements for the degree of
Doctor of Philosophy

In

The Interdepartmental Program of
Animal and Dairy Sciences

by

Jairo Alberto Sarmiento
DVM, National University of Colombia, 2001
December 2014

ACKNOWLEDGEMENTS

First, the author would like to thank the members of his committee, Dr. Glen Gentry, Dr. Robert Godke, and Dr. Daniel Burba, for their scientific and academic support and their willingness to collaborate with his requests. The author would like to sincerely thank his advisor, Dr. Ken Bondioli, for the opportunity to work with him at LSU, for always being available to help, and for challenging him when necessary and guiding him when he was lost. Special gratitude is due also to Dr. John Lynn for his teaching, mentoring, and close collaboration during the author's experiments.

Thanks to the faculty members in the Animal Science Department, including Dr. Hay, Dr. Thompson, Dr. McMillin, and Dr. Williams, for their teaching and guidance. The help of the staff at the School of Animal Sciences, the Reproductive Biology Center, and Central Station is also greatly appreciated, especially Sally Turner, Cassandra Rattle, Manuel Persica, Dana Caldwell, Rebecca Lirette, Mark Vidrine, James Sterling, Joe Navarre, James Desselle, and Randy Morell. What the author learned from them about life is prized as much as the academic education he received at LSU.

A huge thanks to all of the author's fellow graduate students who have provided assistance, especially April Waguespack Levy, Michael Stout, Angelica Giraldo, Alicia Picou, Tricia Adams, Javier Jarazo, Brittany Foster, Paige Hardin, Bethany Fisher, and Erin Oberhaus. Special recognition deserves to be given Cody Bailey for his exemplary work ethics and permanent contributions to this project. Thanks also to the undergraduate students in the reproduction and artificial insemination classes for their contribution to the development of the author's teaching skills.

The author would also like to thank Sarah Farmer and her family. She has changed his life in the time that they have been together and has opened the authors mind and life to new ideas, places, people, scenarios, and possible futures. Sarah provided unconditional support

during the long and dark hours, as well as during the happy and bright moments. Sarah's family has opened the door of their house and the souls of their members to make the author comfortable in a new home, far away from home.

Lastly, the author would like to express his deepest gratitude to his sister, brother, and most especially to his mother, who taught him that love, education, and hard work are the pathway to fulfilling one's dreams. Their constant and unconditional support has allowed the author to reach academic success in his professional career and countless moments of personal satisfaction. Without family, and the struggles that come with it, life becomes a pointless endeavor.

TABLE OF CONTENTS

ACKNOWLEDGEMENTS	ii
LIST OF TABLES	vi
LIST OF FIGURES	viii
LIST OF ABBREVIATIONS	ix
ABSTRACT	xi
CHAPTER	
I. INTRODUCTION	1
II. LITERATURE REVIEW	3
2.1 Histone Methylation	5
2.2 Histone Ubiquitination	19
2.3 Histone Acetylation	21
2.4 Histone Phosphorylation	22
III. DIFFERENCES IN LEVELS OF HISTONE METHYLTRANSFERASE TRANSCRIPTS BETWEEN IMMATURE, IN VITRO MATURED, AND IN VIVO MATURED CUMULUS CELLS AND OOCYTES	25
3.1 Introduction	25
3.2 Materials and Methods	27
3.3 Results	37
3.4 Discussion	53
IV. RELATIVE ABUNDANCE OF HISTONE 3 LYSINE 9 TRI-METHYLATED IN EARLY BOVINE EMBRYOS PRODUCED IN VITRO USING IN VIVO AND IN VITRO MATURED OOCYTES	61
4.1 Introduction	61
4.2 Materials and Methods	62
4.3 Results	69
4.4 Discussion.....	73
V. SUMMARY AND CONCLUSIONS	80
LITERATURE CITED	84
APPENDIX A: PROTOCOLS	92
APPENDIX B: STOCK SOLUTIONS AND MEDIA FORMULATIONS.....	100

APPENDIX C: EQUIPMENT AND MATERIALS USED.....	102
APPENDIX D: ADDITIONAL DATA TABLES.....	103
VITA	114

LIST OF TABLES

3.1	PCR primers	35
3.2	Relative expression for the ASH1L gene in Experiment one	39
3.3	ANOVA analysis for the ASH1L gene in Experiment one	39
3.4	Relative expression for the SUV39H1 gene in Experiment one	40
3.5	ANOVA analysis for the SUV39H1 gene in Experiment one	40
3.6	Relative expression for the KDM6B gene in Experiment one	41
3.7	ANOVA analysis for the KDM6B gene in Experiment one	41
3.8	Relative expression for the EHMT2 gene in Experiment one	42
3.9	ANOVA analysis for the EHMT2 gene in Experiment one	42
3.10	Pair-wise comparisons (Tukey's test) for the EHMT2 gene in Experiment one	43
3.11	Relative expression for the ASH1L gene in Experiment two	45
3.12	ANOVA analysis for the ASH1L gene in Experiment two	45
3.13	Pair-wise comparisons (Tukey's test) for the ASH1L gene in Experiment two	46
3.14	Relative expression for the EHMT2 gene in Experiment two	46
3.15	ANOVA analysis for the EHMT2 gene in Experiment two	46
3.16	Relative expression for the SUV39H1 gene in Experiment two	47
3.17	ANOVA analysis for the SUV39H1 gene in Experiment two	47
3.18	Relative expression for the KDM6B gene in Experiment two	47
3.19	ANOVA analysis for the KDM6B gene in Experiment two	48
3.20	Relative expression for the ASH1L gene in Experiment three	50
3.21	ANOVA analysis for the ASH1L gene in Experiment three	50

3.22	Relative expression for the EHMT2 gene in Experiment three	51
3.23	ANOVA analysis for the EHMT2 gene in Experiment three	51
3.24	Relative expression for the SUV39H1 gene in Experiment three	51
3.25	ANOVA analysis for the SUV39H1 gene in Experiment three	52
3.26	Relative expression for the KDM6B gene in Experiment three	52
3.27	ANOVA analysis for the KDM6B gene in Experiment three	52
4.1	Student's t test of in vitro matured oocytes vs. in vivo matured oocytes	71
4.2	Student's t test of embryos derived from in vitro matured oocytes versus embryos derived from in vivo matured oocytes	72
D.1	Geometric mean of housekeeping genes in Experiment one	103
D.2	QPCR values in Experiment one	104
D.3	Geometric mean of housekeeping genes in Experiment two	105
D.4	QPCR values in Experiment one	106
D.5	Geometric mean of housekeeping genes in Experiment three	107
D.6	QPCR values in Experiment one	108
D.7	Fluorescent intensity data for Experiment four	109
D.8	Fluorescent intensity data for Experiment five	110

LIST OF FIGURES

3.1	Synchronization protocol for transvaginal ultrasound-guided aspiration of immature oocytes	30
3.2	Synchronization protocol for transvaginal ultrasound-guided aspiration of In vivo matured oocytes	31
3.3	Relative expression of histone methyltransferase transcripts in cumulus-oocyte Complexes (COCs)	43
3.4	Relative expression of histone methyltransferase transcripts in oocytes	49
3.5	Relative expression of histone methyltransferase transcripts in cumulus cells	53
4.1	Synchronization protocol for transvaginal ultrasound-guided aspiration of immature oocytes	64
4.2	Synchronization protocol for transvaginal ultrasound-guided aspiration of in vivo matured oocytes	65
4.3	Analysis of fluorescent intensity during Experiment four	70

LIST OF ABBREVIATIONS

ASH1L	Bos taurus absent, small, or homeotic-like Drosophila gene
cAMP	Cyclic adenosine monophosphate
CDK2	Cyclin-dependant protein kinase 2
CIDR	Control internal drug release device
COCs	Cumulus-oocyte complexes
CRC	Chromatin remodeling complex
DFR	Dominant follicle removal
DNA	Deoxyribonucleic acid
Dnmt3a	DNA methyltransferase protein 3a
Dnmt3b	DNA methyltransferase protein 3b
EHMT2	Bos taurus euchromatic histone-lysine N-methyltransferase 2 gene
eIF1A	Eukaryotic initiation factor
FIB	Fluorescent intensity from the background
FIRI	Fluorescent intensity from the regions of interest
FIS	Fluorescent intensity of the sample
GA	Genomic activation
GADPH	Bos taurus glyceraldehyde 3-phosphate dehydrogenase gene
GnRH	Gonadotropin releasing hormone
H2A	Histone 2A
H2B	Histone 2B
H3K4	Histone 3 lysine 4
H3K9	Histone 3 lysine 9
H3K20	Histone 3 lysine 20
H3K27	Histone 3 lysine 27
H4K20	Histone 4 lysine 20
HMTs	Histone methyltransferases
HOX	Homeotic genes/protein
HP1	Heterochromatin protein 1
ING2	Inhibitor of growth protein 2
JmjC	Jumonji C domain
KDM6B	Bos taurus lysine (K)-Specific Demethylase 6B gene
MLL	Mixed lineage leukemia proteins family
mRNA	Messenger ribonucleic acid
NANOG	Pluripotent transcription factor NANOG
NuRD	Nucleosome remodeling deacetylase
OCT4	Pluripotent transcription factor NANOG
Pc	Drosophila polycomb protein family
PCR	Polymerase chain reaction
PGF2 α	Prostaglandin F2 alpha
Poly A	Bos taurus poly (A) polymerase gene
PRMTs	Protein arginine methyltransferases
QPCR	Real time polymerase chain reaction
Rad6	Ubiquitin acceptor/catalyzer enzyme
RNA	Ribonucleic acid
SAM	S-adenosyl-L-methionine
SET	Methyltransferase protein domain
SMYD3	Methyltransferase protein domain

SOX2	Pluripotent transcription factor SOX2
STAT1	Signal transducers and activators of transcription
SUV39H1	Bos taurus suppressor of variegation 3-9 homologue 1 gene
TUGA	Transvaginal ultrasound guided aspiration
UTX	Lysine (k)-specific demethylase 6A enzyme

ABSTRACT

Histone proteins are proteins found in eukaryotic cells that associate with DNA to form the most basic structural unit of chromatin, called nucleosomes. The post-translational modifications of histones regulate developmental competence in bovine oocytes and early embryos. The difference in developmental competence between in vitro matured oocytes and in vivo matured oocytes was used to investigate the accumulation of transcripts for histone methyltransferases (HMTs) during oocyte maturation. Methyltransferases ASH1L, EHMT2, SUV39H1 and KDM6B were selected as genes of interest. Transvaginal ultrasound-guided aspiration (TUGA) was used to collect immature and in vivo matured bovine cumulus-oocyte complexes (COCs). Immature COCs collected via TUGA were randomly assigned to either the immature or the in vitro mature treatments. Transcriptome analysis was performed in COCs, oocytes, and cumulus cells. Results showed no differences in transcriptome levels between immature and in vivo treatments, suggesting that there are no major accumulations of transcripts for HMTs during the antral phase of oocyte maturation in vivo. Higher accumulations of transcripts for the EHMT2 and ASH1L genes were found in the in vitro maturation Treatment for COCs and oocytes ($p = 0.005$ and $p = 0.001$, respectively). Immunocytochemistry was used to investigate the consequences of this increase in transcripts accumulation for HMTs during in vitro maturation of oocytes. Methylation levels of lysine 9 in histone 3 measured in both oocytes at the metaphase II stage and early embryos showed that the increase in the accumulation of transcripts coding for HMTs during in vitro maturation correlates with a decrease in the level of methylation of lysine 9 in histone 3 in oocytes at the metaphase II stage, as well as a decrease in the levels of methylation of lysine 9 in histone 3 in the blastomeres of early cleaving embryos. The decrease in the levels of tri-methylation of lysine 9 in histone 3 potentially affect the capacity of the oocyte and early embryo to silence gene and stabilize heterochromatic regions and potentially compromise the developmental potential of the embryo.

CHAPTER I

INTRODUCTION

Epigenetic reprogramming studies the molecular modifications of DNA, DNA associated proteins and chromatin associated with changes in gene expression. These modifications contain inheritable information that does not depend upon the sequences of bases in the DNA molecule, and are usually referred as the epigenetic status of a cell. Genome-wide modifications of the epigenetic status of the cell (epigenetic reprogramming) occur twice naturally during early embryo development: soon after fertilization and during gametogenesis. After fertilization, the paternal and maternal genomes must undergo dramatic changes in their nuclear morphology and chromatin structure to achieve a configuration that allows the gene expression pattern required to progress further in development.

The epigenetic status of a cell can be modified by the methylation of cytosine bases in the DNA, the post-translational modification of histone proteins, the positioning of the nucleosomes, and topological changes in the chromosomes. The modification of histones is one of the most versatile mechanisms involved in epigenetic reprogramming because they can be used as markers for proteins that modify chromatin structure. As a general rule, enzymes that covalently modify histones target specific amino acids and a different enzyme is responsible for removing the epigenetic mark.

Histones can be methylated on either lysine or arginine residues. The numerous lysine and arginine residues on the histone tail, the multiple levels of methylation that each residue can take, and the possible combination of multiple methylation sites, on top of the possibility of methylation marks interacting with other types of epigenetic marks, makes histone methylation a complex, flexible, and effective regulatory mechanism (Shi and Whetstone, 2007).

EHMT2 (Euchromatic histone-lysine N-methyltransferase) and SUV39H1 (Homolog 1 of the position-effect variegation 3-9) are both histone methyltransferases that catalyze the mono-, di-, and tri-methylation of lysine 9 in histone 3 (Tachibana et al., 2002; Park et al., 2014). The

difference in their activity is based on the tendency of EHMT2 to associate with silent genes in euchromatic regions whereas SUV39H1 is a signal for pericentric heterochromatin and for the establishment of transcriptional repression.

ASH1L (Absent, Small or Homeotic disk 1) is a histone methyltransferase involved in epigenetic reprogramming due to its capacity to catalyze the methylation of histone 3 at lysine 4. This epigenetic mark is important during early embryo development because it has been associated with regions of active gene transcription and very stable chromatin structure (Gregory et al., 2007; Gao et al., 2010). KDM6B is a demethylase enzyme, having an antagonistic role to the histone methyltransferases described earlier. KDM6B has the capacity to remove repressive marks, prevent the activity of heterochromatic proteins, and enhance gene expression (Agger et al., 2007).

ASH1L, EHMT2, SUV39H1, and KDM6B work together with other epigenetic markers to modify the epigenetic landscape of the DNA in the paternal and maternal gametes in order to create an all-new epigenetic landscape for the embryo that supports both the maternal-zygote transition of gene regulation and the developmental potential of the early embryo.

The present document describes a series of three experiments that use the well-established difference in developmental potential between in vitro matured oocytes and in vivo matured oocytes to study the accumulation of transcripts coding for ASH1L, EHMT2, SUV39H1, and KDM6B methyltransferase enzymes in cumulus-oocyte complexes, cumulus cells, and oocytes. A fourth experiment investigates the consequences of irregular accumulation of transcripts coding for histone methyltransferases by evaluating the levels of tri-methylation of lysine 9 in histone 3 when comparing in vitro versus in vivo matured oocytes. One further step is taken in the fifth experiment by comparing the epigenetic landscape of in vitro fertilized embryos from in vitro matured oocytes compared with in vitro fertilized embryos from in vivo matured oocytes.

CHAPTER II LITERATURE REVIEW

In 1962 Sir John B. Gurdon replaced the immature nucleus in the egg of a frog with the mature nucleus of a differentiated frog's intestinal cell. The modified egg successfully developed into a tadpole (Gurdon, 1962). With this experiment, Gurdon demonstrated that the regulatory mechanisms that determine the subset of genes to be expressed by a given cell can be modified. Epigenetic reprogramming studies the molecular modifications of DNA, DNA associated proteins, and chromatin associated with changes in gene expression. These modifications contain inheritable information that does not depend upon the sequences of bases in the DNA molecule and are usually referred to as the epigenetic status of a cell.

Genome-wide modifications of the epigenetic status of the cell (epigenetic reprogramming) occur naturally twice during early embryo development: during gametogenesis and soon after fertilization. Experimentally, epigenetic reprogramming can be induced by fusing somatic cells with embryonic stem cells, by cloning via nuclear transfer, and by induction of pluripotency with core transcription factor procedures. Also, changes in gene expression patterns similar to those described during epigenetic reprogramming have been described in some pathological conditions (Koike et al., 2014; Zhang et al., 2014).

During gametogenesis primordial germ cells must change their somatic bi-parental epigenetic marks and acquire the adequate epigenetic marks for gametes of the gender of the embryo. After fertilization, the paternal and maternal genomes must undergo dramatic changes in their nuclear morphology and chromatin structure in order to achieve a configuration that allows the gene expression pattern required to progress further in development.

However, transcription from gametic genomes is tightly regulated for reasons associated with avoidance of activation of selfish DNA elements, reprogramming of the genome, and dense packaging in the male pronuclei (Blaxter, 2014). Therefore, the maternal gamete must provide

either the proteins or the transcripts and the translational machinery responsible for controlling the developmental progress of the early embryo.

The epigenetic status of a cell can be modified by the methylation of cytosine bases in the DNA, the post-translational modification of histone proteins, the positioning of the nucleosomes, and topological changes in the chromosomes. The modification of histones is one of the most versatile mechanisms involved in epigenetic reprogramming. Histones are proteins that associate with DNA in the chromosomes of eukaryotic cells. Their structural function is to organize the DNA in the form of nucleosomes, which are further arranged into higher-order chromatin structures. By controlling chromatin structure, histone proteins regulate the accessibility of proteins to DNA, especially transcription factors and RNA polymerase, therefore modifying gene expression.

Consequent with their dual function, histone proteins have two regions: the core and the N-terminal tails. The core is characterized by a close attachment of the protein to the DNA lead by hydrogen bonds, hydrophobic interactions, and salt linkages. The N-terminal tails are exposed on the outside of the nucleosome and are considered the regulatory regions because they interact with other elements to control chromatin structure and function.

The post-translational modifications of histones (via covalent modifications of the histone N-terminal tails) serve as markers that recruit specific protein complexes. These markers allow or deny access to the DNA by other protein complexes, thereby regulating biological functions. The amino acid side chains of the histone tails are subject to covalent modifications including acetylation, phosphorylation, ubiquitination, and methylation. These modifications regulate diverse chromatin functions such as gene expression, DNA replication, and chromosome segregation (Zhang and Reinberg, 2001).

The post-translational modification of histone proteins is one of the mechanisms that modifies the epigenetic status of a cell. Other mechanisms include the methylation of cytosine

bases in DNA, the repositioning of nucleosomes, topological changes in chromosomes, and the relative positioning of genes within the nucleus.

Proteins that carry out epigenetic modifications do not act alone, but interact with one another, often by forming large protein complexes. These protein complexes regulate high-order chromatin structure and the accessibility to chromatin of proteins that regulate transcription (Li, 2002). The modification of the epigenetic status of a cell at any given time can be started by single residue modifications in the histone tail, or by a combination of modifications in the same histone or even in different histone proteins within the same nucleosome. The function of a given histone modification is given by the type of regulatory protein it recruits (Bannister and Kouzarides, 2005).

The covalent addition of marks in histone tails is a dynamic process, with marks being added and removed at different rates depending on their chromosomal location, status of the cell in the cell cycle, and environmental conditions and stimulus. This implies that all post-translational modifications of histones must be reversible, an idea that was very controversial only ten years ago. Nowadays, a large number (but not all) of the enzymes responsible for these modifications have been identified and characterized (Beisel et al., 2002; Andreu-Vieyra et al., 2010). As a general rule, enzymes that covalently modify histones target specific amino acids and a different enzyme is responsible for removing the epigenetic mark.

2.1 Histone Methylation

Histones can be methylated on either lysine or arginine residues. The numerous lysine and arginine residues on the histone tail, the multiple levels of methylation that each residue can acquire, and the possible combination of multiple methylation sites on top of the possibility of methylation marks interacting with other types of epigenetic marks makes histone methylation a complex, flexible, and effective regulatory mechanism (Shi and Whetstine, 2007).

Methylation of histone proteins induces changes in chromatin structure, but the relatively small size of methyl groups and the fact that their addition to lysine and arginine residues does

not neutralize their charges makes it unlikely that methylation alone changes chromatin structure enough to induce changes in gene expression (Bannister and Kouzarides, 2005). It is more likely that the modification of histone tails creates binding sites for regulatory proteins with specific binding domains.

The mechanisms by which histone methyltransferases recognize the specific sections of chromatin to be methylated is not clearly understood. It has been postulated that methyltransferases can be recruited by DNA binding factors or by the transcriptional machinery. They may also be recruited by proteins capable of recognizing methylation and other epigenetic marks on histone residues. These proteins reside within complexes that are associated with enzymatic activities operating on the chromatin template (Ruthenburg et al., 2007). There is also some evidence that non-coding RNAs transcribed from specific regions within target genes have the ability to recruit histone methyltransferases and DNA methyltransferases to the tails of histone 3 proteins associated with the target gene (Sanchez-Elsner et al., 2006). This mechanism, however, was described in the *Drosophila* and it is not yet known if it occurs in mammalian cells. The authors propose, though, that these types of epigenetic mechanisms are generally well preserved throughout evolution.

There are three main groups of proteins that regulate histone methylation as an epigenetic mark. The trithorax group is the main family of proteins responsible for maintaining chromatin in a permissive state via histone methylation, and the Polycomb group mediates the addition of methyl residues that propend for repressive configurations of chromatin (Gao et al., 2010). The third group, the Jumonji C domain containing family, is mainly responsible for removing the methylation marks.

Methylation of histone tails was previously considered an irreversible modification. It was not until 2005 that members of the Jumonji C domain containing proteins started to be identified by their histone demethylase activity (Trewick et al., 2005). Since then, the JmjC domain has been identified in more than one hundred proteins, in organisms from bacteria to eukaryotes.

The large number of enzymes with potential to demethylate histone proteins, the multiple residues in the histone tails susceptible of methylation, and the possible interactions between multiple modifications suggest that demethylases represent an important mechanism to dynamically regulate histone methylation as an epigenetic mark (Shi and Whetstine, 2007).

There seems to be differences in the regulatory mechanisms of histone methylation between gametes and somatic cells in mice. In the oocyte, methylation of specific histone residues are enzyme-specific, and transgenic mice carrying double mutations of specific histone methyltransferase genes fail to fertilize and/or develop; whereas, genetically modified cumulus cells with double mutations of single histone methyltransferase genes show an increase in the levels of transcripts of similar enzymes with a compensatory increase of the epigenetic modification (Andreu-Vieyra et al., 2010).

2.1.1. Methylation of Lysine Residues

Histone 3 can be methylated at lysine residues 4, 9, 27, 36, and 79; histone 4 can be methylated at lysine 20 (H3K4, H3K9, H3K27, H3K36, H3K79, H4K20, respectively). Lysine residues can be mono-, di- or tri-methylated (Gregory et al., 2007). Both the site and the extent of lysine methylation affect the interaction between chromatin and effector proteins.

Since the outcome of any epigenetic mark depends on the location of the modification, the combination of one or more modifications, and the enzyme involved in the particular modification, the biological outcomes of methylation of lysine residues in histone proteins are associated with multiple and diverse cell processes (Nishioka et al., 2002). Lysine methylation is involved in the progression of the cell cycle, DNA replication and apoptosis. It can be a mark of accessible DNA for effector proteins or it can recruit proteins that organize heterochromatin and induce gene silencing. When regulation is lost, lysine methylation of histone tails has been associated with pathological conditions such as prostate, breast, and hematopoietic cancers, as well as neurological disorders (Shi and Whetstine, 2007). Sometimes antagonist marks coincide to co-regulate the expression of pluripotency genes.

Therefore, the methylation of lysine residues in histone tails can be better understood by studying specific lysine residue modifications in combination with the enzyme responsible for the modification.

2.1.1.1. Methylation of Histone 3 at Lysine 4

Methylation of histone 3 at lysine 4 is an evolutionarily conserved mark associated mainly with transcriptionally active chromatin, although transcriptional repression has been described in association with H3K4me2/3 in some cases (Shi et al., 2006). The methylation of histone 3 at lysine 4 was first described by Honda et al, in 1975. They were characterizing other known methylation forms in histone 3 when they discovered what they described as “an additional minor site for histone 3 methylation” (Honda et al., 1975b). At that time, methylation of histones was thought to be not only a stable, irreversible modification but also part of a temporal sequence of events that begins with histone synthesis and is followed by histone acetylation, deacetylation, methylation, and phosphorylation (Honda et al., 1975a).

High levels of H3K4 tri-methylation are regularly associated with the 5' region of the majority of active genes in vertebrates, with many authors suggesting a strong positive correlation between this modification and an increase in transcription rates, active polymerase II occupancy, and histone acetylation (Bernstein et al., 2005; Ruthenburg et al., 2007). The di-methylated stage of H3K4 has been associated with open chromatin frames, but not with transcriptional activation, since tri-methylated H4 accumulates around the promoter region of transcriptionally active genes but di-methylated H3K4 does not (Bernstein et al., 2002; Santos-Rosa et al., 2002).

There are some situations where methylation of H3K4 does not follow the criteria described previously. One example is the regions where genes of the Hox family are located. Genes of the Hox family show broad patterns of methylation along the whole cluster, instead of just around the promoter region, and it has been suggested that this difference in the methylation patterns has to do with the role of these genes during early embryo development

(Bernstein et al., 2005). Another exception occurs when H3K4me_{2/3} is recognized by proteins of the histone deacetylase complex, such as ING2. In these cases transcriptional repression occurs (Shi et al., 2006).

The biological effects of methylation of lysine 4 in histone 3 acquire a new order of complexity as regulatory mechanisms when methylation of H3K4 interacts with other epigenetic marks. For example, the acetylation of histone 3 tails is followed by the methylation of lysine 4 in histone 3, resulting in the opening of the chromatin structure (Strahl et al., 1999). Methylation of H3k4 also precludes methylation of H3K9 by SUV39H1, but not by KDM6B (Nishioka et al., 2002), affecting the formation of heterochromatin but not gene silencing within euchromatic regions. Also, H3K4 methylation can have a regulatory effect on chromatin structure and gene expression, since it interferes with demethylases such as NuRD binding to chromatin (Nishioka et al., 2002).

The role of methylation of lysine 4 during early development is still a matter of study. In humans, there is evidence that the tri-methylation of lysine 4 in histone 3 is a constant epigenetic mark throughout development, beginning in oocytes at the germinal vesicle stage, going into the metaphase II stage, and in pre-implantation embryos. (Zhang et al., 2012). The relative abundance of this specific epigenetic mark, measured using immunocytochemistry, showed that there is no significant difference in the levels of tri-methylation of H3K4 between oocytes at different stages of maturation. However, there was an increase in the relative abundance of H3K4me₃ in early embryos compared with oocytes and the levels decreased to the lowest values by the occurrence of genomic activation in the embryos.

Studies with animal models suggest that tri-methylation of H3K4 is a common mark of the oocyte genome in most mammalian species. In mammalian early embryos, the H3K4me₃ mark has two elements of interest. First, H3K4me₃ is an asymmetric mark in the parental pronuclei, since high levels of H3K4me_{3/2} have been found in the female pronuclei, but not in the male counterpart (Ross et al., 2008). Secondly, levels of H3K4me₃ decreased after

fertilization in pig embryos (Gao et al., 2010). The interpretation of these results remains controversial, questioning the role of H3K4 methylation in chromatin remodeling and gene expression in the early embryo. It is not clear whether the decrease in H3K4me3 levels is due to active demethylation or if it is the result of dilution caused by the addition of non-methylated histones during cell division.

Thus far, nine enzymes have been identified as being capable of methylating lysine 4 in histone 3 in vertebrates. These enzymes include ASH1L, SET7/9, SMYD3, Meisets, and five members of the Mixed Lineage Leukemia proteins family (MLL). Out of these nine, ASH1L is the only one associated directly with early embryo development (Gregory et al., 2007; Gao et al., 2010).

2.1.1.1.1. Absent, Small, or homeotic Disk 1 (ASH1L)

ASH1L is the common name to refer to the mammalian homologue of the *Drosophila melanogaster* tritorax group protein, called Absent, Small or Homeotic disk 1. It has been also called “Absent, Small, or Homeotic like Drosophila”, “Absent, Small, and Homeotic disk protein 1 homologue”, “Lysine N-methyltransferase 2H”, “KMT2H”, and “Histone Lysine N-methyltransferase”, among others. Experimentally, ASH1L has shown the capacity to methylate histone 3 at lysines 4, 9 and 20 in the *Drosophila* (Beisel et al., 2002). However, its spatial distribution in vertebrates correlates well with H3K4me3, but not as well with H3K9 and H3K20 (Gregory et al., 2007).

ASH1L is a large, multi-domain protein complex that contains multiple motifs associated with chromatin remodeling. The PRE-SET and the SET domain are responsible for the methyltransferase activity (Beisel et al., 2002), but it contains at least nine more motifs that can potentially interact with chromatin-protein complexes. It has been proposed that ASH1L uses these motifs to establish epigenetically active structures during epigenetic activation (Gregory et al., 2007). ASH1L actively interacts with Heterochromatin Protein 1 (HP1), *Drosophila* Polycomb (Pc) and the Chromatin Remodeling Complex (CRC) (Beisel et al., 2002).

High levels of ASH1L transcripts were found at the 4-cell stage in porcine oocytes. The high level of transcripts matched the high levels of tri-methylation of H3K4 reported at the same time. These findings suggest that ASH1L plays an important role in stabilizing chromatin structure and keeping the open-frame status required for the porcine embryo to progress through early development and genomic activation (Gao et al., 2010).

ASH1L occupies the 5'-transcribed region of active genes and it is not usually associated with the transcribed region of inactive genes, unlike MLL1. Therefore, it has been postulated that there is a synergic or coupled activity between ASH1L and MLL1 in many mammalian genes, implying that different methyltransferase enzymes from the tritorax family might work together during activation of transcription (Gregory et al., 2007).

The close association between a peak in the expression of ASH1L and the activation of a cluster of genes of the Hox family in pig embryos has been used to postulate that ASH1L-mediated H3K4 tri-methylation plays a major role during development in the pre-implantation embryo (Gao et al., 2010). These findings contradict the low levels of ASH1L activity described by Whitworth in the 4-cell porcine embryo (Whitworth et al., 2005).

2.1.1.1.2. SET Domain Containing Protein 7

First described in 2002 (Nishioka et al., 2002), Set 9 is a histone 3 lysine 4 methyltransferase mainly associated with open chromatin frames and active gene transcription. Set 9 methylase activities are determined by a 50kD single polypeptide containing a SET motif as a catalytic unit, like most of mammalian histone methyltransferases. However, regardless of the evolutionarily highly conserved origins of histone proteins and its modifiers, it lacks the PRE-SET and POST-SET motifs that other enzymes of this family require for their catalytic activity (Nishioka et al., 2002). This is relevant because the PRE-SET and POST-SET domain are responsible for recognizing the specific residues where HMT enzymes are to be recruited for activity. This requires SET 9 to be directed to the selected nucleosomes by a yet unidentified factor that recognizes the right substrates to be modified.

SET 9 also seems to facilitate transcription by a slightly different mechanism than most HMTs. It does not recruit protein complexes that enhance transcription; SET 9 precludes the association of NuRD (a histone 3 deacetylase enzyme associated with gene silencing) and SUV39H1 (a H3K9 methyltransferase associated with gene silencing) with the tail of histone 3 (Nishioka et al., 2002). Moreover, SET 9 precludes the activity of SUV39H1 but has no effect on EHMT2. This means that the recognition of residues by these two H3K9 methyltransferases can be independently regulated by other modifications within the same tail (Nishioka et al., 2002).

2.1.1.2. Methylation of Histone 3 at Lysine 9

Methylation of lysine 9 in histone 3 proteins has been associated with transcriptional gene silencing and it is considered the epigenetic mark of constitutively repressed heterochromatin. It has been well established that H3K9me3 complements DNA methylation, inhibits serine phosphorylation (Chen et al., 1999), and actively participates in the recruitment of heterochromatin protein 1 (HP1) during the formation of heterochromatin leading to gene silencing. Furthermore, the tri-methylation of lysine 9 at histone 3 has also been recently associated with active genes (Gregory et al., 2007).

Five histone 3 lysine 9 methyltransferases have been identified so far and they display subtle differences in their ability to do so. EHMT1 and EHMT2 mediate di-methylation in euchromatic regions, SUV39H1 and SUV39H2 regulate formation of heterochromatin and SETDB1 has been associated with the silencing of retrovirus-like elements dispersed in the euchromatic regions in mammalian cells (Park et al., 2011).

Methylation at H3K9 is generally associated with repressive chromatin status; however, the degree of methylation modifies the significance of the modification. For example, the tri-methylated state of lysine 9 in histone 3 is associated with pericentric heterochromatin, whereas the mono- and di-methylated status of lysine 9 are more associated with silent domains within euchromatic regions (Lehnertz et al., 2003; Peters et al., 2003). However, tri-methylation of

H3K9 can also serve as a mark for active gene expression when the tri-methylated histones are located within the body of the gene (Shi and Whetstone, 2007).

The presence of tri-methylated H3K9 has been described in immature ovine oocytes, and remains during oocyte growth and maturation. It has been proposed that H3K3me3 works synergistically with the progressive methylation of DNA in maturing oocytes to create a repressed chromatin status in the fully differentiated oocyte and to underlie the silencing of imprinted genes (Russo et al., 2013). This synergic mechanism between histone methylation and DNA methylation has been described as fundamental in the establishment and maintenance of epigenetic gene silencing regulation of cell determination and function (Vire et al., 2006).

Both the tri-methylated and the di-methylated forms of H3K9 are present in the developing mouse oocyte, and the levels of methylation change in similar manners, suggesting that both stages are under the same regulatory mechanism (Liu et al., 2004). In mice, the methylation status present in H3K9 during oocyte maturation and growth is maintained after fertilization, whereas the paternal genome remains under-methylated even though H3K9 HMTs transcripts and enzymes are present in the ooplasm after fertilization. Paternal and maternal genomes remained asymmetrically methylated until genomic activation, where methylation levels increased symmetrically. These findings suggest that H3K9 HMTs are inactive during early embryonic stages and that the role of H3K9 methylation is not to regulate heterochromatin formation and gene expression in the early embryo, but to mark the maternal genome so it can be differentiated from the paternal genome by the cellular machinery (Liu et al., 2004).

2.1.1.2.1. Euchromatin Histone-Lysine N-Methyltransferase 2 (EHMT2)

EHMT2 also has been called “Histone3-K9 methyltransferase”, “Lysine N-Methyltransferase 1C”, “Protein G9a”, “G9a”, “Lysine 9 Specific 3”, “H3-K9-HMTase 3”, “HLA-B-Associated Transcrip 8”, “Chromosome 6 open reading frame 30”, “GAT8”, and “Ankyrin Repeat-Containing Protein”. It regulates mono- and di-methylation of histone 3 at lysine 9 in

euchromatic regions and has been associated with inactive chromatin stages and with repression of gene expression during embryogenesis (Park et al., 2011).

There have been two mechanisms proposed for EHMT2: it creates local heterochromatic architecture in euchromatic regions by methylating H3K9 that recognize subpopulations of HP1 proteins, and/or (since it also methylates H3K27 in vitro) histone 3 proteins methylated at both lysine residues may recruit chromatin modifying proteins that influence chromatin structure and gene expression (Tachibana et al., 2002).

There is an early embryonic lethality on *EHMT2*^{-/-} mice, with the developmental arrest occurring from the E9 stage until the E12 stage (the time of neural plate formation, formation of amniotic cavities, and the end of gastrulation in mice) characterized by the reorganization of tissues, widespread alterations in gene expression profiles, and chromatin reorganization (Tachibana et al., 2002). These elements suggest that EHMT2 mediated histone methylation of euchromatin is a key component of the mechanisms that regulate early stages of embryogenesis. Retardation of embryonic growth was also noticed, which was explained by the significant increase of apoptotic cells in *EHMT2*^{-/-} embryos.

EHMT2 deficiency affects genes that are imprinted in the trophoblast which are not dependent on DNA methylation for the somatic maintenance of their allelic silencing (Park et al., 2011). However, there was no significant change in the in vitro developmental potential of porcine embryos injected with EHMT1/2 RNAi; changes in the transcript abundance of eIF1A, but not OCT4, NANOG, or SOX2 suggest that only a subset of genes that undergo changes in transcript abundance are regulated by histone modifying enzymes (Park et al., 2011).

2.1.1.2.2. Suppressor of variegation3-9 Homolog 1 (SUV39H1)

Also called “Position-Effect Variegation 3-9 Homolog”, “KMT1A”, “Lysine N-methyltransferase 1A”, and “H3-K9 HMTase 1”, SUV39H1 has classically being associated with inactive chromatin and repression of gene expression because SUV39H1 mediates the recruitment of HP1 via tri-methylation of H3K9. Moreover, it is considered to control the

inheritance of repressive chromatin regions since SUV39H1 is the trans-generational signal for pericentric heterochromatin formation in mouse early embryos, which plays a crucial role in chromosome segregation and establishment of transcriptional repression (Tachibana et al., 2002).

Additional roles other than heterochromatin formation have been proposed for H3K9 tri-methylation by SUV39H1. It has been implicated in chromatin remodeling during DNA repair since modifications in the interaction of SUV39H1 and chromatin have resulted in altered DNA repair mechanisms and modification of the lifespan of mice (Liu et al., 2013). SUV39H1 has been recently associated with the mechanisms of chromosome condensation and alignment, since mutant forms of the enzyme result in misalignment and failure of chromosome segregation during mitosis (Chu et al., 2012; Wang et al., 2013). Moreover, SUV39H1 has been suggested to play a role in the regulation of the cell cycle by facilitating the replication of heterochromatin (Chu et al., 2012).

The cell cycle dependent protein kinase CDK2 has the potential to phosphorylate SUV39H1 at serine 391 during G1-S transition in vivo and in vitro (Park et al., 2014). The phosphorylated SUV39H1 dissociates from chromatin, allowing histone demethylases such as JMJD2A to access to heterochromatic loci. The induced structural modification of heterochromatin would facilitate DNA replication and the progression through the cell cycle.

The tri-methylation of H3K9 by SUV39H1 works synergistically with DNA methyltransferases Dnmt3a and Dnmt3b to generate heterochromatic DNA at pericentric satellite repeats (Lehnertz et al., 2003). The control of the DNA methylation process at centromeric repeats seems to be regulated by a different pathway, since SUV39H1 mutant cells were capable of undergoing chromatin condensation at the centromeric repeats.

Lastly, it has been suggested to have a specific role during early embryo cleavage because the injection of RNAi targeting SUV39H1 in porcine embryos affected in vitro development. There was a decrease in cell number in embryos injected with the RNAi, but there

was no interference with the transcript abundance of NANOG, SOX2, OCT4 or eIF1A. Results indicated that this HMT is not involved in the regulation of transcription of these genes, and their effect has to be in other epigenetic pathways which also control early embryo development (Park et al., 2011). Also, double mutant *SUV39h1/2*^{-/-} mice are not lethal, questioning the relevance of the role of this enzyme in mammalian embryonic development (Tachibana et al., 2002).

2.1.1.3. Methylation of Histone 3 at Lysine 27

Methylation of lysine 27 in histone 3 is a repressive modification and it is considered the epigenetic mark of facultative heterochromatin. The Polycomb repressive complex 2 is responsible for keeping lysine 27 at histone 3 in a tri-methylated or di-methylated state, and it also has the ability to recruit repressive proteins that modify the chromatin structure into a repressive state (Gao et al., 2010). UTX and KDM6B are enzyme members of the trithorax family responsible for the removal of methyl groups of the tri-methylated and di-methylated state of H3K27. This group of enzymes is characterized by the presence the JmjC domain, which is the motif with the demethylase activity. KDM6B induces strong demethylation of H3K27 in vivo and causes delocalization of Polycomb proteins in vivo (Agger et al., 2007). Other regulatory mechanisms that control or decide the methylation status of H3K27 and its biological activity are yet to be discovered.

Some authors report the levels of relative abundance of tri-methylation of lysine 27 in histone 3 to be stable during oocyte maturation and early embryo development in humans, and that only embryos around the time of genomic activation show a significant decrease in the global methylation pattern of the nuclei (Zhang et al., 2012). Some other authors report a rapid decrease in the levels of tri-methylation of H3K27 during embryogenesis and stem cell differentiation. The former group suggests that H3K27 is required for stem cell renewal, is considered important in maintaining pluripotency, and plays a role in the regulation of the

expression of the three key pluripotency genes OCT4, NANOG and SOX2 during early differentiation in embryonic stem cells.

Studies in humans reported that after fertilization only one of the two pronuclei (the one closest to the polar bodies) had a positive signal for H3K27me3, whereas both of the polar bodies produced a strong H3K27me3 signal. The authors considered the H3K27 tri-methylated pronuclei as the maternal one, and the pronuclei without H3K27me3 as the paternal one (Zhang et al., 2012). This phenomenon has also been described in bovine embryos (Ross et al., 2008).

In early porcine embryos, the levels of methylation of H3K27 follow the levels of histone methyltransferase transcripts. At the 1-cell stage, transcript levels of histone methyltransferases are high, demethylases levels are almost undetectable, and tri-methylation of lysine 27 is at its highest level. When the early porcine embryo reaches the 4-cell stage (time of genomic activation in the species) levels of histone methyltransferases are low, levels of demethylases are high, and levels of tri-methylation of lysine 27 in histone 3 have decreased (Gao et al., 2010).

2.1.1.3.1 Lysine (K)-specific demethylase 6B (KDM6B)

Also known as the Jumonji Domain Containing 3, Jumonji Domain Containing protein 3, JmjC Domain-Containing protein 3, and Lysine demethylase 6B. KDM6B specifically demethylates lysine 27 in histone. Because its demethylase activity was first identified associated with the expression of genes of the HOX family, its activity has been related to the regulation of the homeotic development of the early embryo.

The role of KDM6B has not been clearly established, but it has been demonstrated to have the capacity to remove repressive marks, add activating marks, and prevent the activity of Polycomb proteins by not prohibiting access to regulatory regions of genes associated with cell fate decisions (Agger et al., 2007).

In both bovine and porcine models, early embryos show a progressive decrease in the level of H3K27me3, reaching the lowest levels by the time of genomic activation (Ross et al.,

2008; Gao et al., 2010). The expression of H3K27me3 demethylases UTX was undetectable at the 1-cell stage and had minimal levels at the 4-cell stage (the maternal-zygote transition point in the pig) with levels of KDM6B peaking at the 4-cell stage (Gao et al., 2010).

2.1.2. Methylation of Arginine Residues

Arginine methylation is a very well conserved mechanism through evolution (Wang et al., 2001) and it has been associated with active transcription, using a mechanism similar to histone methylation, by modifying the interactions between chromatin and effector proteins. However, information about arginine methylation is limited and difficult to interpret since this modification is difficult to detect *in vivo*. Its synthesis and activity seems to be cyclical, and methyl-arginine binding proteins are yet to be identified (Lepikhov and Walter, 2004).

Protein Arginine methyltransferases (PRMTs) catalyze the transfer of methyl groups from s-adenosyl-L-methionine (SAM) to the guanidine nitrogens of arginine residues. Arginine residues in histone proteins can be mono-methylated or di-methylated; the di-methylation can be symmetrical or asymmetrical. The enzymes that catalyze this process have been divided into two types, with the type I catalyzing the formation of asymmetric di-methyl arginine residues, whereas the type II enzyme catalyzes the formation of symmetric di-methyl arginine residues (Zhang and Reinberg, 2001).

PRMT as a protein family has multiple target proteins, but at least two of its members have been identified to methylate arginine residues in histone proteins: PRMT1 and CARM1, also called PRMT4 (Zhang and Reinberg, 2001). What makes PRMTs particularly interesting is that they seem not to be exclusively histone methyltransferases. They appear to share their role of transcriptional regulators among other tasks. CARM1 methylates *in vitro* histone 3 at arginine 2, 17, and 26, as well as members of the p160 family of co-activators of transcription (Chen et al., 1999). PRMT1 regulates the interferon signaling pathway (Abramovich et al., 1997), protein regulators of transcription such as STAT1 (signal transducers and activators of transcription) (Mowen et al., 2001), and Histone 4 at arginine 3 (Wang et al., 2001). The mechanisms by

which PRMT coordinates their dual regulation of transcription (regulating chromatin structure and regulating transcription activators) has yet to be elucidated.

The role of PRMTs during embryo development is not clear (Wang et al., 2001). PRMT mutant mouse embryos fail to develop further than the blastocyst stage, suggesting an important role during early embryo development, but at a cellular level PRMTs are not required for cell survival. It is questionable if the main role of PRMT during early embryo development is actually associated with the methylation of histone tails or with its interaction with other nuclear proteins (Pawlak et al., 2000).

Two enzymes have been described as active histone arginine methyltransferases: PRMT1 and CARM1. PRMT1 was first isolated and purified by Wang, et al. in 2001 and it is the most abundant H4-specific HMT. A 42-kD polypeptide, it has been proven to methylate H4R3 both in vivo and in vitro (Wang et al., 2001). PRMT1 lacks any lysine methyltransferase activity, is inhibited by acetylation of lysine residues, and shows high affinity RNA binding proteins in vivo, but the significance and biological implications of these characteristics are poorly understood. The other histone arginine methyltransferase, CARM1, has been associated with transcriptional activation (Chen et al., 1999).

2.2. Histone Ubiquitination

Ubiquitin is a 76 amino acid protein that can modify proteins by being transferred from the intermediary enzyme to lysine residues in the target protein. Substrates can be mono- or poly-ubiquitinated, with poly-ubiquitination being a frequent mark for protein degradation and mono-ubiquitination a mark for subsequent modifications in the target protein. Ubiquitination is a reversible modification; ubiquitin-specific proteases are responsible for removing this mark. Histone 2A is ubiquitinated at lysine 119 and histone 2B is ubiquitinated at lysine 120 by Rad6 in mammalian cells, with ubiquitination of H2A being far more prominent than ubiquitination of H2B.

Ubiquitination of H2A has been associated with transcriptional silencing by recruiting chromatin modifying proteins such as members of the Polycomb repressive complex 1 or by being functionally coupled to methylation of other H3 lysines that regulate gene silencing (Baarends et al., 2005). Transcriptional repression due to stimulation of high-order chromatin formation has also been postulated (Weake and Workman, 2008).

Ubiquitination of histone H2B regulates gene expression by participating in transcriptional activation after histone associated ubiquitin proteins interact with RNA polymerase II (Weake and Workman, 2008). It has also been proposed that H2B works as a check point at which RNA polymerase II pauses during early transcription elongation. H2B ubiquitination has also been described as an epigenetic regulator due to its interactions with other covalent modifications in histone residues. Specifically, it regulates the methylation of histone H3 at lysines 4 and 79, but not the methylation of histone H3 at lysine 36.

Ubiquitination of H2B at lysine 123 is mediated by the enzyme Rad6, also known as ubiquitin-conjugating enzyme. The mutation of RAD6 induces a lack of methylation at lysines 4 and 79, but does not alter the methylation at lysine 36. Therefore, it has been proposed that ubiquitination of H2B works as an epigenetic switch that marks subsequent epigenetic modifications (Briggs et al., 2002). However, mutations at lysine 79 do not interfere with the regulation of Lysine 4 by ubiquitination of H2B and vice versa, showing that the regulatory mechanism is unidirectional and independent from each other (Briggs et al., 2002).

The regulatory mechanisms that use histone ubiquitination are still incompletely characterized; it is not clear why H2B is a mark associated with the transcribed region of most genes, but it only appears to have a regulatory role in a small subset of these genes. An alternative mechanism suggests that ubiquitination participates in transcriptional regulation indirectly, since ubiquitination of H2B has been reported as necessary for the demethylation of H3K4 and H3K79 in eukaryotes (Dover et al., 2002; Sun and Allis, 2002). It has also been reported that levels of H2B increase during cell differentiation processes and alterations in the

levels of ubiquitin-conjugating enzymes induce modification in the differentiation process of human or mice embryonic stem cells, but no clear mechanisms have been described yet (Fuchs et al., 2012; Karpiuk et al., 2012).

2.3 Histone Acetylation

Acetylation of histone tails regulates gene expression by modifying chromatin structure. In general, acetylation of histone tails correlates with the opening of chromatin structures, increasing the DNA accessibility for transcription factors resulting in an increase in gene expression (Vandel and Trouche, 2001; Zhang and Reinberg, 2001). The p300/CBP protein complex apparently has intrinsic histone acetyl transferase activity. But this protein complex is also associated with the transcriptional activation of several transcription factors (Giordano and Avantaggiati, 1999). Histone acetylation has the potential to link two different mechanisms of transcriptional regulation controlled by the same protein complex.

The levels of histone acetylation in vivo are very dynamic; they are balanced out by two opposing sets of enzymes: histone acetyl transferases and histone deacetylase. They work antagonistically, but simultaneously lead to the changes in gene expression required by the cell to adjust to changing environments (Cheung et al., 2000). The easily reversible acetylation marks provide the cell with the means to respond quickly to changes in the environment by rapid changes in gene expression patterns (Shi and Whetstone, 2007).

Many enzymes have been reported with histone acetyl transferase activity, most of them having specific affinity for lysine residues in H3 and H4 N-terminal tails. Gnc5 was the first family of histone acetyl transferase proteins to be identified (Brownell et al., 1996). It is highly conserved among eukaryote organisms. It seems that Gnc5 is recruited by the interaction between activator proteins and the promoter region of a specific cluster of genes (Lo et al., 2000). After recruitment, Gnc5 acetylates histone proteins within the basal promoters of these genes, facilitating the access of transcription factors.

Histone acetylation of histone 3 at lysine 12 showed a dynamic pattern during bovine oocyte maturation with a strong signal at the GV and GVBD stages, and a marked decrease in MI and MII stages. This observation was constant regardless of the size of the follicle from which the oocyte was collected before maturing them in vitro (Racedo et al., 2009).

2.4. Histone Phosphorylation

There is an increase in phosphorylation of histone 1 during mitosis in eukaryote cells (Bradbury et al., 1973), and there is a site specific phosphorylation of core histone 3 at serine 10 during mitosis in mammalian cells (Gurley et al., 1978). These two findings made scientists believe for a long time that there was a direct association between histone phosphorylation and chromatin condensation prior to mitosis in the cell cycle. However, it was later shown that neither histone 1 phosphorylation (Guo et al., 1995) nor histone 1 itself (Ohsumi et al., 1993) were necessary for mitotic chromosome condensation. Therefore, scientists have been very careful about postulating an association of causality between histone phosphorylation and chromatin condensation.

Based on evidence that indicates that phosphorylation of serine 10 in histone 3 only occurs during mitosis in mammalian cells in vivo (Wei et al., 1999) have proposed two possible theories for the link between histone phosphorylation and chromatin condensation. Histone phosphorylation causes a transient decondensation of chromatin that facilitates the binding of chromatin condensing proteins to the DNA and/or the phosphorylated histone itself might act as a mark for chromatin condensation factors (Wei et al., 1999).

However, phosphorylation brings a negative charge into the positively charged H3 amino terminus, reducing the interaction between H3 and DNA and theoretically inducing more decondensation than condensation of the chromatin structure. Furthermore, phosphorylation of H3S10 by Aurora B protein disrupts the interaction between H3K9 and HP1 when the cell enters the M phase of the cell cycle. This means that during interphase, HP1 can stay associated with tri-methylated H3K9. However, before mitosis takes place, HP1 and H3K9me3 must dissociate,

and the phosphorylation of H3S10 changes the affinity of H3K9 for HP1, allowing a cell cycle-dependent dissociation of heterochromatic regions (Fischle et al., 2005).

And the links between histone phosphorylation and the regulation of the cell cycle do not end there. Phosphorylation of histone 3 has been associated with the regulation of transcription of families of protein kinases involved in cell cycle regulation (Sassone-Corsi et al., 1999), with the transcriptional activation of mitogen-stimulated response genes, such as c-fos and c-jun (Mahadevan et al., 1991), and with proteins of the MAP signaling pathway. All these interactions suggest an important role of the histone 3 phosphorylation in regulation of cell cycle, mitosis, cell proliferation, and cell differentiation.

A second regulatory mechanism involving histone phosphorylation has been postulated based in the frequency that phosphorylation overlaps prior to post-translational modifications on the same histone tail. A well-documented example is the interaction between the phosphorylation of serine 10 and the acetylation of lysine 14 in histone 3. Gcn5, the histone acetylase, displays up to a 10-fold greater affinity for phosphorylated serine 10 in histone 3 as a substrate compared to the unmodified form of H3, and phosphorylation of serine 10 in histone 3 has been functionally linked in vitro and in vivo to Gcn5-mediated acetylation at lysine 14 (Lo et al., 2000). This type of interaction has been described as “dimodified status of histone tails” (Cheung et al., 2000).

Based on this dimodified status of the histone 3 tail, some authors suggests that histone proteins might also follow the regulatory mechanisms described for other families of regulatory proteins, in which several modifications regulate different levels of enzymatic activity (Cheung et al., 2000). Other authors suggest that since covalent modifications work as interaction signals for effector proteins, the presence of more than one modification simultaneously might serve as a highly specific marker for regulatory proteins (Mahadevan et al., 1991). However, the transcription associated phosphorylation of histone 3 only occurs in discrete areas of the genome; it means that the acetylation of lysine 14 also occurs independently of phosphorylation

and that single modifications are more the rule than the exception. At this point, the understanding of the mechanism that regulate histone modifications, as well as the consequences of such modifications, are only partially understood. More effort and research is needed before we can affirm that the histone code has been broken.

CHAPTER III

DIFFERENCES IN LEVELS OF HISTONE METHYLTRANSFERASE TRANSCRIPTS BETWEEN IMMATURE, IN VITRO MATURED, AND IN VIVO MATURED BOVINE CUMULUS CELLS AND OOCYTES

3.1. Introduction

The difference in developmental competence between in vitro matured oocytes and in vivo matured oocytes has been well established, with in vivo matured oocytes reaching higher rates of embryo development than their in vitro matured counterparts. It has also been established that the different phenotypes of oocytes matured in vivo compared with oocytes matured in vitro offers the possibility to compare their mRNA content (Labrecque and Sirard, 2014). During the experiments described in this chapter, the difference in developmental competence between immature oocytes, in vitro matured oocytes and in vivo matured oocytes is used as a system to explore possible differences in the accumulation of transcripts during the final maturation of the oocyte.

Soon after fertilization the gametes must undergo extensive epigenetic reprogramming to achieve the epigenetic landscape required to establish the totipotent stage characteristic of early embryo development. However, genomic activation (GA) does not occur in the bovine embryo until the eight- to 16-cell stages (day 2.5 – 3 after fertilization), suggesting that the proteins required for the epigenetic reprogramming prior to the eight-cell stage cannot be synthesized by the early embryo and must be provided in the form of mRNAs by the oocyte. These mRNAs are synthesized and accumulated during the final maturation of the oocyte. The experiments in this chapter conduct transcriptome analysis of mRNAs accumulated during the final stages of oocyte maturation that code for proteins associated with epigenetic reprogramming.

The post-translational modification of histone proteins has been identified as one of the key regulatory mechanisms involved in epigenetic reprogramming. Histone methyltransferase

proteins have the potential to modify chromatin structure and, therefore, regulate gene expression. This regulation has been proven to be critical in the early embryo since genes leading to early totipotent development (which remain silent in most somatic cells and gametes) must be actively expressed, whereas every other gene that is not critical for developmental potential must be silenced. The experiments described in this chapter study transcripts of enzymes responsible for the post-translational modification of histones.

The preponderant role that cumulus cells play during oocyte maturation has been well established. Bilateral communication exists between the oocyte and the surrounding cumulus cell which includes paracrine signaling and the transfer of small molecules via gap junctions. Cumulus cells even regulate the beginning of nuclear maturation by constantly supplying the oocyte with cyclic adenosine monophosphate (cAMP), which prevents the enzymatic cascades responsible for resumption of meiosis. It has been proposed that it is the rupture of the link between the cumulus cells and the oocyte which causes the decline in the levels of cAMP in the ooplasm, leading to the resumption of meiosis. Even more, recent research suggests that during the period of transcriptional incompetence due to the resumption of meiosis, cumulus cells transfer critical mRNAs required for embryonic development to the oocyte (Macaulay et al., 2014). During the experiments presented in this chapter, cumulus-oocyte complexes were used for transcriptome analysis, which was additionally performed in oocytes and cumulus cells separately.

This chapter describes three experiments using the difference in developmental competence between immature oocytes, in vitro matured oocytes, and in vivo matured oocytes as a system to research the accumulation of mRNAs transcripts during the final stages of oocyte maturation. These experiments centered on mRNAs that are involved in epigenetic reprogramming in the early embryo by selecting four transcripts, which code for three histone methyltransferases and one histone demethylase for analysis. These transcripts were studied in bovine cumulus-oocyte complexes, denuded oocytes and biopsies of cumulus cells.

3.2. Materials and Methods

3.2.1. Animal husbandry

Experimental procedures in this study were approved by the Louisiana State University Animal Care and Use Committee and conducted at the Louisiana State University Agricultural Center Reproductive Biology Laboratory (RBC) - Embryo Biotechnology Laboratory (EBL) in Saint Gabriel, Louisiana from August 2012 through July 2013.

Non lactating crossbred (Angus x Red Angus x Brangus) cows (n=40) 4 to 7 years of age, maintained as the experimental physiology herd at the LSU RBC, were used throughout the course of this study. The cows displayed regular estrous cycles, were all in moderate to good body condition, and were maintained on pastures planted with Bermudagrass (*Cynodon dactylon*) and White clover (*Trifolium repens*). Hay was provided ad libitum during the winter season.

The Louisiana State University RBC is located in South Louisiana. It is situated at 30°16' north latitude, 91°06' west longitude, and has a subtropical climate. The elevation is nine meters above the sea level, the average annual precipitation is 150 meters, and the average day length is 12.6 hours.

3.2.2. Experimental design

Three experiments were conducted to investigate the relative abundance of histone methyltransferase transcripts in bovine cumulus cells and oocytes:

- Experiment one: Cumulus-oocyte complexes were used to investigate differences in transcripts for histone methyltransferases ASH1L, EHMT2, SUV39H1 and KDM6B between immature cumulus-oocyte complexes, in vitro matured cumulus-oocyte complexes and in vivo matured cumulus-oocyte complexes.
- Experiment two: Oocytes were used to investigate differences in transcripts for histone methyltransferases ASH1L, EHMT2, SUV39H1 and KDM6B between immature oocytes, in vitro matured oocytes and in vivo matured oocytes.

- Experiment three: Samples of cumulus cells were used to investigate differences in transcripts for histone methyltransferases ASH1L, EHMT2, SUV39H1 and KDM6B between immature cumulus cells, in vitro matured cumulus cells and in vivo matured cumulus cells.

For all three experiments presented in this chapter, the experimental unit was defined as the oocyte and the sampling unit was defined as the oocyte. In order to study the possible differences in gene expression between cumulus cells and oocytes, three experimental treatments were defined for each experiment:

- Treatment one: Immature cumulus cells and/or oocytes were used for transcriptome analysis after transvaginal ultrasound guided aspiration when still at a germinal vesicle stage.
- Treatment two: In vitro matured cumulus cells and/or oocytes were used for transcriptome analysis after transvaginal ultrasound guided aspiration of oocytes at the germinal vesicle stage and maturation in vitro until arrested at the metaphase II stage.
- Treatment three: In vivo matured cumulus cells and/or oocytes were used for transcriptome analysis after in vivo maturation and transvaginal ultrasound guided aspiration when at a metaphase II stage.

3.2.3. Synchronization for collection of cumulus-oocyte complexes

Two synchronization protocols were used for these experiments. The first was used to collect immature oocytes (germinal vesicle stage) and the second was used to collect in vivo matured oocytes (metaphase II stage). These synchronization protocols are based on those described by Rizos (Rizos et al., 2002) and used by others to collect both in vitro matured and in vivo matured cumulus-oocyte complexes for transcriptome analysis (Tesfaye et al., 2009; Assidi et al., 2013; Spencer et al., 2013).

Synchronization protocol one was used to retrieve immature oocytes for use in experimental treatments one and two. An outline of this protocol is presented in Figure 3.1. A controlled internal release device with progesterone (Easi-Breed™ CIDR cattle insert®, Zoetis laboratories) was placed intravaginally for ten days and prostaglandin $F_{2\alpha}$ (PGF_{2 α} , 25 mg of dinoprost tromethamine, Lutalize®, single dose, intramuscular) was given the day of CIDR removal. Cows were observed for signs of estrous behavior 48 to 72 hours after the administration of PGF_{2 α} , and cows displaying standing estrus were identified and recorded. Cows that failed to display estrus during the observation period were also identified, but they were not removed from the experimental group. Eight days after starting estrus, growth of all dominant follicles was impaired using an ultrasound-guided needle. Then, four days after dominant follicle removal (DFR), transvaginal ultrasound-guided aspiration of follicles was performed.

Synchronization protocol two was similar to protocol one; an outline of the protocol is presented in Figure 3.2. A CIDR in combination with PGF_{2 α} was used to synchronize estrus. Dominant follicle removal was performed eight days after standing estrus and PGF_{2 α} was administered four days after DFR. Cows displaying estrous behavior were given PGF_{2 α} and Gonadotropin releasing hormone (GnRH, 100 µg of Gonadorelin hydrochloride, Factrel®, single dose) intramuscular 48 hours later. Transvaginal ultrasound-guided aspiration of oocytes was performed 12 hours after the administration of GnRH.

Protocol one was used in ten cows, whereas protocol two was used in 40 animals. There was an interval of, at least, 40 days between the end of protocol one and the beginning of protocol two. When environmental factors, such as high temperatures during the summer, affected the quality of the oocytes, collections were suspended until conditions returned to normal and cows recovered their cyclicity. Cows used in protocol one were selected randomly from the physiology herd, and all 40 cows from the physiology herd were used for protocol two.

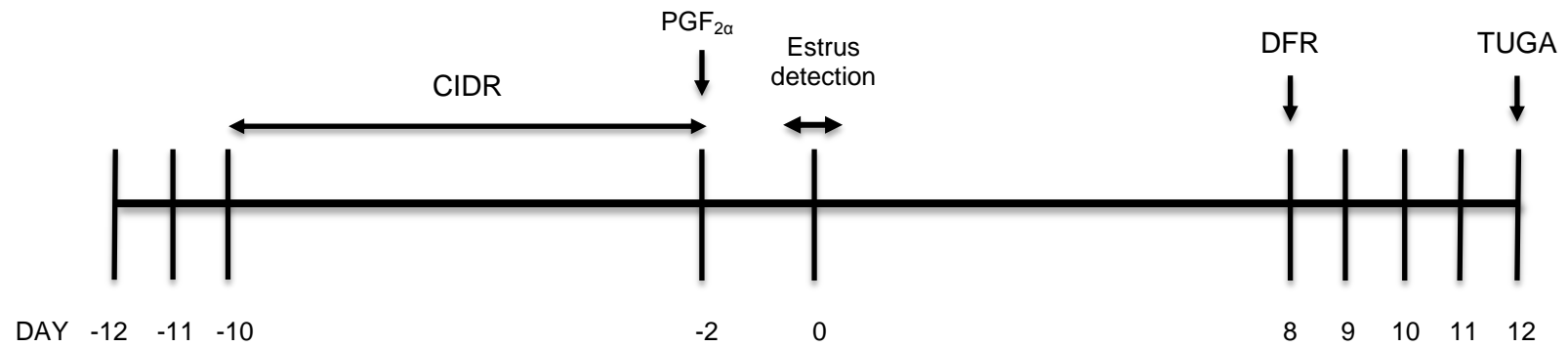


Figure 3.1. Synchronization protocol for transvaginal ultrasound-guided aspiration of immature oocytes. CIDR is controlled internal drug release device; PGF_{2α} is prostaglandin F 2 alpha; DFR is dominant follicle removal; TUGA is transvaginal ultrasound-guided aspiration.

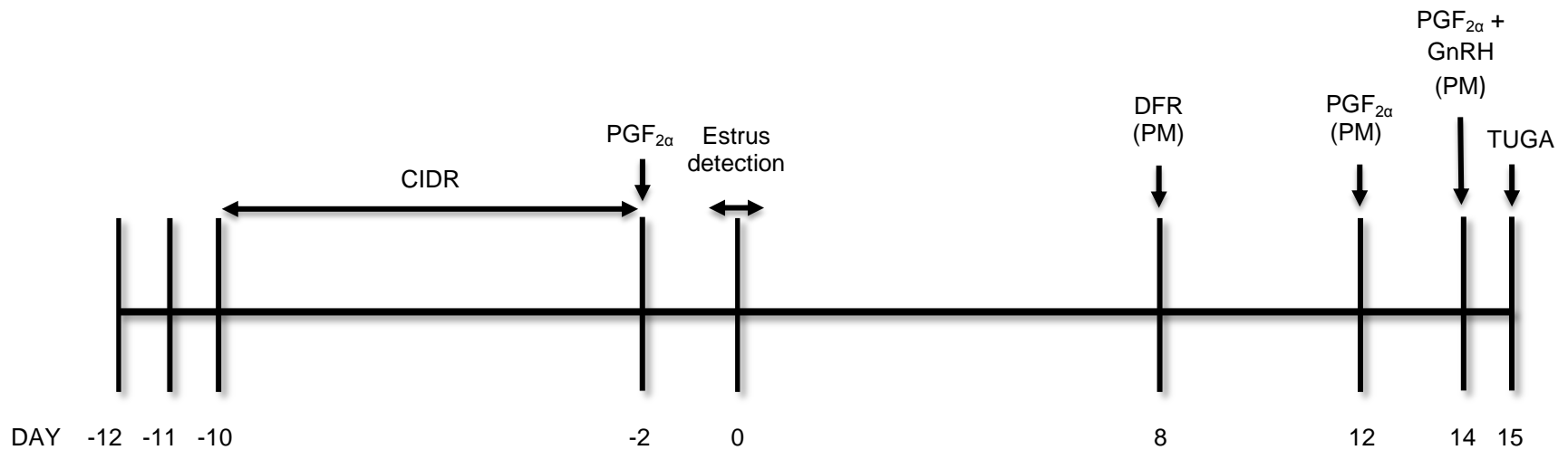


Figure 3.2. Synchronization protocol for transvaginal ultrasound-guided aspiration of in vivo matured oocytes. CIDR is controlled internal drug release device; PGF_{2α} is Prostaglandin F 2 alpha; DFR is dominant follicle removal; GnRH is Gonadotropin Releasing Hormone, TUGA is transvaginal ultrasound-guided aspiration. PM indicates that treatments were applied in the afternoon.

3.2.4. Collection of cumulus-oocyte complexes

Cumulus-oocyte complexes (COCs) were collected by transvaginal ultrasound-guided aspiration (TUGA) of antral follicles. Equipment and materials used for TUGA are presented in Appendix C. Cows were briefly restrained in a holding chute and given an epidural injection of six mL of lidocaine 2% (lidocaine hydrochloride, VETone[®] pharmaceuticals). A 7.5 MHz ultrasound transducer was used trans-vaginally as the ovaries were manipulated trans-rectally. The image provided by the ultrasound was used by the technician to identify the follicles and direct an 18g X 88.9mm needle to aspirate the follicular contents. The needle was connected by tubing to a bovine embryo filter with a 75 micron membrane (EmCom[™] Filter). A vacuum pump was connected to the filter to apply negative pressure, enhancing the recovery of follicular contents.

Oocyte collection medium (OCM) used to lubricate the surfaces with the potential to be in contact with the follicular contents and provide an isotonic, isothermal environment for the oocytes within the collection system. OCM used was Dulbecco's phosphate-buffered saline 10X (DPBS, Sigma, D1283) diluted to a working concentration (1X) supplemented with 1% calf serum and 10 IU/mL of heparin (Heparin sodium, Sagent[®] pharmaceuticals). Detailed information about the OCM can be found in Appendix B. Immediately following collection, oocytes were transferred to a gridded dish and stereoscopic microscopes were used to search, rinse and collect cumulus-oocyte complexes.

3.2.5. Sample evaluation and freezing

The evaluation protocol was the same for all three treatments in all three experiments. Cumulus-oocyte complexes which were expected to be at germinal vesicle stage were evaluated based on the homogeneity of the ooplasm and the presence of several layers of compact cumulus cells. Cumulus-oocyte complexes expected to be at the metaphase II stage were evaluated based on the homogeneity of the ooplasm and evidence of ongoing cumulus cell expansion.

Samples for all experiments and treatments were placed in 1.8 mL centrifuge tubes in a volume of less than 5 μ L of DPBS containing 0.1% polyvinyl alcohol (PVA) and stored at -80°C for later RNA analysis.

3.2.6. Sample processing

The processing of samples was different between experiments because Experiment one used cumulus-oocytes complexes (COCs), Experiment two used oocytes, and Experiment three used cumulus cells. In Experiment one cumulus-oocyte complexes were used as samples without any further processing. For Experiment three, a small group of cumulus cells were removed from the outer layers of the cumulus to be used as the sample. For Experiment two, cumulus cells of the COCs used in Experiment three were removed using a 0.1% hyaluronidase solution (Sigma® H-3506). COCs were held in hyaluronidase solution at 39°C for seven minutes and then vortexed for ten minutes. The resulting denuded oocytes were used as the sample.

3.2.7. In vitro maturation of cumulus-oocyte complexes

Treatment two of all three experiments required in vitro maturation of the cumulus-oocyte complexes (COCs). The protocol for in vitro oocyte maturation can be found in Appendix A, the formulation for the maturation medium can be found in Appendix B, and a list of the equipment and materials used during in vitro maturation are presented in Appendix C. Immediately after collection and evaluation, COCs assigned to Treatment two were washed four times through standard maturation medium and transferred into 35 μ L drops of maturation medium covered with 570 μ L of mineral oil and incubated in 5% CO₂ at 39° C for 22 hours. Maturation medium was tissue culture medium 199 supplemented with 10% fetal bovine serum, 0.2 mM sodium pyruvate, 2 mM glutamine, 5 μ m/mL of FSH and 1% penicillin/streptomycin.

3.2.8. Primer selection and validation

Three genes coding for three histone methyltransferases (ASH1L, EHMT2, and SUV39H1) and one gene coding for a histone demethylase (KDM6B) were selected as genes of

interest, and two housekeeping genes (Poly A polymerase and GADPH) were selected as reference genes. Primers (forward and reverse) for each gene were acquired from Invitrogen™. Primers accession numbers, sequences and product size can be found in table 3.1.

RNA was extracted from ovarian tissue and reverse transcriptase PCR was used to produce an initial calibrator. The main characteristic of this initial calibrator is to contain the DNA sequences for the four genes of interest and the two housekeeping genes. The initial calibrator was used to produce purified PCR product for each gene, which was used to determine the optimal annealing temperature for each set of primers, to corroborate that each set of primers was amplifying a single product, and to spike the initial calibrator with purified PCR product from each gene to produce a final calibrator. This final calibrator was used to generate the QPCR standard curves for each gene, and as a reference positive control in each QPCR reaction performed in the samples.

Basic PCR reactions consisted of 25 µL Jumpstart™ Red taq® Ready Mix (P0982, Sigma), 2 µL of the forward primer, 2 µL of the reverse primer, 10 µL of DNA from a calibrator, and 11 µL of dH₂O for a total of 50 µL. The thermocycler was programmed for four steps. Step one was 94°C for two minutes; step two was 35 cycles of 30 seconds at 94°C, 30 seconds at the specific annealing temperature of each set of primers, and one minute at 72°C for elongation; step three was one cycle of five minutes at 72°C for final extension and step four was holding the PCR product at 4°C until removed from the thermocycler.

Real time PCR reactions consisted of 4 µL of calibrator, 10 µL of SsoFast™ EvaGreen® supermix (172-5200, Sigma), 10 µmol of forward primer, 10 µmol of reverse primer and 4 µL of nuclease-free water. The thermocycler was programmed for three steps. The first step was one minute at 95 °C; the second step was 40 cycles of 30 seconds at 95 °C and 30 seconds at 61°C and the third step consisted of 68 cycles with 0.5°C increases every ten seconds, starting at 61°C and finishing at 95°C. The complete protocols for PCR amplification can be found in Appendix A.

Table 3.1. PCR primers

Primer ¹	GeneBank Accession Number	Sequence	Product size (bp)
ASH1L	NM_001192743	F 5' -ACCTCCTCCATCGCCTTC R 5' -TGTGCTCAACCATCCAACC	215
EHMT2	NM_001206263	F 5' -CTCTACTATGATTCCTACTCTG R 5' -CATCTTCCTCTTCTTCTTCC	163
SUV39H1	NM_001046264	F 5' -ACTAAGCGACTTCACTTCAC R 5' -GGCACCTCCTCAGTATCC	216
KDM6B	XM_003587412	F 5' -CCATCAAGAGAACAACAAC R 5' -GAAGCATAGAGGTCATCC	174
Poly A	X63436	F 5' -AAGCAACTCCATCAACTACTG- 3' R 5' -ACGGACTGGTCTTCATAGC- 3'	169
GAPDH	U85042	F 5' -CCTTCATTGACCTTCACTACATGGTCTA- 3' R 5' -TGGAAGATGGTGATGGCCTTTCCAT- 3'	127

¹ASH1L: *Bos taurus* absent, small, or homeotic-like Drosophila, mRNA; EHMT2: *Bos taurus* euchromatic histone-lysine N-methyltransferase 2, mRNA; SUV31: *Bos taurus* suppressor of variegation 3-9 homologue 1, mRNA; KDM6B: PREDICTED: *Bos taurus* lysine (K)-Specific Demethylase 6B, mRNA; Poly A: *Bos taurus* poly(A) polymerase (Poly A)- reference gene; GAPDH: *Bos taurus* glyceraldehyde 3-phosphate dehydrogenase - reference gene.

3.2.9. RNA extraction

Total RNA was extracted using RNeasy® Plus Micro Kit (74034, Qiagen®) following the manufacturer recommendations of the fabricant. A copy of the RNA extraction protocol can be found in Appendix A. Briefly, lysing buffer was added to frozen samples to prevent mRNA losses during thawing, and an affinity column was used to remove the genomic DNA; a second affinity membrane is used to retain the RNA while organic solvents remove any remaining lipids and proteins from the sample. Total RNA in each sample was eluted in 15 µL of RNase-free water and used immediately for reverse-transcriptase PCR.

3.2.10. Complementary DNA

After mRNA isolation, each sample was processed with Bio-Rad iScript™ cDNA Synthesis Kit (170-8891, Bio-Rad laboratories) according to the manufacturer recommendations. The iScript reverse transcriptase uses a blend of oligo-di-nucleotides and random hexamer primers to transcribe mRNA into cDNA. A complete copy of the RT-PCR protocol is in Appendix A.

The protocol used in the thermocycler to synthesize complementary DNA consisted of four steps. In the first step, the PCR reaction is heated to 25°C for five minutes to activate the enzyme. In step two, the PCR reaction is heated to 42°C for 30 minutes to allow the activity of the reverse transcriptase polymerase. Step three heated the PCR reaction to 85°C to denature the enzyme and finish the reaction. The last step held the PCR product at 4°C until the reactions were removed from the thermocycler.

3.2.11. Quantitative real-time PCR

Transcriptome levels for histone methyltransferases were quantified using real-time PCR. The protocol used can be found in detail in Appendix A. Briefly, 10 µL of SsoFast™ EvaGreen® Supermix, 2 µL of forward primer, 2 µL of reverse primer, 4 µL of cDNA from samples and 2 µL of dH₂O were used per reaction. SsoFast™ was chosen because of its high efficiency, sensitivity, and strong fluorescent signal.

Thermocycler was programmed to three steps. Step one was set to 95°C for one minute, step two was selected to be 40 cycles of 95°C for 5 seconds followed for 30 seconds at 61°C, and step three was set to perform the melting curve with increments of 0.5°C every ten seconds starting at 61°C and finishing when reaching 95°C.

Q-PCR analysis was performed for two housekeeping genes (Poly A polymerase and GADPH) in each sample. Housekeeping genes were selected based on previous experiences at the lab. The geometrical mean was used as the “reference values for the housekeeping gene” to normalize the QPCR values of the samples for the four genes of interest.

The $2^{-\Delta\Delta CT}$ method was used to normalize the CT value of the samples. This method uses a two-step process to normalize Q-qPCR data in a semi-quantitative analysis. First, data were normalized against the reference value of the housekeeping genes within the same sample. The second normalization compares the difference in threshold values from the first step against the reference value, called the calibrator, which was a known positive control that remains constant for every PCR run of every gene in all experiments.

3.2.12. Statistical Analysis

Values of relative abundance of transcripts were calculated using the “Delta Delta Ct” method. After testing for normality (Kolmogorov-Smirnov test), a one-way ANOVA followed by pair-wise comparisons using Tukey’s test were performed using SigmaStat® Statistical Software (version 3.5). Differences of $p < 0.05$ were considered to be significant.

3.3. Results

3.3.1. Experiment One

Ten cows were synchronized following protocol one and 73 cumulus-oocyte complexes were recovered, yielding an average of 7.3 immature cumulus-oocyte complexes per cow. Morphological selection was used to select 64 cumulus-oocyte complexes. Half of these cumulus-oocyte complexes (n=32) were randomly selected to be matured in vitro. The remaining half was immediately frozen in two oocytes per sample, resulting in 16 samples of

immature cumulus-oocyte complexes. After in vitro maturation was completed on the first set of cumulus-oocyte complexes, these were also frozen randomly in two cumulus-oocyte complexes per sample (16 samples total) and stored at -80°C until further processing.

Synchronization protocol two was used 40 days later in 40 cows, and 19 in vivo matured cumulus-oocyte complexes were recovered, yielding an average of 0.75 cumulus-oocyte complexes per cow. A total of 16 cumulus-oocyte complexes were selected based on the expansion of the cumulus cells and the homogeneity of the ooplasm, and these were frozen one COC per sample (16 samples total).

The analysis of variance for the treatments (immature oocyte, in vitro matured oocytes and in vivo matured oocytes) when the transcriptome from cumulus-oocyte complexes was analyzed showed that there was no difference between any of the treatments for the genes ASH1L, SUV39H1, and KDM6B ($p = 0.882$, $p = 0.510$, $p = 0.068$, respectively). The powers of the performed tests were 0.049, 0.049 and 0.354 respectively.

There was a difference ($p = 0.005$) between the treatments for the EHMT2 gene. There was an increase in the number of transcripts for the EHMT2 gene in in vitro matured oocyte treatment compared with the in vivo matured treatment ($p = 0.007$) and immature treatment ($p = 0.021$). There was no difference between the in vivo and the immature treatments ($p = 0.907$). The power of this test was 0.798. The relative abundance of transcripts for the ASH1L, SUV39H1, KDM6B and EHMT2 for each sample in each treatment in Experiment one can be found in tables 3.2, 3.4, 3.6 and 3.8, respectively.

The tables detailing the ANOVA analysis comparing the immature, in vitro matured, and in vivo matured treatments for the ASH1L, SUV39H1, KDM6B and EHMT2 genes in Experiment one can be found in the tables 3.3, 3.5, 3.7 and 3.9, respectively. The pair-wise comparisons (Tukey's test) between treatments for the EHMT2 gene in Experiment one can be found in table 3.10. Histograms comparing the relative abundance of transcript for ASH1L, SUV39H1, KDM6B and EHMT2 genes can be found in figure 3.3.

Table 3.2 Relative expression for the ASH1L gene in Experiment one

Treatment	Immature COCs	In vitro matured COCs	In vivo matured COCs
Calibrator	1.000	1.000	1.000
Sample 1	0.022	0.115	0.011
Sample 2	0.034	0.543	9.396
Sample 3	0.012	0.034	0.010
Sample 4	0.050	0.074	0.038
Sample 5	0.346	0.037	0.035
Sample 6	0.012	0.352	0.087
Sample 7	0.113	0.060	0.056
Sample 8	0.014	0.014	0.022
Sample 9	0.061	0.036	0.532
Sample 10	0.035	0.051	0.108
Sample 11	0.029	0.193	0.031
Sample 12	0.019	0.248	0.012
Sample 13	0.484	0.749	0.038
Sample 14	0.011	1.041	0.185
Sample 15	8.477	0.370	0.060
Sample 16	0.020	1.824	0.005

Relative expression calculated as $2^{-\Delta\Delta CT}$ with Calibrator =1.

Table 3.3 ANOVA analysis for the ASH1L gene in Experiment one

Treatment	N	Missing	Mean	Std Dev	SEM
Immature COCs	16	0	0.609	2.103	0.526
In vitro matured COCs	16	0	0.359	0.409	0.122
In vivo matured COCs	16	0	0.664	2.332	0.583

Source of Variation	DF	SS	MS	F	P
Between groups	2	0.846	0.423	0.126	0.882
Residual	45	151.484	3.366		
Total	47	152.330			

Table 3.4 Relative expression for the SUV39H1 gene in Experiment one

Treatment	Immature COCs	In vitro matured COCs	In vivo matured COCs
Calibrator	1.000	1.000	1.000
Sample 1	0.681	0.299	0.076
Sample 2	13.164	1.769	0.142
Sample 3	0.325	0.269	0.071
Sample 4	1.325	0.269	0.093
Sample 5	3.524	0.815	0.113
Sample 6	0.471	1.624	0.094
Sample 7	0.248	2.694	0.110
Sample 8	3.101	0.233	0.074
Sample 9	0.049	1.173	6.631
Sample 10	0.030	1.839	0.433
Sample 11	0.058	0.645	0.572
Sample 12	0.096	0.403	0.562
Sample 13	0.451	1.848	1.150
Sample 14	0.028	0.104	0.242
Sample 15	0.424	17.101	0.391
Sample 16	0.588	0.552	0.228

Relative expression calculated as $2^{-\Delta\Delta CT}$ with Calibrator =1.

Table 3.5 ANOVA analysis for the SUV39H1 gene in Experiment one

Treatment	n	Missing	Mean	Std Dev	SEM
Immature COCs	16	0	1.535	3.276	0.819
In vitro matured COCs	16	0	1.977	4.106	1.027
In vivo matured COCs	16	0	0.686	1.611	0.403

Source of Variation	DF	SS	MS	F	P
Between groups	2	13.769	6.884	0.684	0.510
Residual	45	452.830	10.063		
Total	47	466.598			

Table 3.6 Relative expression for the KDM6B gene in Experiment one

Treatment	Immature COCs	In vitro matured COCs	In vivo matured COCs
Calibrator	1.000	1.000	1.000
Sample 1	0.539	0.298	0.103
Sample 2	2.890	12.972	0.481
Sample 3	2.979	3.070	0.144
Sample 4	4.372	0.951	0.077
Sample 5	4.552	1.548	0.144
Sample 6	2.319	3.119	0.231
Sample 7	0.704	1.313	2.755
Sample 8	4.802	0.588	0.302
Sample 9	0.158	0.612	0.482
Sample 10	0.495	1.209	0.767
Sample 11	0.625	2.220	0.138
Sample 12	0.140	0.632	0.152
Sample 13	0.404	441.252	0.198
Sample 14	0.223	2.345	0.243
Sample 15	1.049	129.660	4.032
Sample 16	1.137	1.018	0.068

Relative expression calculated as $2^{-\Delta\Delta CT}$ with Calibrator =1.

Table 3.7 ANOVA analysis for the KDM6B gene in Experiment one

Treatment	n	Missing	Mean	Std Dev	SEM
Immature COCs	16	0	1.712	1.687	0.422
In vitro matured COCs	16	3	1.455	0.947	0.263
In vivo matured COCs	16	0	0.645	1.113	0.278

Source of Variation	DF	SS	MS	F	P
Between groups	2	9.817	4.909	2.861	0.068
Residual	42	72.048	1.715		
Total	44	81.866			

Table 3.8 Relative expression for the EHMT2 gene in Experiment one

Treatment	Immature COCs	In vitro matured COCs	In vivo matured COCs
Calibrator	1.000	1.000	1.000
Sample 1	0.005	0.099	0.018
Sample 2	0.011	1.172	0.018
Sample 3	0.011	0.155	0.004
Sample 4	0.252	0.673	0.003
Sample 5	0.057	1.188	0.007
Sample 6	0.008	1.543	0.012
Sample 7	0.166	1.463	0.014
Sample 8	0.018	0.588	0.002
Sample 9	0.100	2.062	0.485
Sample 10	0.258	0.281	0.225
Sample 11	0.144	0.092	0.129
Sample 12	0.245	0.055	0.111
Sample 13	0.782	0.032	0.163
Sample 14	0.093	0.135	0.068
Sample 15	0.655	4.645	0.110
Sample 16	0.309	0.033	0.058

Relative expression calculated as $2^{-\Delta\Delta CT}$ with Calibrator =1.

Table 3.9 ANOVA analysis for the EHMT2 gene in Experiment one

Treatment	n	Missing	Mean	Std Dev	SEM
Immature COCs	16	0	0.195	0.230	0.057
In vitro matured COCs	16	0	0.888	1.196	0.299
In vivo matured COCs	16	0	0.089	0.125	0.031

Source of Variation	DF	SS	MS	F	P
Between groups	2	6.034	3.017	6.042	0.005
Residual	45	22.473	0.499		
Total	47	28.508			

Table 3.10 Pair-wise comparisons (Tukey's test) for the EHMT2 gene in Experiment one

Comparison	Diff of means	p	q	P	p < 0.050
In vitro vs. in vivo	0.799	3	4.525	0.007	Yes
In vitro vs. immature	0.694	3	3.927	0.021	Yes
Immature vs. in vivo	0.106	3	0.597	0.907	No

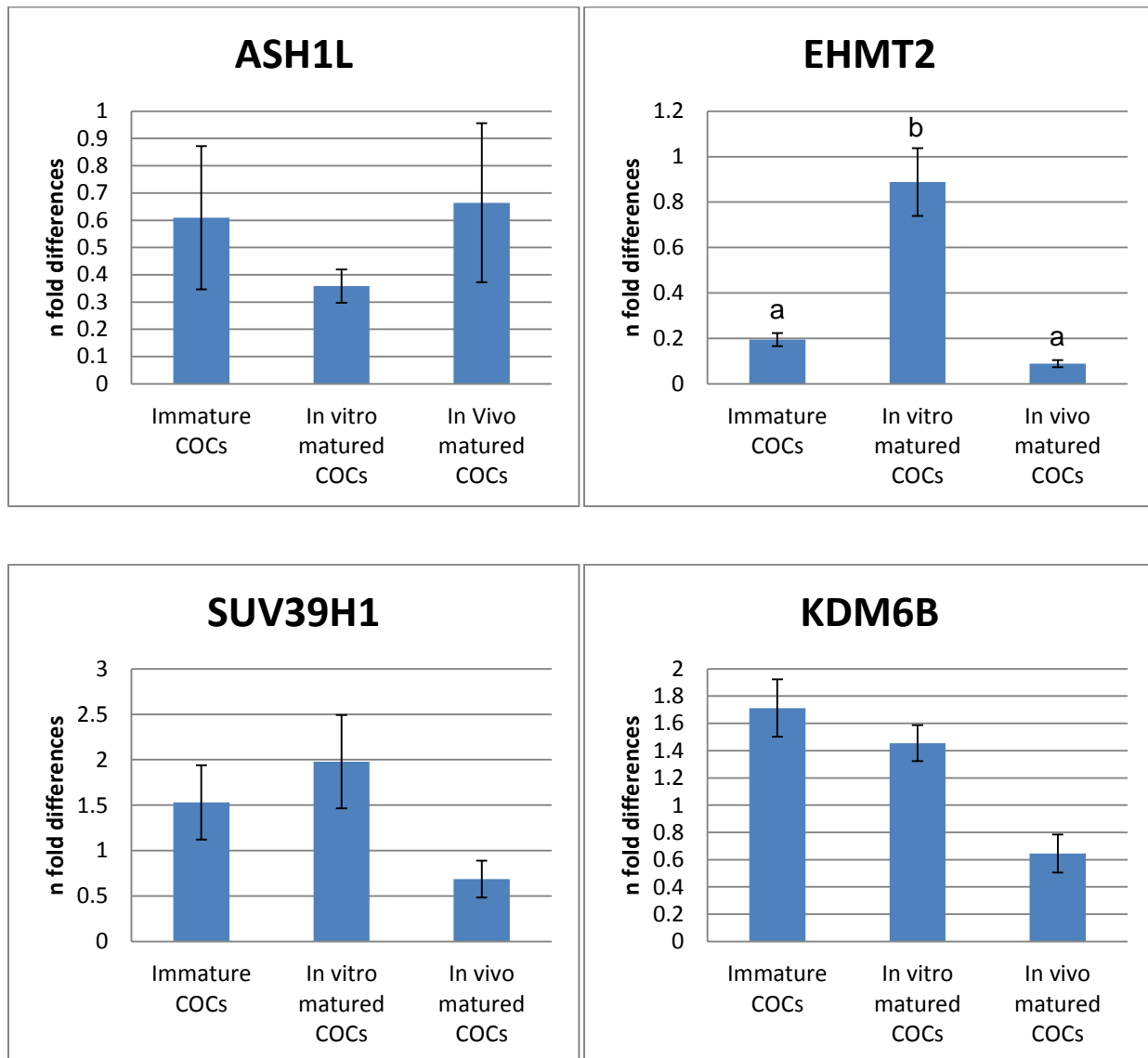


Figure 3.3 Relative expression of histone methyltransferase transcripts in cumulus-oocyte complexes (COCs).

3.3.2. Experiment Two

Ten cows were synchronized following protocol one and 59 cumulus-oocyte complexes were recovered, yielding an average of 5.9 immature cumulus-oocyte complexes per cow. Morphological selection was used to select 28 cumulus-oocyte complexes with enough layers of cumulus cells to allow for a biopsy of the cumulus cells. 14 cumulus-oocyte complexes were randomly selected, the biopsy of the cumulus cells was performed, and the cumulus cells were saved for use in Experiment three. The remaining cumulus cells were removed using a hyaluronidase solution, and the denuded immature oocytes were frozen in a 1.8 mL centrifuge tube (two per sample) and stored at -80°C for further processing. The remaining 14 cumulus-oocyte complexes were matured in vitro and then a biopsy of the cumulus cells was performed. Remaining cumulus cells were once again removed using hyaluronidase and the denuded in vitro matured oocytes were frozen and stored at -80°C for further processing. Cumulus cell biopsies from the in vitro matured oocytes were also saved to be used in Experiment three.

Synchronization protocol two was started 40 days later in 40 cows. 12 in vivo matured oocytes were recovered, yielding 0.3 cumulus-oocyte complexes per cow. Seven oocytes with evidence of cumulus cell expansion were selected and a biopsy of the cumulus cells was performed. Cumulus cells were saved to be used in Experiment three, then the oocytes were denuded using hyaluronidase and frozen using one oocyte per sample (7 samples total).

No difference was found for EHMT2, SUV39H1, KDM6B genes ($p = 0.614$, $p = 0.320$, and $p = 0.178$, respectively). There was a difference ($p < 0.001$) for the ASH1L gene between treatments. There was an increase in gene expression of the ASH1L gene in oocytes in the in vitro matured treatment compared with the in vivo matured treatment ($p < 0.001$), and the immature treatment ($p < 0.001$). There was no difference between the in vivo and the immature treatments ($p = 0.453$). The power of the ANOVA tests performed on the ASH1L, EHMT2, SUV39H1, and KDM6B genes in Experiment two were 1.0, 0.049, 0.077 and 0.175 respectively.

The relative abundance of transcripts for the ASH1L, SUV39H1, KDM6B and EHMT2 for each sample in each treatment in Experiment two can be found in tables 3.11, 3.14, 3.16 and 3.18, respectively. The tables detailing the ANOVA analysis comparing the immature, in vitro matured, and in vivo matured treatments for the ASH1L, SUV39H1, KDM6B and EHMT2 genes in Experiment two can be found in the tables 3.12, 3.15, 3.17 and 3.19, respectively. The pair-wise comparisons (Tukey's test) between treatments for the EHMT2 gene in Experiment one can be found in table 3.13. Histograms comparing the relative abundance of transcript for ASH1L, SUV39H1, KDM6B and EHMT2 genes can be found in figure 3.4.

Table 3.11 Relative expression for the ASH1L gene in Experiment two

Treatment	Immature oocytes	In vitro matured oocytes	In vivo matured oocytes
Calibrator	1.000	1.000	1.000
Sample 1	0.005	0.997	0.008
Sample 2	0.118	0.922	0.002
Sample 3	0.005	0.997	0.009
Sample 4	0.004	0.997	0.002
Sample 5	0.005	0.996	0.003
Sample 6	0.003	0.998	0.019
Sample 7	0.728	0.604	0.011

Relative expression calculated as $2^{-\Delta\Delta CT}$ with Calibrator =1.

Table 3.12 ANOVA analysis for the ASH1L gene in Experiment two

Treatment	n	Missing	Mean	Std Dev	SEM
Immature oocytes	7	0	0.124	0.270	0.102
In vitro matured oocytes	7	0	0.930	0.147	0.055
In vivo matured oocytes	7	0	0.008	0.006	0.002

Source of Variation	DF	SS	MS	F	P
Between groups	2	3.533	1.766	56.289	<0.001
Residual	18	0.565	0.031		
Total	20	4.097			

Table 3.13 Pair-wise comparisons (Tukey's test) for the ASH1L gene in Experiment two

Comparison	Diff of means	p	q	P	p < 0.050
In vitro vs. in vivo	0.922	3	13.775	<0.001	Yes
In vitro vs. immature	0.806	3	12.040	<0.001	Yes
Immature vs. in vivo	0.116	3	1.735	0.453	No

Table 3.14 Relative expression for the EHMT2 gene in Experiment two

Treatment	Immature oocytes	In vitro matured oocytes	In vivo matured oocytes
Calibrator	1.000	1.000	1.000
Sample 1	0.050	0.029	0.012
Sample 2	0.098	0.040	0.053
Sample 3	0.035	0.024	0.019
Sample 4	0.071	0.049	0.017
Sample 5	0.065	0.250	0.051
Sample 6	0.118	0.181	0.293
Sample 7	0.018	0.210	0.231

Relative expression calculated as $2^{-\Delta\Delta CT}$ with Calibrator =1.

Table 3.15 ANOVA analysis for the EHMT2 gene in Experiment two

Treatment	n	Missing	Mean	Std Dev	SEM
Immature oocytes	7	0	0.065	0.035	0.013
In vitro matured oocytes	7	0	0.112	0.097	0.037
In vivo matured oocytes	7	0	0.097	0.116	0.044

Source of Variation	DF	SS	MS	F	P
Between groups	2	0.008	0.004	0.502	0.614
Residual	18	0.144	0.008		
Total	20	0.152			

Table 3.16 Relative expression for the SUV39H1 gene in Experiment two

Treatment	Immature oocytes	In vitro matured oocytes	In vivo matured oocytes
Sample 1	0.135	0.035	0.055
Sample 2	0.065	0.032	0.074
Sample 3	0.034	0.054	0.139
Sample 4	0.097	0.064	0.025
Sample 5	0.172	1.693	0.105
Sample 6	0.068	0.604	0.127
Sample 7	0.031	0.228	0.635

Calibrator = positive control used to normalize QPCR values between samples.

Table 3.17 ANOVA analysis for the SUV39H1 gene in Experiment two

Treatment	n	Missing	Mean	Std Dev	SEM
Immature oocytes	7	0	0.086	0.052	0.020
In vitro matured oocytes	7	0	0.337	0.612	0.231
In vivo matured oocytes	7	0	0.166	0.211	0.080
Source of Variation	DF	SS	MS	F	P
Between groups	2	0.341	0.170	1.215	0.320
Residual	18	2.527	0.140		
Total	20	2.868			

Table 3.18 Relative expression for the KDM6B gene in Experiment two

Treatment	Immature oocytes	In vitro matured oocytes	In vivo matured oocytes
Sample 1	0.008	0.008	0.021
Sample 2	0.013	0.009	0.004
Sample 3	0.019	0.004	0.001
Sample 4	0.012	0.012	0.016
Sample 5	0.011	0.086	-----
Sample 6	0.015	0.023	0.015
Sample 7	0.005	0.211	0.005

Relative expression calculated as $2^{-\Delta\Delta CT}$ with Calibrator =1.

Table 3.19 ANOVA analysis for the KDM6B gene in Experiment two

Treatment	n	Missing	Mean	Std Dev	SEM
Immature oocytes	7	0	0.012	0.005	0.002
In vitro matured oocytes	7	0	0.051	0.076	0.029
In vivo matured oocytes	7	0	0.009	0.008	0.003

Source of Variation	DF	SS	MS	F	P
Between groups	2	13.769	6.884	0.684	0.510
Residual	45	452.830	10.063		
Total	47	466.598			

3.3.3. Experiment Three

Ten cows were synchronized following protocol one and 59 cumulus-oocyte complexes were recovered, yielding an average of 5.9 immature cumulus-oocyte complexes per cow. Morphological selection was used to select 28 cumulus-oocyte complexes with enough layers of cumulus cells to allow for a biopsy of the cumulus cells. 14 cumulus-oocyte complexes were randomly selected and a biopsy of the cumulus cells was performed. Cumulus cells from two oocytes were sampled together and stored at -80°C for further processing. For the remaining 14 cumulus-oocyte complexes, biopsies of cumulus cells were performed after in vitro maturation and 7 samples (two biopsies per sample) were stored at -80°C.

Synchronization protocol two was used 40 days later in 40 cows, and 12 in vivo matured oocytes were recovered yielding 0.3 cumulus-oocyte complexes per cow. Seven oocytes with evidence of cumulus cell expansion were selected and a biopsy of the cumulus cells was performed. 7 samples (1 biopsy per sample) were stored at -80°C.

The analysis of variance for the three treatments (immature, in vitro matured, and in vivo matured) when transcriptome of denuded oocytes was analyzed showed that there was no difference between any of the treatments for the genes ASH1L, EHMT2, SUV39H1 and KDM6B

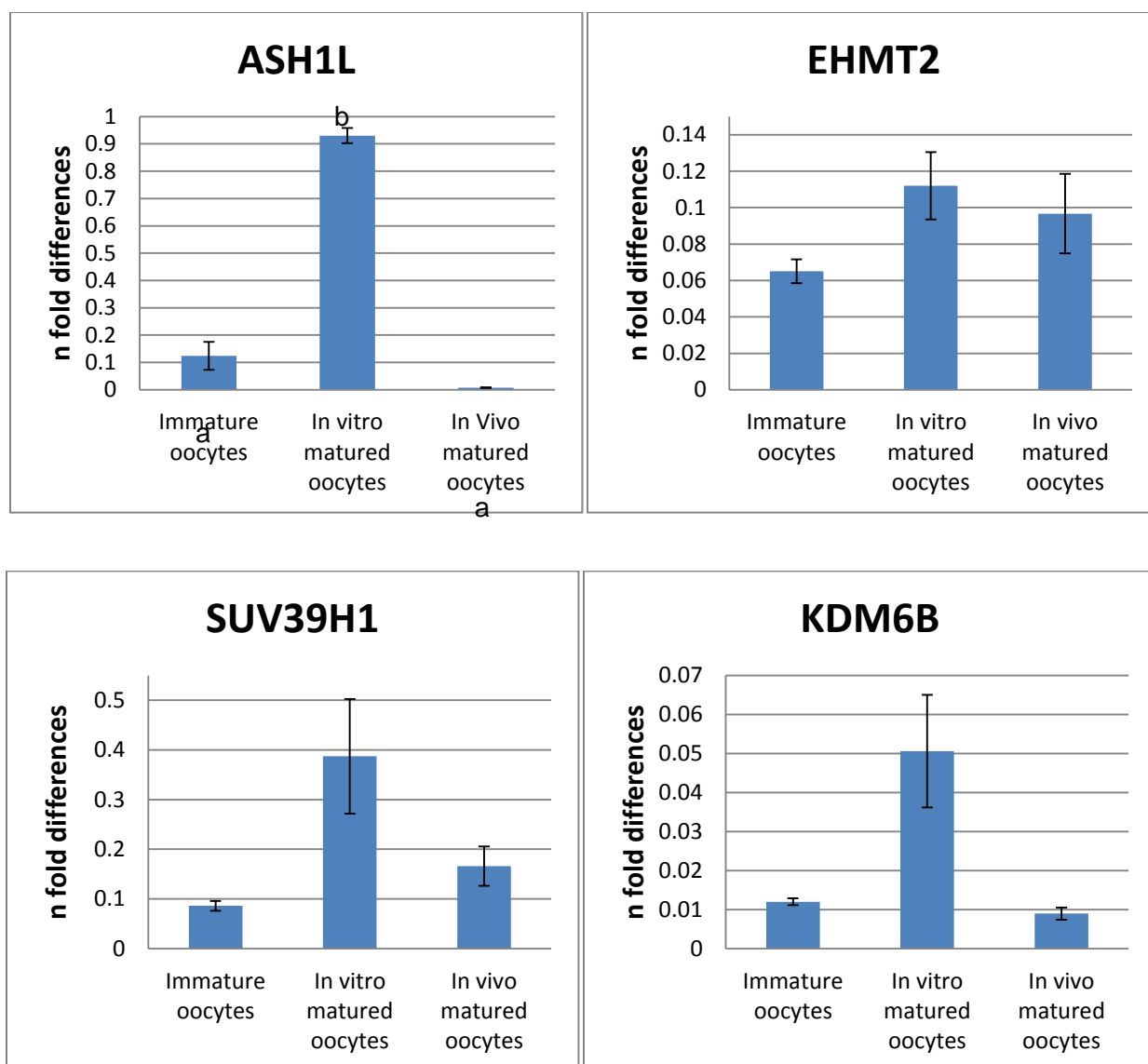


Figure 3.4 Relative expression of histone methyltransferase transcripts in oocytes.

($p = 0.285$, $p = 0.093$, $p = 0.5$, and $p = 0.086$, respectively). The powers of the tests performed were 0.095, 0.304, 0.049, and 0.319 respectively.

It is important to mention that, even though no statistical significant differences were found in this experiment, two of the genes analyzed, EHMT2 ($p = 0.093$) and KDM6B ($p = 0.086$), had p values that were not significant at the 0.05 level, but would have been significant at the 0.1 level. Also, the power of the ANOVA tests performed is significantly low, which is due to the small sample size used during these experiments. The recovery of in vivo matured

oocytes via TUGA is particularly challenging in the cow and limits the number of samples included in the experiments.

The relative abundance of transcripts for the ASH1L, SUV39H1, KDM6B and EHMT2 for each sample in each treatment in Experiment three can be found in tables 3.20, 3.22, 3.24 and 3.26, respectively. The tables detailing the ANOVA analysis comparing the immature, in vitro matured, and in vivo matured treatments for the ASH1L, SUV39H1, KDM6B and EHMT2 genes in Experiment three can be found in the tables 3.21, 3.23, 3.25 and 3.27, respectively. Histograms comparing the relative abundance of transcript for ASH1L, SUV39H1, KDM6B and EHMT2 genes can be found in figure 3.5.

Table 3.20 Relative expression for the ASH1L gene in Experiment three

Treatment	Immature cumulus cells	In vitro matured cumulus cells	In vivo matured cumulus cells
Calibrator	1.000	1.000	1.000
Sample 1	0.004	0.005	0.007
Sample 2	0.001	0.052	0.003
Sample 3	0.005	0.007	0.004
Sample 4	0.002	0.008	0.008
Sample 5	0.004	0.006	0.002
Sample 6	0.007	0.448	0.001
Sample 7	0.005	0.007	0.002

Relative expression calculated as $2^{-\Delta\Delta CT}$ with Calibrator =1.

Table 3.21 ANOVA analysis for the ASH1L gene in Experiment three

Treatment	n	Missing	Mean	Std Dev	SEM
Immature cumulus cells	7	0	0.004	0.002	0.001
In vitro matured cumulus cells	7	0	0.076	0.165	0.062
In vivo matured cumulus cells	7	0	0.004	0.002	0.001
Source of Variation	DF	SS	MS	F	P
Between groups	2	0.024	0.012	1.348	0.285
Residual	45	0.163	0.009		
Total	47	0.187			

Table 3.22 Relative expression for the EHMT2 gene in Experiment three

Treatment	Immature cumulus cells	In vitro matured cumulus cells	In vivo matured cumulus cells
Sample 1	0.013	0.040	0.015
Sample 2	0.013	0.009	0.010
Sample 3	0.014	0.018	0.016
Sample 4	0.014	0.024	0.009
Sample 5	0.018	0.018	0.007
Sample 6	0.010	0.141	0.001
Sample 7	0.028	0.041	0.014

Relative expression calculated as $2^{-\Delta\Delta CT}$ with Calibrator =1.

Table 3.23 ANOVA analysis for the EHMT2 gene in Experiment three

Treatment	n	Missing	Mean	Std Dev	SEM
Immature cumulus cells	7	0	0.016	0.006	0.002
In vitro matured cumulus cells	7	0	0.041	0.046	0.017
In vivo matured cumulus cells	7	0	0.010	0.005	0.002

Source of Variation	DF	SS	MS	F	P
Between groups	2	0.004	0.002	2.722	0.093
Residual	45	0.013	0.001		
Total	47	0.017			

Table 3.24 Relative expression for the SUV39H1 gene in Experiment three

Treatment	Immature cumulus Cells	In vitro matured cumulus Cells	In vivo matured cumulus cells
Calibrator	1.000	1.000	1.000
Sample 1	0.015	0.003	0.006
Sample 2	0.010	0.010	0.002
Sample 3	0.007	0.019	0.010
Sample 4	0.011	0.008	0.005
Sample 5	0.013	0.026	0.006
Sample 6	0.229	0.269	0.001
Sample 7	0.017	0.013	0.013

Relative expression calculated as $2^{-\Delta\Delta CT}$ with Calibrator =1.

Table 3.25 ANOVA analysis for the SUV39H1 gene in Experiment three

Treatment	n	Missing	Mean	Std Dev	SEM
Immature cumulus cells	7	0	0.043	0.082	0.031
In vitro matured cumulus cells	7	0	0.050	0.097	0.037
In vivo matured cumulus cells	7	0	0.006	0.004	0.002
Source of Variation	DF	SS	MS	F	P
Between groups	2	0.008	0.004	0.720	0.500
Residual	45	0.097	0.005		
Total	47	0.104			

Table 3.26 Relative expression for the KDM6B gene in Experiment three

Treatment	Immature cumulus cells	In vitro matured cumulus cells	In vivo matured cumulus cells
Sample 1	0.006	0.013	0.003
Sample 2	0.001	0.005	0.005
Sample 3	0.006	0.007	0.001
Sample 4	0.002	0.013	0.001
Sample 5	0.003	0.011	0.003
Sample 6	0.005	0.070	0.001
Sample 7	0.002	0.005	0.000

Relative expression calculated as $2^{-\Delta\Delta CT}$ with Calibrator =1.

Table 3.27 ANOVA analysis for the KDM6B gene in Experiment three

Treatment	n	Missing	Mean	Std Dev	SEM
Immature cumulus cells	7	0	0.003	0.002	0.001
In vitro matured cumulus cells	7	0	0.018	0.023	0.009
In vivo matured cumulus cells	7	0	0.002	0.002	0.001
Source of Variation	DF	SS	MS	F	P
Between groups	2	0.001	0.001	2.815	0.086
Residual	45	0.003	0.000183		
Total	47	0.004			

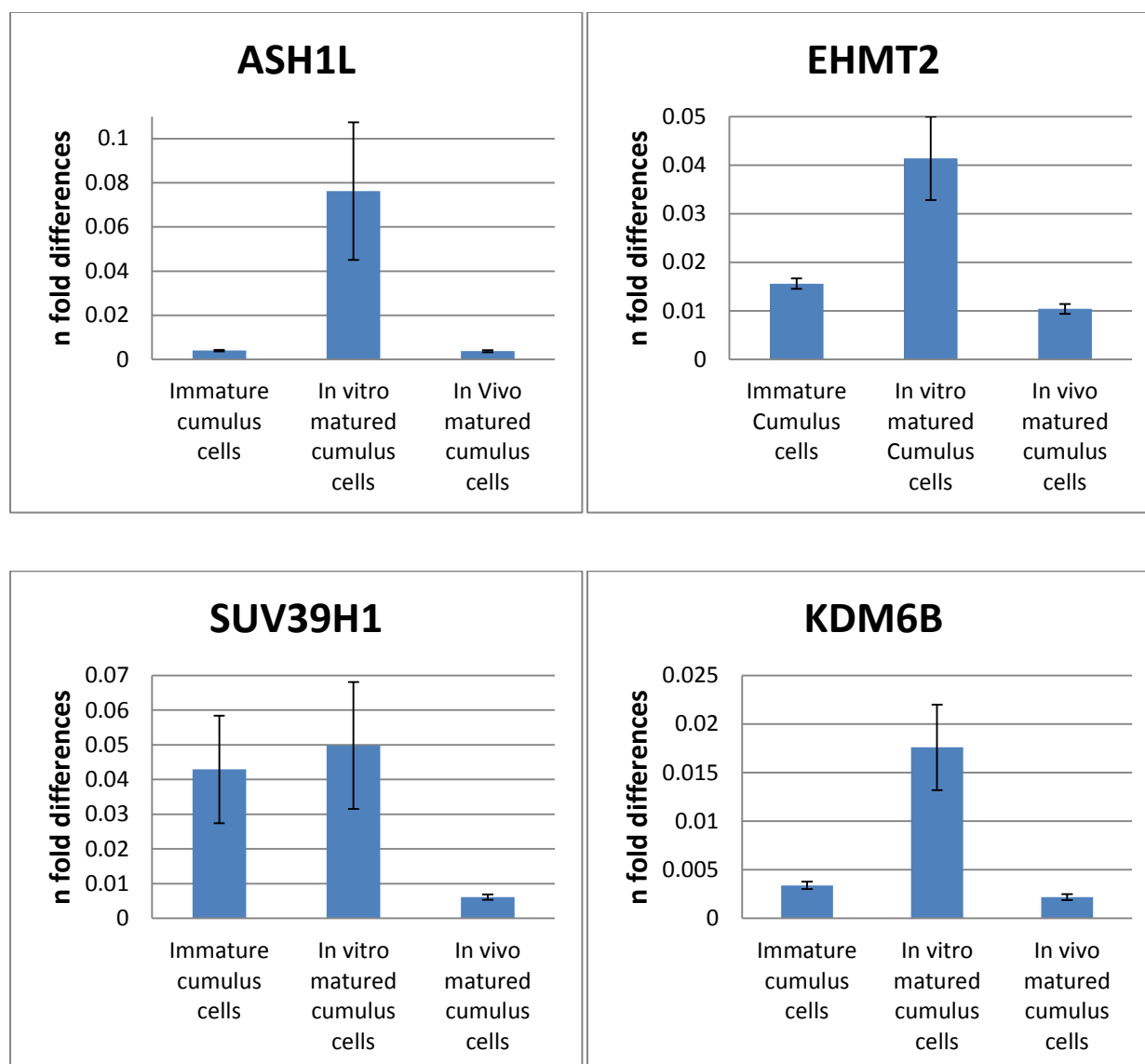


Figure 3.5 Relative expression of histone methyltransferase transcripts in cumulus cells.

3.4. Discussion

The objective of the experiments described in this chapter was to use the difference in developmental competence between in vivo matured oocytes and in vitro matured oocytes to study the level of relative abundance of transcripts for selected histone methyltransferase enzymes in cumulus-oocyte complexes, oocytes and cumulus cells. Transcriptome analyses are particularly useful in the characterization of the in vitro vs. in vivo model because there seems not to be any major differences in nuclear maturation or fertilization rates between these two

embryo production systems. But the differences between them become evident in the developmental potential of the oocytes.

The developmental potential of in vivo matured oocytes has long been known to be superior to the developmental potential of in vitro matured oocytes (Leibfried-Rutledge et al., 1987). When comparing oocytes matured in vivo versus oocytes matured in vitro, even with the constant improvement in technology, culture systems cannot provide the same environment as does the maternal reproductive system. This situation has been extensively documents in cattle (Labrecque and Sirard, 2014). Experimental results show in vivo matured oocytes as having significantly higher blastocyst rates (57.65%) compared with in vitro matured oocytes (40%) (Humblot et al., 2005). The epigenetic landscape in bovine embryos has been correlated with their developmental potential (Santos et al., 2003), and delayed and incomplete reprogramming in bovine oocytes has been reported in bovine embryos produced in vitro via nuclear transfer (Bourc'his et al., 2001).

Results of the experiments showed that there is no difference in the relative abundance of transcripts coding for histone methyltransferases ASH1L, KDM6B and SUV39H1 in cumulus-oocyte complexes. There was a difference in the accumulation of transcripts for histone methyltransferase EHMT2 between cumulus-oocytes complexes from different maturation systems. Transcript levels in the in vitro matured treatment were greater than the immature treatment and the in vivo matured treatment. No difference was found between the immature and the in vivo matured treatments when cumulus-oocyte complexes were evaluated.

When oocytes were removed from their cumulus cells before transcriptome analysis the results changed. No differences were found for transcripts of the EHMT2, SUV39H1 and KDM6B genes. Significant differences were found for transcripts of the gene ASH1L. Pair-wise comparisons among the treatments again showed higher levels of transcripts in the in vitro treatment compared to the immature and in vivo matured treatments. No difference was

detected between the immature and the in vivo matured treatments when denuded oocyte were studied.

The analysis of the cumulus cells showed no differences in the accumulation of transcripts for any of the four genes of interest (ASH1L, EHMT2, SUV39H1 and KDM6B) among treatments when the criteria for rejection was set at the 0.05 level. However, higher accumulations of transcripts in the in vitro treatment for the genes EHMT2 and KDM6B could have been found if the criteria were changed to the 0.1 level. Furthermore, analysis of the histograms suggest possible differences between treatments in transcripts of the SUV39H1 and KDM6B genes in oocytes and KDM6B in cumulus cells that did not show up during the statistical analysis. This failure to detect differences between treatments is most likely due to the lack of power resulting from the limited sample size.

The first conclusion obtained from these results is that there are no differences between the immature and the in vivo matured treatments. Results of experiments one, two and three showed that there are no differences in the relative abundance of transcripts for any of the four histone methyltransferases included in this study (ASH1L, EHMT2, SUV39H1 and KDM6B) between immature cumulus-oocyte complexes, oocytes or cumulus cells and their in vivo matured counterparts.

It is known that the transcription of mRNA coding for histone methyltransferases must occur during oocyte maturation, since epigenetic marks such as the tri-methylation of lysine 9 in histone 3 are not present in oocytes from primordial follicles (Fair et al., 1997) and no transcript accumulation for SUV39H1 was found in either primordial or primary follicles in cattle. Follicles start to accumulate transcripts for this gene at the small secondary follicle stage (40-60 μm) and the level of transcript accumulation remained constant until the large secondary follicle stage (65-85 μm). It was not until the antral follicle stage that accumulation of transcripts was significantly higher than in more immature stages (Bessa et al., 2013). Transcript levels for histone methyltransferases and histone methylation levels have been reported to remain at

constant levels in secondary follicles, mature oocytes, and early embryos in murine, mice and humans (Sarmiento et al., 2004; Kageyama et al., 2007; Qiao et al., 2010).

Immature oocytes are collected from antral follicles sized 3 mm or larger. Results from these experiments support the idea that, by this point in the development of the oocyte, the levels of transcripts coding for histone methyltransferases has already reached the level that will be maintained until ovulation. This observation coincides with reports made for Oliveri et al. in 2003 describing that no differences in the accumulation of transcripts were found in the levels of mRNA of SUV39H1, using both micro-array and QPCR technologies, between germinal vesicle and metaphase II oocytes in mice.

Results from the present experiments, however, contradict another report suggesting that the accumulation of transcripts of EHMT2 and SUV39H1 in mice oocytes was evident during oocyte maturation. Immature oocytes showed basal levels of transcripts for both transcripts, whereas matured oocytes had between 3.5 and 5 times more transcripts for SUV39H1 and between 4.5 and 10 times more transcripts for EHMT2 (Kageyama et al., 2007).

Unfortunately, the model used for most experiments comparing difference in transcriptome between immature and in vivo matured oocytes use mice as the model, making it difficult to extrapolate and compare results. Differences among species have been postulated, although no experiment has yet compared differences in oocyte transcriptome among species. Nevertheless, histone proteins and the mechanism that regulate them are among the most conserved traits throughout evolution.

Species is not the only element makes the results from transcriptome analysis during oocyte maturation difficult to interpret. The experimental designs, the housekeeping genes of reference selected, and the starting material are major sources of variation between experiments.

The selection of the reference housekeeping genes has profound repercussions in transcriptome analysis. Due to the variable efficiency of the RNA extraction and PCR

amplification techniques, the values of the real time PCR performed on the samples for the genes of interest must to be normalized using the value of the real time PCR performed on the samples for the housekeeping genes. This approach assumes that the abundance of transcripts of the selected housekeeping genes remains constant during the oocyte maturation process. Different studies have utilized different housekeeping genes, but there is a lack of information in regard to the transcriptional profile of the genes used frequently as reference genes in transcriptome analysis during maturation of mammalian oocytes.

Also, the use of both oocytes and cumulus-oocyte complexes during transcriptome analysis generates differences among experiments. Bessa et al. in 2013 attributed the difference in the results to the methodologies followed, and elaborated that in their experiments oocyte measurements are more precise because they dissected the oocytes, whereas other experiments did not discriminate about the presence of cumulus cells.

The reason why cumulus cells were not taken into account in most experimental designs, I propose, was the assumption that the oocyte was solely responsible for transcriptome variations, making the transcriptome of the cumulus cells irrelevant. However, there is evidence now supporting the hypothesis of mRNA transfer from the cumulus cells into the bovine oocyte. Trans-zonal projections of the cumulus cells protrude into the zona pellucida and reach the oocyte membrane, and RNA-containing particles have been found in these projections. The projections in the bovine cumulus-oocyte complex develop at the same time as the oocyte undergoes cytoplasmic maturation, and the size of the projections (2 μm) would likely allow the transfer of larger molecules such as mRNA. Moreover, there is evidence that newly transcribed mRNA is sent into the projections, supporting the idea that there is an efflux of specific mRNAs from the cumulus cells into the transcriptionally-inactive bovine oocyte around the time of the germinal vesicle breakdown (Macaulay et al., 2014).

These experiments may also provide the most reliable answer to the question about the accumulation of transcripts in the oocyte during the maturation period in bovine oocytes. They

showed that transcripts were accumulated during oocyte maturation, but only when the cumulus cells were present, suggesting that the cumulus cells act as an exogenous source of transcripts for the oocyte (Macaulay et al., 2014). This supports the approach taken during the experiments described in this chapter, analyzing oocytes, cumulus cells and cumulus-oocyte complexes separately.

The most important findings during these experiments are the differences in transcript accumulation between in vitro and the other two treatments. In vitro matured cumulus-oocyte complexes had higher levels of transcripts coding for EHMT2 compared with the immature and in vivo matured treatments, and in vitro matured oocytes had higher levels of transcripts coding for ASH1L compared with the immature and in vivo matured treatments. Additionally, the in vitro matured cumulus cells had higher levels of transcripts coding for EHMT2 and KDM6B compared with the immature and in vivo matured treatments that were not significant at the $p=0.05$ level, but would have been significant at the $p = 0.1$ level ($p = 0.093$ and $p = 0.086$, respectively).

The results of the experiments described in this document contradict the results from other studies that suggest that there is a decrease in the levels of methyltransferases during in vitro oocyte maturation. However, the differences in the experimental designs make a plain comparison of the results difficult.

It has been reported that there was no difference in the levels of relative abundance of transcripts for EHMT2 across different stages of bovine oocyte maturation in cattle (Racedo et al., 2009), but there was a decrease in the transcript abundance of SUV39H1 at the metaphase II stage. This results contradict the increase in transcripts of the EHMT2 gene found in cumulus-oocyte complexes and cumulus cells ($p=0.021$ and 0.093 respectively) and no difference in the levels of SUV39H1 transcripts ($p=0.882$). However the mentioned experiment reports that the relative abundance of transcripts for EHMT2 and SUV39H1 was significantly higher in bovine oocytes isolated from larger follicles (2-8 mm in size) compared with oocytes from smaller follicles (<2 mm in size) when the average relative abundance at four stages of development

(germinal vesicle, germinal vesicle breakdown, metaphase I, and metaphase II) were analyzed together, and concludes that in cattle the relative abundance of HMTs EHMT2 and SUV39H1 is affected by follicular size, with bigger follicles accumulating a larger number of transcripts (Racedo et al., 2009). Oocytes recovered from follicles smaller than 2 mm are highly immature, and perform poorly when cultured and fertilized in vitro. Comparing them against more competent oocytes (collected from larger follicles) might not be commensurable.

Another study reporting a decrease in the levels of relative abundance of transcripts for the EHMT2 and SUV39H1 during oocyte maturation used the comparison between immature oocytes, in vitro matured oocytes, parthenogenetically activated oocytes and embryos produced via somatic-cell nuclear transfer as the experimental model (Nowak-Imialek et al., 2008) and the focus was on the methylation level induced in the embryo by the type of somatic cell used during the cloning process.

Results from the present set of experiments suggest a loss of the regulatory mechanisms of transcription of histone methyltransferases when cumulus-oocyte complexes are cultured in vitro. There is a general up regulation of transcripts coding for histone methyltransferases in the in vitro culture COCs. The miss-regulation of transcripts associated with the developmental potential of in vitro cultured embryos has been reported previously (Niemann and Wrenzycki, 2000). In this case, the major changes in gene expression were attributed to the use of bovine serum in the maturation and culture medium. No bovine serum was used in the fertilization and culture media of the present experiment, but fetal bovine serum was used in the maturation medium.

A direct association between changes in the expression of genes regulating epigenetic modifications, such as DNA methylation and histone modifications, and developmental potential of bovine embryos has been made (Wrenzycki et al., 2005). There has also been changes reported in the accumulation of transcripts which are important in the developmental potential of embryos produced via somatic cell nuclear transfer (Sawai et al., 2005). These reports support

the results of the present set of experiments, postulating that there are changes in the accumulation of transcripts for histone methyltransferases induced during the in vitro culture of the oocytes.

Transcriptome analysis provide further insight of the oocyte maturation process, but their interpretation is limited because suboptimal quality oocytes, uncontrollable variables in the in vitro culture system, and the lack of support from proteomic analysis make it difficult to associate the changes in mRNA levels with the change in the phenotype observed (Labrecque and Sirard, 2014). Therefore, the biological interpretation of the analysis of transcriptome in this chapter will be evaluated in conjunction with the results of Experiments four and five, where the phenotype of the transcripts included in the study can be evaluated.

CHAPTER IV

RELATIVE ABUNDANCE OF HISTONE 3 LYSINE 9 TRI-METHYLATED IN EARLY BOVINE EMBRYOS PRODUCED IN VITRO USING IN VIVO AND IN VITRO MATURED OOCYTES

4.1 Introduction

By the time of ovulation, the mammalian oocyte must have acquired the elements that will provide it with the developmental potential to undergo fertilization, begin cleaving, develop into an embryo capable of inducing a pregnancy in the mother and deliver a healthy offspring. In the in vitro embryo production system, ovulation is replaced by the moving of in vitro matured oocytes from the maturation dish into the fertilization dish, but the expectations about the developmental potential of in vitro matured oocytes remain the same as for their in vivo matured counterparts.

Regardless of the intense efforts to develop in vitro production systems that accurately mimic the in vivo conditions for embryo development, the developmental competence of in vitro produced embryos remains significantly lower than the developmental potential of in vivo produced embryos. Multiple factors have been reported as responsible, at least partially, of the decreased developmental potential of in vitro produced embryos. The accumulation of transcripts in the maturing oocyte is one of factors with the potential to compromise the developmental potential of the oocyte.

In the previous chapter, evidence suggesting a miss-regulation in the accumulation of transcripts coding for proteins that regulate chromatin structure in in vitro matured oocytes was presented. In this chapter, the effect of this miss-regulation was evaluated. The levels of tri-methylation of lysine 9 in histone 3 incorporated to chromatin was measured using immunocytochemistry. Comparisons between in vitro matured oocytes and in vivo matured oocytes were made, as well as comparisons between embryos produced in vitro from both in vivo matured oocytes and in vitro matured oocytes.

4.2 Materials and Methods

4.2.1. Animal husbandry

Experimental procedures in this study were approved by the Louisiana State University Animal Care and Use Committee in the protocol number A2012-16 signed on July 23rd 2012 and were conducted at the Louisiana State University Agricultural Center Reproductive Biology Laboratory (RBC) - Embryo Biotechnology Laboratory (EBL) (Saint Gabriel, Louisiana) from August 2012 through July 2013.

Non lactating crossbred (Angus x Red Angus x Brangus) cows (n=40) aged 4 to 7 years, maintained as the experimental physiology herd at the LSU RBC, were used throughout the course of this study. The cows displayed regular estrous cycles, were all in moderate to good body condition, and were maintained on pastures planted with Bermudagrass, Rye grass and supplemented with hay during the winter time.

4.2.2. Experimental design

Two experiments were conducted to investigate the relative abundance of tri-methylated lysine 9 in histone 3 in matured oocytes and early embryos.

Experiment four: Immunocytochemistry was used to study the differences in the levels of the tri-methylated state of lysine 9 in histone 3 between in vitro matured oocytes and in vivo matured oocytes. Experiment five: Immunocytochemistry was used to study the differences in the levels of the tri-methylated state of lysine 9 in histone 3 between pre-genomic activation embryos fertilized in vitro after in vivo or in vitro maturation.

The experimental unit in both experiments was defined as the oocyte; the sampling unit in Experiment four was defined as the oocyte, whereas the experimental unit in Experiment five was defined as the blastomere.

4.2.3 Synchronization for collection of cumulus-oocyte complexes

Two synchronization protocols were used for these experiments. The first was used to collect immature oocytes (germinal vesicle stage) and the second was used to collect in vivo

matured oocytes (metaphase II stage). These synchronization protocols are based on those described by Rizos (Rizos et al., 2002) and used by others to collect both in vitro matured and in vivo matured cumulus-oocyte complexes for transcriptome analysis (Tesfaye et al., 2009; Assidi et al., 2013; Spencer et al., 2013).

Synchronization protocol one was used to retrieve immature oocytes for use in experimental treatments one and two. An outline of this protocol is presented in Figure 3.1. A controlled internal release device with progesterone (Easi-Breed™ CIDR cattle insert®, Zoetis laboratories) was placed intravaginally for ten days and prostaglandin $F_{2\alpha}$ (PGF_{2 α} , 25 mg of dinoprost tromethamine, Lutalyse®, single dose, intramuscular) was given the day of CIDR removal. Cows were observed for signs of estrous behavior 48 to 72 hours after the administration of PGF_{2 α} , and cows displaying standing estrus were identified and recorded. Cows that failed to display estrus during the observation period were also identified, but they were not removed from the experimental group. Eight days after starting estrus, growth of all dominant follicles was impaired using an ultrasound-guided needle. Then, four days after dominant follicle removal (DFR), transvaginal ultrasound-guided aspiration of follicles was performed.

Synchronization protocol two was similar to protocol one; an outline of the protocol is presented in Figure 3.2. A CIDR in combination with PGF_{2 α} was used to synchronize estrus. Dominant follicle removal was performed eight days after standing estrus and PGF_{2 α} was given four days after DFR. Cows displaying estrous behavior were given PGF_{2 α} and Gonadotropin releasing hormone (GnRH, 100 µg of Gonadorelin hydrochloride, Factrel®, single dose) intramuscular 48 hours later. Transvaginal ultrasound-guided aspiration of oocytes was performed 12 hours after the administration of GnRH.

Protocol one was used in ten cows, whereas protocol two was used in 40 animals. There was an interval of 40 days between the end of protocol one and the beginning of protocol two.

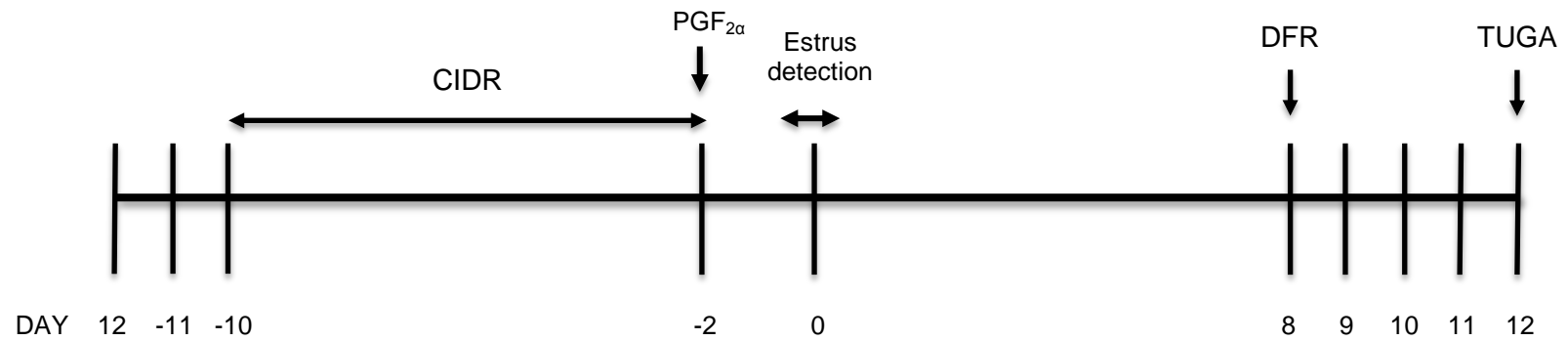


Figure 4.1. Synchronization protocol for transvaginal ultrasound-guided aspiration of immature oocytes. CIDR is controlled internal drug release device; PGF_{2α} is prostaglandin F_{2α}; DFR is dominant follicle removal; TUGA is transvaginal ultrasound-guided aspiration.

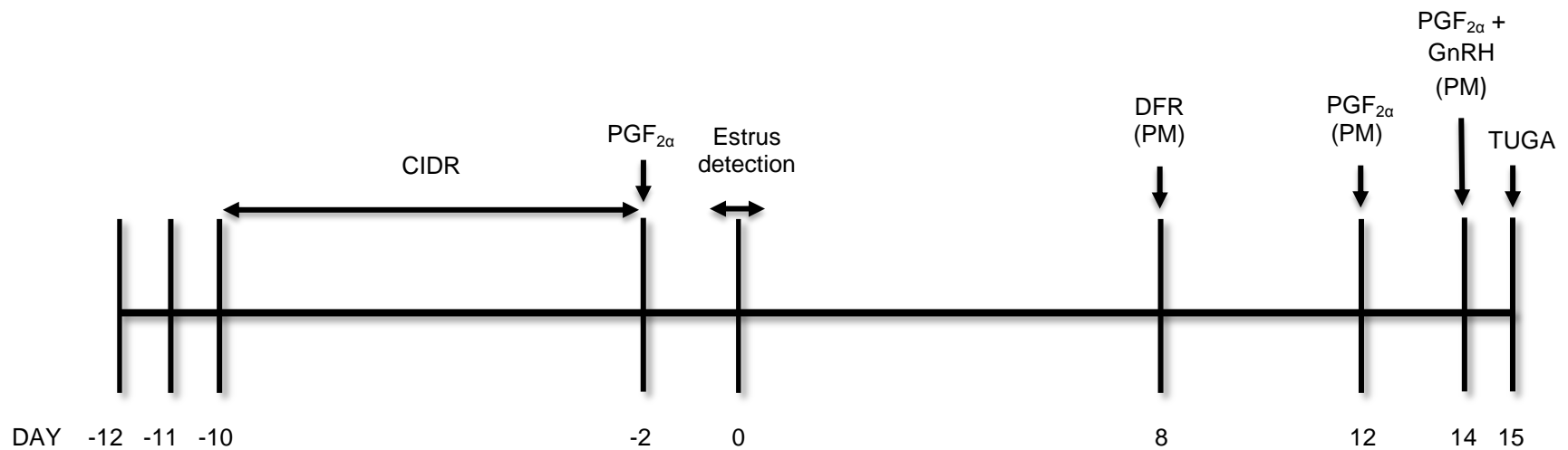


Figure 4.2. Synchronization protocol for transvaginal ultrasound-guided aspiration of in vivo matured oocytes. CIDR is controlled internal drug release device; $\text{PGF}_{2\alpha}$ is Prostaglandin $\text{F}_{2\alpha}$; DFR is dominant follicle removal; GnRH is Gonadotropin Releasing Hormone, TUGA is transvaginal ultrasound-guided aspiration. PM indicates that treatments were applied in the afternoon.

Cows used in protocol one were selected randomly from the physiology herd, and all 40 cows from the physiology herd were used for protocol two.

4.2.4. Collection of cumulus-oocyte complexes

Oocytes were collected by transvaginal ultrasound guided aspiration (TUGA) of antral follicles. Equipment and materials used for TUGA are presented in Appendix C. Cows were briefly restrained in a holding chute and given an epidural injection of 6 mL of lidocaine 2% (lidocaine hydrochloride, VETone[®] pharmaceuticals). A 7.5 MHz ultrasound transducer was used trans-vaginally as the ovaries were manipulated trans-rectally. The image provided by the ultrasound was used by the technician to identify the follicles and direct an 18g X 8.89 cm needle to aspirate the follicular contents. The needle was connected by tubing to a bovine embryo filter with a 75 micron membrane (EmCom[™] Filter). A vacuum pump was connected to the filter to apply negative pressure, enhancing the recovery of follicular contents.

Oocyte collection medium (OCM) was used to lubricate the surfaces with the potential to be in contact with the follicular contents and provide an isotonic, isothermal environment for the oocytes within the collection system. OCM used was Dulbecco's phosphate-buffered saline 10X (DPBS, Sigma, D1283) diluted to a working concentration supplemented with 1% calf serum and 10 IU/ mL of heparin (Heparin sodium, Sagent[®] pharmaceuticals). Information about OCM can be found in Appendix B. Following collection, cumulus-oocyte complexes were transferred to a gridded dish and stereoscopic microscopes were used to search, rinse and collect COCs.

4.2.5. In vitro maturation of cumulus-oocyte complexes

Treatment two of all three experiments required in vitro maturation of the cumulus-oocyte complexes. The protocol for in vitro oocyte maturation can be found in Appendix A, the formulation for the maturation medium can be found in Appendix B, and a list of the equipment and materials used during in vitro maturation are presented in Appendix C. Immediately after collection and evaluation, cumulus-oocyte complexes assigned to treatment two were washed four times through standard maturation media and transferred into 35 μ L drops of maturation

medium covered with 570 μ L of mineral oil and incubated in 5% CO₂ at 39° C for 22 hours.

Maturation medium was tissue culture medium 199 supplemented with fetal bovine serum, sodium pyruvate, glutamine, FSH and a mix of penicillin and streptomycin.

4.2.6. In vitro fertilization of cumulus-oocyte complexes

After oocytes were matured, in vitro fertilization was performed as per the protocol in Appendix A. Refer to Appendix B for media formulations. Oocytes were moved in groups of approximately ten to 48 μ L IVF-TALP drops covered with 570 μ L of mineral oil in four-well plates, which had been equilibrated in 5% CO₂ at 39°C for at least two hours prior to the addition of the oocytes. Two straws of bull semen were thawed at 37°C for 30 seconds in a water bath and added on top of an ISolate[®] (99264, Irvine Scientific[®]) density gradient. The gradient was centrifuged at 400g for 20 minutes, washed with 5 mL of IVF-TALP and centrifuged for 10 minutes, then washed with 2 mL of IVF-TALP and centrifuged for 5 minutes. The number of sperm in the pellet was counted using a hemocytometer and a fertilization suspension of IVF-TALP and sperm was prepared at a 1×10^6 sperm/mL concentration. A 2 μ L volume of this sperm suspension was added to each 48 μ L drop of IVF-TALP with oocytes, and the dishes were placed back into the 5% CO₂ incubator at 39°C.

4.2.7. In vitro culture of embryos

At 18 hours post-fertilization, the presumptive zygotes were removed from IVF drops, placed into a warmed hyaluronidase solution and vortexed at max speed for 4 to 7 minutes until all cumulus cells were removed. They were then washed through a pre-warmed, pre-equilibrated SOFaa culture medium and placed into 35 μ L drops of culture medium under 570 μ L of mineral oil in four-well plates. Embryos were then cultured for 60 hours in 5% CO₂ at 39°C. Refer to Appendix B for media formulations.

4.2.8 Immunocytochemistry

Mature oocytes were fixed by placing the samples into a paraformaldehyde solution (15710, Electron Microscopy Sciences) and then moved into a 88% methanol solution (M1775-

1GA, Sigma-Aldrich™). Membranes were permeated with a PBST solution containing Tween 20 (161-0781, BIO-RAD®). Unspecific binding was prevented by blocking the samples in a commercial blocking solution (Maxblock Blocking Medium®, 15252, Active Motif™) overnight at 4°C. After washing the samples with Maxwash™ Washing Medium (15254, Active Motif®) for 10 minutes on top of a shaking plate, oocytes were incubated for one hour at 37°C within a polyclonal antibody to histone 3 tri-methylated lysine 9 (GR164977-1, Abcam®) produced in rabbits. Samples were washed 3 times with Maxwash™ Washing Medium (15254, Active Motif®) for 10 minutes on top of a shaking plate before being incubated for one hour at 37°C within a goat anti-rabbit IgG labeled Chromeo™ 488 (15041, Active Motif®) diluted in Maxbind™ Staining Medium (15253, Active Motif®). Samples were washed 4 times with Maxwash™ Washing Medium (15254, Active Motif®) for 10 minutes on top of a shaking plate before being mounted in microscopy slides using ProLong® gold antifade reagent (P36930, Molecular proves® by life technologies™).

4.2.9. Deconvolution microscopy

A Leica DM RXA2 upright microscope with DAPI (ex 340-380/em450-490) and FITC/GFP (ex 460-500/em512-542) filter sets was used to capture the microscope images. The exposure time and the Z-stack distance were maintained constant within and between treatments. Fluorescent intensity from regions of interest (FIRI) was measured using SlideBook 5.5® digital microscopy software (3i™). Regions of interest were defined as an area of the image that completely contained one and only one structure of interest (metaphase plate of the oocyte in Experiment 4 and the nucleus of each blastomere in Experiment 5) from which fluorescent intensity could be calculated. These regions of interest had constant area within treatments and between treatments in each experiment. Fluorescent intensity from the background (FIB) was measured in an area equal to the regions of interest and from a section of the image representative of the intensity of the background. The value of fluorescent intensity

of the sample (FIS) was defined as $FIS = FIRI - FIB$ (Fluorescent intensity of the sample = Fluorescent intensity of the regions of interest - Fluorescent intensity of the background).

4.2.10. Confocal microscopy

A Zeiss SteREO Lumar V.12[®] upright microscope with DAPI (ex 359-371/LP397) and FITC/GFP (ex 450-490/em500-550) filter sets was used to capture the microscope images. The exposure time and the Z-stack distance were maintained constant within and between treatments. Fluorescent intensity from regions of interest (FIRI) was measured using SlideBook 5.5[®] digital microscopy software (3i[™]). Regions of interest were defined as an area of the image that completely contained one and only one structure of interest (metaphase plate of the oocyte in Experiment 4 and the nucleus of each blastomere in Experiment 5) from which fluorescent intensity could be calculated. These regions of interest had constant area within treatments and between treatments in each experiment. Fluorescent intensity from the background (FIB) was measured in an area equal to the regions of interest and from a section of the image representative of the intensity of the background. The value of fluorescent intensity of the sample (FIS) was defined as $FIS = FIRI - FIB$ (Fluorescent intensity of the sample = Fluorescent intensity of the regions of interest - Fluorescent intensity of the background).

4.2.11. Statistical Analysis

Fluorescence analysis was performed using SlideBook[®] 5.5 (3i intelligent imaging innovations[™]) digital microscopy imaging software. A picture of the analysis of fluorescence intensity can be shown in Figure 4.3. Fluorescence data was exported in Microsoft Excel 2010 spreadsheet format. Differences in fluorescence levels between treatments were analyzed using Student's t-test using SigmaStat[®] Statistical Software (version 3.5). Differences of $P < 0.05$ were considered to be significant.

4.3. Results

In experiment four, ten cows were synchronized following protocol 1 and 54 cumulus-oocyte complexes were recovered, yielding an average of 5.4 immature cumulus-oocyte

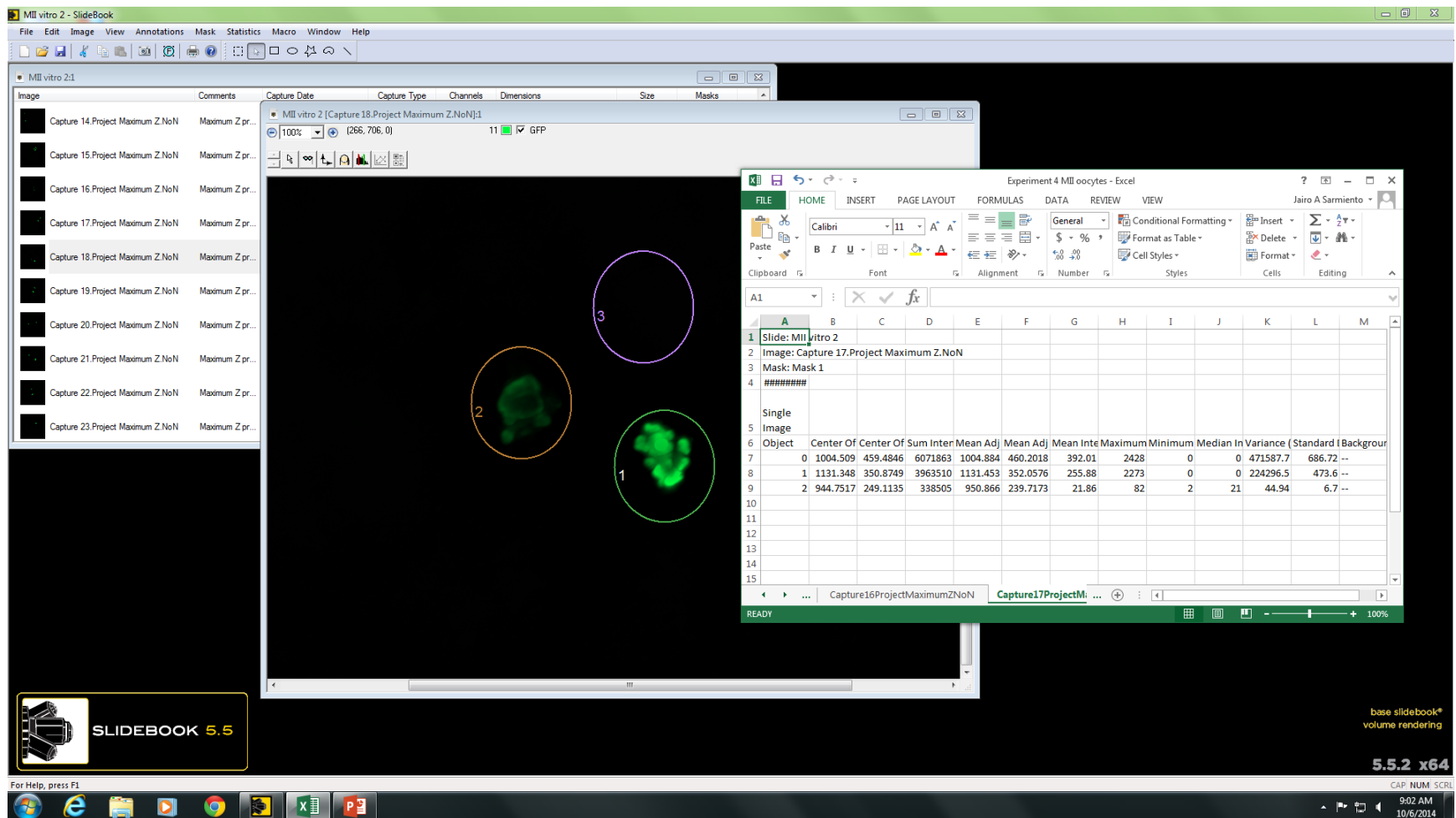


Figure 4.3 Analysis of fluorescent intensity during Experiment four. Fluorescent intensity is measured using Slidebook 5.5[®] software. The sample is an in vitro matured oocytes shortly before reaching the metaphase II stage. Intensities from two areas of interest where the fluorescent tri-methylated lysine 9 in histone 3 signals are detected are captured and exported to Excel[®] Microsoft Office[™] software for further analysis. A third region of interest capturing the intensity of the background is also taken to be used to normalize the data.

complexes collected per cow. Cumulus-oocyte complexes were matured in vitro for 22 hours. 40 cows were synchronized using protocol two and 15 in vivo matured oocytes were recovered, yielding an average of 0.0375 oocytes per cow. Morphological evaluation was used to select 24 cumulus-oocyte complexes from the in vitro matured group and 6 cumulus-oocyte complexes from the in vivo matured group. Morphological evaluation was based on homogeneity of the ooplasm and clear evidence of cumulus expansion.

Cumulus cells were removed before fixing and staining the oocytes. A primary antibody developed in rabbits against tri-methylated lysine 9 in histone 3 was complemented with a secondary goat-anti rabbit antibody labeled with a fluorescent probe. Samples in both treatments were stained simultaneously using the same batch of staining solutions to minimize difference due to sample processing.

Fluorescence intensity was captured using a deconvolution microscope and analyzed using microscopy imaging software. The results are presented in Table 4.1 There were lower levels of tri-methylation of lysine 9 in histone 3 in in vitro matured oocytes compared with in vivo matured oocytes ($p < 0.001$).

Table 4.1 Student's t test of in vitro matured oocytes versus in vivo matured oocytes

Treatment	n	Missing	Mean	Std Dev	SEM
In vitro matured oocytes	6	0	468941.67	485620.92	198253.91
In vivo matured oocytes	24	0	5109783.17	2892383.11	590405.23

$t = -3.867$ with 26 degrees of freedom ($p < 0.001$). Power of the test with $\alpha = 0.05$: 0.964

In experiment five, ten cows were synchronized following protocol 1 and 62 cumulus-oocyte complexes were recovered, yielding an average of 6.4 immature cumulus-oocyte complexes collected per cow. Cumulus-oocyte complexes were matured in vitro for 22 hours. 40 cows synchronized using protocol two were aspirated and 17 in vivo matured oocytes were recovered, yielding an average of 0.425 oocytes per cow. Morphological selection was used to

select 35 cumulus-oocyte complexes from the in vitro matured group and ten cumulus-oocyte complexes from the in vivo matured group. Fluorescence intensity was captured using a deconvolution microscope and analyzed using microscopy imaging software. The results are presented in Table 4.2.

Table 4.2 Student's t test of embryos derived from in vitro matured oocytes versus embryos derived from in vivo matured oocytes

Treatment	n	Missing	Mean	Std Dev	SEM
Blastomeres from embryos from in vitro matured oocytes	89	0	136375.63	75967.22	8052.51
Blastomeres from embryos from in vivo matured oocytes	24	0	204348.54	122960.08	25099.12

t = -3.366 with 111 degrees of freedom (p < 0.001). Power of the test with alpha = 0.05: 0.909.

Morphological selection was based on clear evidence of cumulus expansion. Oocytes from both treatments were fertilized in vitro simultaneously but separately. Embryos from both treatments were cultured in vitro for 60 hours simultaneously, under the same culture condition, in separate dishes. Six embryos (60%) cleaved from the ten in vivo matured oocytes fertilized in vitro: one embryo developed to the two-cell stage (16%), two embryos developed to the three-cell stage (33.3%), two embryos developed to the four-cell stage (33.3%), and one embryo developed to the eight-cell stage (16%). 22 embryos (62.85%) developed from the 35 in vitro matured oocytes fertilized in vitro: two embryos developed to the two-cell stage (9.09%), three embryos developed to the three-cell stage (13.6%), 13 embryos developed to the four-cell stage (54.16%), two embryos developed to the five-cell stage (9.09%), one embryo developed to the six-cell stage (4.54%), and one embryo developed to the eight-cell stage (4.54%).

After culture, a primary antibody developed in rabbits against tri-methylated histone 3 lysine 9 was complemented with a secondary goat-anti rabbit antibody labeled with a fluorescent dye. Samples in both treatments were stained simultaneously using the same batch of staining solutions to minimize differences due to sample processing.

There was a significant difference ($p < 0.001$) in the level of tri-methylation of lysine 9 in histone 3 between in the blastomeres of embryos derived from in vitro matured oocytes compared with embryos derived from in vivo matured oocytes.

4.4. Discussion

Collection of immature cumulus-oocyte complexes (COCs) yielded an average of 7.3 COCs per cow in Experiment one, 5.9 COCs per cow in Experiments two and three, 5.4 oocytes per cow in Experiment four and 6.4 oocytes per cow in Experiment five. An in vivo matured cumulus-oocyte complex was collected from 47.5% of the cows aspirated for Experiment one, 30% of the cows aspirated for Experiments two and three, 37.5% of the cows aspirated in Experiment four, and 42.5% of the cows aspirated in Experiment five. The recovery rate of immature COCs is close to the commercial recovery rates for cows that do not receive ovarian stimulation during the synchronization protocol. Reduced recovery rates are associated with proximity to ovulation (Humblot et al., 2005) and represents the main reason why commercial biotechnology companies working with cattle collect almost exclusively immature oocytes for their in vitro embryo production systems.

The use of drug-mediated ovarian stimulation was considered during the design of the synchronization protocols. It was evident that it would benefit the number of samples that could be collected, the timeframe of the experiment, and the amount of work required. However, evidence that the use of superstimulating drugs induce changes in gene expression in both cumulus cells and oocytes, specifically genes associated with oxidative stress and differentiation (Dias et al., 2013), was used to decide against any ovarian stimulation.

GnRH was used in the synchronization protocol to stimulate the release of LH, which is responsible for the final nuclear maturation of the intrafollicular oocyte. It has been shown that the use of GnRH for a LH surge induction does not provide any substantial changes in regard to the transcriptional status of the preovulatory oocyte (Humblot et al., 2005).

These synchronization protocols yielded follicles for aspiration from 3 to 12 mm in diameter, which were all aspirated. Follicular size was not considered during the collections because developmental competence of the oocyte does not relate to follicular size or developmental competence of the follicle, and factors negatively affecting follicular development (such as atresia) can enhance oocyte competence (Arlotto et al., 1996).

Morphological evaluation of immature cumulus-oocyte complexes in Experiment one was used to select 87.6% of the oocytes collected to be assigned either to the immature or the in vitro matured treatment. The percentage of immature cumulus-oocyte complexes that passed the morphological evaluation was 47.4% in Experiments two and three, 44% in Experiment four, and 56.4% in Experiment five. The large variability in the quality of the oocytes retrieved via transvaginal ultrasound guided aspiration of follicles (TUGA) can be explained by differences in follicular counts between cows, variability in the response to the synchronization protocols, changes in management conditions of the herd and conditions during the collection session.

The differences in follicular counts between cows in the physiology herd are substantial. There are some cows that average 35 COCs recovered per collection session whereas others average no more than 4 COCs per session (data not shown). The cows were selected randomly from the herd to prevent bias, resulting in high variability in the recovery rates.

Cows respond differently to synchronization protocols, and even though most of the cows were in the middle of a follicular wave, some cows had dominant follicles at the time of TUGA, producing oocytes that were reasonably questionable within the selection criteria for the experiment, which was that the cumulus-oocyte complex had not had the opportunity to undergo maturation in vivo. Rejecting COCs suspected of in vivo maturation affected the recovery rates of the project.

The changes in management that affected the recovery rates were mainly associated with changes in the weather and, therefore, in the nutritional status of the herd. The limited number of cows in the physiology herd at the RBC, the length of the synchronization protocols,

the rest intervals given to the cows between protocols, and other research projects conducted in parallel with this project resulted in collection sessions that were months apart from each other. Changes in the average number of follicles present in the ovaries of the cows were observed among the different seasons in which the cows were examined with ultrasound equipment.

Changes in the conditions during the oocyte collection sessions can influence the recovery rates and the quality of the cumulus-oocyte complexes retrieved. Changes in personnel, effectiveness and duration of the epidural anesthesia, cow temperament and behavior, room temperature and effective negative pressure of the vacuum pump determined the number and quality of the cumulus-oocyte complexes recovered.

However, cows that did not display estrus after the CIDR + prostaglandin portion of the protocol were not removed from the experimental group because the developmental competence of the oocyte relates directly to the developmental status of the follicle, but no association has been found with the corpus luteum (Vassena et al., 2003) and developmental competence has been proposed to be independent of the phase of the estrus cycle where oocytes are collected (Arlotto et al., 1996). Therefore, even if a small group of cows failed to become synchronized with the majority of the herd, as long as they respond to the final injections of prostaglandin given and develop a dominant follicle while displaying estrous behavior, a competent in vivo mature oocyte should be retrieved during the follicular aspiration.

In the in vivo matured oocyte treatment, the percentage of oocytes that passed the morphological evaluation was 84.2% in Experiment one, 58.3% in Experiments two and three, 40% in Experiment four and 58.8% in Experiment five. The criteria to select an in vivo matured oocyte were homogeneous ooplasm and evidence of substantial expansion of the cumulus cells. The use of cumulus expansion as a criterion for oocyte maturation has been questioned because there is evidence that human oocytes occasionally expand the cumulus cells without reaching the metaphase II stage (Veeck, 1988). However, there is no difference in the fertilization rates between oocytes confirmed to be in MII and oocytes with cumulus expansion

with no clear meiosis status. This means that even though a small number of oocytes may have delayed nuclear maturation, cytoplasmic and molecular maturation have taken place before cumulus expansion (Veeck, 1988).

However, cumulus cell expansion was kept as a selection criterion for technical reasons. During the collection of large follicles it is recommended not to access the dominant follicle with the needle coming from the top directly into the few layers of granulosa cells surrounding the antral cavity because disruption of the follicular wall of large follicles tends to occur when contacted with the needle, and when this happens the oocytes are seldom recovered. Instead, large follicles must be approached with the needle going through the ovarian medulla. Unfortunately, during this approach immature cumulus-oocyte complexes can get in contact with the needle, resulting in the unintended collection of immature Cumulus-oocyte complexes instead of the mature cumulus-oocyte complex targeted for collection. .

The percentage of oocytes that cleaved after fertilization was 60% in the in vivo matured treatment and 62.85% in the in vitro matured treatment. The results of IVF following TUGA of oocytes vary greatly. There are reports of blastocyst rates as low as 54% (Merton et al., 2003) and some others with 81.9% +/- 8.7% morula rates and 80.4% +/- 9.4% blastocyst rates (Blondin et al., 2002). In Experiment five, the percentage of embryos that cleaved in the in vitro matured oocyte treatment seemed high, because it is expected that embryos developing from oocytes matured in vitro have lower developmental competence than their in vivo matured counterparts. The reason for this high cleavage rate is unknown, but it might have been influenced by the strict morphological selection applied after collection, allowing a healthy cohort of oocytes to develop better than average. Also, 22.6% of the embryos in the in vitro matured oocyte treatment did not develop further than the three-cell stage in the 60 hours of culture. This percentage can be interpreted as embryos that cleaved, but lacked developmental potential to continue growing.

Experiments four and five demonstrated a difference in the levels of tri-methylation of lysine 9 in histone 3 between embryos developing from in vitro matured oocytes and in vivo matured oocytes. These findings are consistent with the loss of regulation in the accumulation of transcripts for histone methyltransferases during the in vitro maturation of bovine oocytes described in Experiments one, two, and three. The specific characteristics of the ooplasm that determine the developmental competence of the oocyte are still unknown, but it is accepted that the embryonic programs for developmental competence are embedded during oocyte maturation, which is done in part by accumulation of reserves of molecules that later support embryonic development (Macaulay et al., 2014).

Results of Experiment four showed that the level of tri-methylation of lysine 9 in histone 3 is higher in in vivo matured oocytes than in vitro matured oocytes. The influence of oocyte quality on the developmental potential of the embryo has been recognized in the cow more clearly than in any other species (Sirard et al., 2006); It has been demonstrated that developmental potential is higher in in vivo matured oocytes than in vitro matured oocytes, it is plausible that the decrease in the level of tri-methylation of lysine 9 in histone 3 is one of the components involved in the decrease of developmental competence detected during the in vitro maturation of oocytes.

The lower levels of methylation of lysine 9 in histone 3 observed in in vitro matured oocytes in experiment four were also observed in the in vitro produced embryos from in vitro matured oocytes in experiment five. Embryos developing from in vitro matured oocytes showed lower levels of H3K9 tri-methylation than the embryos developing from in vivo matured oocytes in the present study.

Experiments one through three showed a lack of regulation in the accumulation of transcripts for histone methyltransferases in oocytes matured in vitro. One of the effects of this lack of regulation seems to be the decrease in the level of tri-methylation of H3K9 in the in vitro derived embryos. Based on the superior developmental competence of embryos produced from

oocytes matured in vivo compared against oocytes matured in vitro, results in the present set of experiments suggest that the up regulation of transcripts for histone methyltransferases causes a decrease in the level of histone methylation in the embryo that compromises its developmental potential.

Following the rationale behind the central dogma of molecular biology, the increase in the level of transcripts of histone methyltransferases suggest a consequent increase in the level of methylation of histone 3. But this assumption contradicts the decrease in the methylation levels observed in Experiments four and five. Therefore, it is possible that the in vitro culture of bovine oocytes induces a lack of regulation in the accumulation of transcripts coding for some histone methyl transferases and mechanisms associated with the posttranscriptional regulation of transcripts. It is possible to postulate that miRNAs target mRNAs for destruction, resulting in a lower expression of the phenotype.

Methylation of histone 3 at lysine 9 is not found in the oocyte at early stages of development, at least in pig oocytes (Bui et al., 2007). However, it becomes a constant epigenetic mark during oocyte maturation (Racedo et al., 2009). It means that the levels of tri-methylation of lysine 9 in histone 3 have to be acquired and maintained during oocyte maturation. Suboptimal maturation of the oocyte (induced by suboptimal in vitro maturation systems) has the potential to generate extensive modifications in the levels of this epigenetic mark.

The methylation of lysine 9 in histone 3 has three biological functions as an epigenetic mark. It serves as a mark to silence genes in euchromatic regions, it regulates the formation of heterochromatin regions, and it serves as an epigenetic mark for genes that are the target of the pluripotency genes in stem cells (when used in combination with other epigenetic marks).

In the metaphase II oocyte, since it is considered transcriptionally incompetent, the biological consequences of hypo-methylation of lysine 9 in histone 3 most likely will not be

related with gene silencing. But in the early embryo, the silencing of unnecessary genes is required to acquire the transcriptome needed to progress to development.

Methylation of histone 3 at lysine 9 is an important regulator of mammalian embryonic development because it serves as a specific binding site for the recruitment of Heterochromatin protein 1, which is one of the major proteins that modify chromatin to create heterochromatic regions and silence genes (Nowak-Imialek et al., 2008). Chromatin configuration of the oocyte is symptomatic of its developmental potential. Chromatin condensation and spatial reorganization have to occur gradually and orderly to maximize competence (Lodde et al., 2013). Therefore, lower levels of tri-methylated lysine 9 in histone three can affect developmental potential of the early embryo by either preventing the condensation of chromatin or by changing the timing of chromatin compaction and gene silencing.

Another important possible consequence of the loss of regulation in the accumulation of transcripts for histone methyltransferases and the lower level of methylation of lysine 9 in histone 3 induced by the in vitro culture of oocyte and embryos is the interference with other elements of the histone code. It has been shown that the combination of epigenetic marks can be used by embryonic stem cells to label genes that are required during early development (Bernstein et al., 2006). Specifically, the presence of the double mark H3K4me3 and H3K9me3 in the same gene suggests that some developmental important genes are pre-activated, but do not become active until the repressive mark is removed (Bernstein et al., 2006).

Finally, hyper-methylation of H3K9 also has been described in embryos produced from somatic cell nuclear transfer (cloning), but the difference in the level of this epigenetic mark was associated to the origin of the somatic cell used during the nuclear transfer process (Nowak-Imialek et al., 2008). It is not clear if the in vitro culture of cloned embryos has any affect in the accumulation of transcripts for histone methyltransferases or the methylation levels in the blastomeres of the early embryo.

CHAPTER V

SUMMARY AND CONCLUSIONS

A set of five experiments was conducted to explore the association between post-translational modification of histones and the developmental competence of bovine oocytes and embryos. In the first three experiments, the well-established difference in developmental competence between in vivo matured oocytes and in vitro matured oocytes was used to investigate possible changes in the accumulation of transcripts of key histone methyltransferase enzymes. In experiments four and five, the changes in transcript accumulation established in experiments one through three was used to study the changes in the level of the accumulation of a specific post-translational modification in mature oocytes and early embryos.

In experiment one, cumulus-oocyte complexes were assigned to one of three treatments: immature, in vitro matured, and in vivo matured. The relative abundance of transcripts for the histone methyltransferases ASH1L, EHMT2, SUV39H1, and KDM6B was calculated using the abundance of the housekeeping genes POLYA and GADPH. Results showed that there is no difference in transcript accumulation for the four genes of interest between the immature and the in vivo treatment. This suggests that there is no major accumulation of transcripts for histone methyltransferases in cumulus-oocyte complexes after the follicle reaches the antral stage. A difference in the accumulation of transcripts for the EHMT2 gene was determined, and the pair-wise comparison showed that the accumulation of transcripts for this gene in in vitro matured oocytes is higher than in the immature and in vivo matured oocytes ($p = 0.021$ and $p = 0.007$, respectively).

In Experiment two, oocytes were assigned one of three treatments: immature, in vitro matured, and in vivo matured. Again, the relative abundance of transcripts for the histone methyltransferases ASH1L, EHMT2, SUV39H1 and KDM6B was calculated following previous protocols. Results showed that there are no difference in transcript accumulation for the four genes of interest between the immature and the in vivo treatment, supporting the prior

conclusion that there are no major accumulations of transcripts for histone methyltransferases in oocytes after they reach the growth phase. A difference in the accumulation of transcripts for the ASH1L gene was determined, and the pair-wise comparison showed that the accumulation of transcripts for this gene in in vitro matured oocytes is higher than in the immature and in vivo matured oocytes ($p = 0.001$ and $p = 0.001$, respectively). This finding suggests that a lack of regulation in the transcription of genes for specific histone methyltransferases can be induced by the in vitro culture conditions.

In Experiment three, cumulus cells were assigned to one of three treatments: immature, in vitro matured, and in vivo matured. Again, the relative abundance of transcripts for the histone methyltransferases ASH1L, EHMT2, SUV39H1, and KDM6B were calculated. Results showed no difference in transcript accumulation for the four genes of interest between the immature cumulus cells and the in vivo matured cumulus cells. Recent studies have demonstrated the transmission of transcript from the cumulus cells to the oocyte during late stages of oocyte maturation when the oocyte is transcriptionally incompetent. Results suggest that the transfer of transcripts coding for histone methyltransferases during in vivo maturation of bovine oocytes is very unlikely.

No differences in the accumulation of transcripts for any of the histone methyltransferases in the study was found in the cumulus cells in the vitro treatment. However, the accumulations of transcripts for the EHMT2 and KDM6B genes would had been significant had the p value been set to $p=0.1$ instead of $p=0.05$. The p values for the ANOVA analysis of these two genes were $p = 0.093$ and $p = 0.086$, respectively. Results in this experiment are inconclusive in regard to the lack of regulation of transcription for histone methyltransferase genes induced by the in vitro culture of embryos.

Based on results of previous experiments suggesting a lack of regulation in the accumulation of transcripts coding for histone methyltransferases induced by the in vitro culture of cumulus-oocyte complexes, experiment four was designed to investigate changes in the

levels of histone methylation between in vivo matured bovine oocytes and in vitro matured oocytes. A polyclonal antibody against the tri-methylated lysine 9 in histone 3 (H3K9me3) was coupled with a secondary antibody labeled with a fluorescent dye to semi-quantify the relative abundance of the H3K9me3 post-translational modification. Results showed that the in vitro matured oocytes displayed lower levels of H3K9me3 than their in vivo matured counterparts.

Since in vivo matured oocytes are more competent than in vitro matured oocytes and post-translational modifications of histones affect developmental competence, results in this experiment suggest that the in vitro culture of oocytes induce modifications in the accumulation of transcripts of the enzyme EHMT2 (which is responsible for the tri-methylation of lysine 9 in histone 3) resulting in lower levels of H3K9me3 that can affect the developmental competence of oocytes matured in vitro.

To provide more support for this idea, in experiment five in vitro matured oocytes and in vivo matured oocytes were fertilized in vitro and the levels of H3K9me3 were evaluated after 60 hours of in vitro culture. It was important to evaluate the embryos at this early stage because we wanted to determine the effect of the maternal transcriptome in the level of post-translational modification of histones, and genomic activation of the bovine embryo occurs around the 8-cell to 16-cell stage.

Results of experiment five showed lower levels of H3K9me3 in the in vitro treatment compared against the in vivo treatment. Once again, there is evidence suggesting that the in vitro culture system induces a lack of regulation in the accumulation of transcripts for histone methyltransferases that results in lower levels of post-translational modification of histone that are crucial for the developmental competence of the embryo.

It is important to elaborate on how an increase in the level of transcripts coding for a methyltransferase enzyme may result in a decrease in the phenotype catalyzed by the enzyme. It could be argued that higher level of transcripts of a histone methyltransferase should result in higher levels of methylation of the histone. But this argument ignores the regulatory

mechanisms and checkpoints that cells have to regulate transcription and translation. We propose that the increase in the transcription levels triggers a posttranscriptional regulatory mechanism within the cell that results in the existing phenotype. It is not clear which post transcriptional mechanisms would be involved, but it is possible to suggest that miRNA targeting transcripts for histone methyltransferases could result in a phenotype with lower levels of histone methylation in the chromatin.

In regard to the biological interpretation of the consequences of the lower levels of histone methylation that have the potential to harm the developmental potential of the embryos, it can be hypothesized that the major effects of the lower levels of H3K9me3 would affect chromatin compaction, gene silencing, and epigenetic marks of genes required during early development. H3K9me3 has been found associated with the promoter regions of genes that are transcriptionally silent. Either by competing with transcription factor or by recruiting chromatin modifying proteins, H3K9me3 has been shown to prevent transcription of targeted genes. H3K9me3 also has the capability to recruit heterochromatin protein 1, which is the major protein factor regulating chromatin compaction and the formation of heterochromatin. Lower levels of H3K9me3 in embryos could affect the compaction of chromatin through the cell cycle as the silencing of clusters of genes.

Lastly, H3K9me3 has been found associated with H3K4me3 in the promoter region of genes that are targeted by the pluripotency genes of embryonic stem cells. This epigenetic mark has been described as a mark for pre-activated genes; genes that are epigenetically labeled to be transcribed but require the removal of the repressive mark to become active. Losing H3K9me3 marks can potentially result in the loss of regulation of these pre-activated genes, which are critical during the early development of the embryo.

LITERATURE CITED

- Abramovich, C., B. Yakobson, J. Chebath, and M. Revel. 1997. A Protein-Arginine Methyltransferase Binds to the Intracytoplasmic Domain of the Ifnar1 Chain in the Type I Interferon Receptor. *EMBO J* 16: 260-266.
- Agger, K., P. A. Cloos, J. Christensen, D. Pasini, S. Rose, J. Rappsilber, I. Issaeva, E. Canaani, A. E. Salcini, and K. Helin. 2007. Utx and Jmjd3 Are Histone H3k27 Demethylases Involved in Hox Gene Regulation and Development. *Nature* 449: 731-734.
- Andreu-Vieyra, C. V., R. Chen, J. E. Agno, S. Glaser, K. Anastassiadis, A. F. Stewart, and M. M. Matzuk. 2010. Mll2 Is Required in Oocytes for Bulk Histone 3 Lysine 4 Trimethylation and Transcriptional Silencing. *PLoS Biol* 8. pii: e1000453. doi: 10.1371/journal.pbio.1000453.
- Arlotto, T., J. L. Schwartz, N. L. First, and M. L. Leibfried-Rutledge. 1996. Aspects of Follicle and Oocyte Stage That Affect in Vitro Maturation and Development of Bovine Oocytes. *Theriogenology* 45: 943-956.
- Assidi, M., F. J. Richard, and M. A. Sirard. 2013. Fsh in Vitro Versus Lh in Vivo: Similar Genomic Effects on the Cumulus. *J Ovarian Res* 6: 68. doi: 10.1186/1757-2215-6-68.
- Baarends, W. M., E. Wassenaar, R. van der Laan, J. Hoogerbrugge, E. Sleddens-Linkels, J. H. Hoeijmakers, P. de Boer, and J. A. Grootegeod. 2005. Silencing of Unpaired Chromatin and Histone H2a Ubiquitination in Mammalian Meiosis. *Mol Cell Biol* 25: 1041-1053.
- Bannister, A. J., and T. Kouzarides. 2005. Reversing Histone Methylation. *Nature* 436: 1103-1106.
- Beisel, C., A. Imhof, J. Greene, E. Kremmer, and F. Sauer. 2002. Histone Methylation by the *Drosophila* Epigenetic Transcriptional Regulator Ash1. *Nature* 419: 857-862.
- Bernstein, B. E., E. L. Humphrey, R. L. Erlich, R. Schneider, P. Bouman, J. S. Liu, T. Kouzarides, and S. L. Schreiber. 2002. Methylation of Histone H3 Lys 4 in Coding Regions of Active Genes. *Proc Natl Acad Sci U S A* 99: 8695-8700.
- Bernstein, B. E., M. Kamal, K. Lindblad-Toh, S. Bekiranov, D. K. Bailey, D. J. Huebert, S. McMahon, E. K. Karlsson, E. J. Kulbokas, 3rd, T. R. Gingeras, S. L. Schreiber, and E. S. Lander. 2005. Genomic Maps and Comparative Analysis of Histone Modifications in Human and Mouse. *Cell* 120: 169-181.
- Bernstein, B. E., T. S. Mikkelsen, X. Xie, M. Kamal, D. J. Huebert, J. Cuff, B. Fry, A. Meissner, M. Wernig, K. Plath, R. Jaenisch, A. Wagschal, R. Feil, S. L. Schreiber, and E. S. Lander. 2006. A Bivalent Chromatin Structure Marks Key Developmental Genes in Embryonic Stem Cells. *Cell* 125: 315-326.
- Bessa, I. R., R. C. Nishimura, M. M. Franco, and M. A. Dode. 2013. Transcription Profile of Candidate Genes for the Acquisition of Competence During Oocyte Growth in Cattle. *Reprod Domest Anim* 48: 781-789.

- Blaxter, M. 2014. Development: The Maternal-Zygotic Transition Revisited. *Curr Biol* 24: R72-75.
- Blondin, P., D. Bousquet, H. Twagiramungu, F. Barnes, and M. A. Sirard. 2002. Manipulation of Follicular Development to Produce Developmentally Competent Bovine Oocytes. *Biol Reprod* 66: 38-43.
- Bourc'his, D., D. Le Bourhis, D. Patin, A. Niveleau, P. Comizzoli, J. P. Renard, and E. Viegas-Pequignot. 2001. Delayed and Incomplete Reprogramming of Chromosome Methylation Patterns in Bovine Cloned Embryos. *Curr Biol* 11: 1542-1546.
- Bradbury, E. M., R. J. Inglis, H. R. Matthews, and N. Sarnier. 1973. Phosphorylation of Very-Lysine-Rich Histone in *Physarum Polycephalum*. Correlation with Chromosome Condensation. *Eur J Biochem* 33: 131-139.
- Briggs, S. D., T. Xiao, Z. W. Sun, J. A. Caldwell, J. Shabanowitz, D. F. Hunt, C. D. Allis, and B. D. Strahl. 2002. Gene Silencing: Trans-Histone Regulatory Pathway in Chromatin. *Nature* 418: 498.(Brief comm.)
- Brownell, J. E., J. Zhou, T. Ranalli, R. Kobayashi, D. G. Edmondson, S. Y. Roth, and C. D. Allis. 1996. Tetrahymena Histone Acetyltransferase A: A Homolog to Yeast Gcn5p Linking Histone Acetylation to Gene Activation. *Cell* 84: 843-851.
- Bui, H. T., N. Van Thuan, S. Kishigami, S. Wakayama, T. Hikichi, H. Ohta, E. Mizutani, E. Yamaoka, T. Wakayama, and T. Miyano. 2007. Regulation of Chromatin and Chromosome Morphology by Histone H3 Modifications in Pig Oocytes. *Reproduction* 133: 371-382.
- Chen, D., H. Ma, H. Hong, S. S. Koh, S. M. Huang, B. T. Schurter, D. W. Aswad, and M. R. Stallcup. 1999. Regulation of Transcription by a Protein Methyltransferase. *Science* 284: 2174-2177.
- Cheung, P., K. G. Tanner, W. L. Cheung, P. Sassone-Corsi, J. M. Denu, and C. D. Allis. 2000. Synergistic Coupling of Histone H3 Phosphorylation and Acetylation in Response to Epidermal Growth Factor Stimulation. *Mol Cell* 5: 905-915.
- Chu, L., T. Zhu, X. Liu, R. Yu, M. Bacanamwo, Z. Dou, Y. Chu, H. Zou, G. H. Gibbons, D. Wang, X. Ding, and X. Yao. 2012. Suv39h1 Orchestrates Temporal Dynamics of Centromeric Methylation Essential for Faithful Chromosome Segregation in Mitosis. *J Mol Cell Biol* 4: 331-340.
- Dias, F. C., M. I. Khan, M. A. Sirard, G. P. Adams, and J. Singh. 2013. Differential Gene Expression of Granulosa Cells after Ovarian Superstimulation in Beef Cattle. *Reproduction* 146: 181-191.
- Dover, J., J. Schneider, M. A. Tawiah-Boateng, A. Wood, K. Dean, M. Johnston, and A. Shilatifard. 2002. Methylation of Histone H3 by Compass Requires Ubiquitination of Histone H2b by Rad6. *J Biol Chem* 277: 28368-28371.

- Fair, T., S. C. Hulshof, P. Hyttel, T. Greve, and M. Boland. 1997. Nucleus Ultrastructure and Transcriptional Activity of Bovine Oocytes in Preantral and Early Antral Follicles. *Mol Reprod Dev* 46: 208-215.
- Fischle, W., B. S. Tseng, H. L. Dormann, B. M. Ueberheide, B. A. Garcia, J. Shabanowitz, D. F. Hunt, H. Funabiki, and C. D. Allis. 2005. Regulation of Hp1-Chromatin Binding by Histone H3 Methylation and Phosphorylation. *Nature* 438: 1116-1122.
- Fuchs, G., E. Shema, R. Vesterman, E. Kotler, Z. Wolchinsky, S. Wilder, L. Golomb, A. Pribluda, F. Zhang, M. Haj-Yahya, E. Feldmesser, A. Brik, X. Yu, J. Hanna, D. Aberdam, E. Domany, and M. Oren. 2012. Rnf20 and Usp44 Regulate Stem Cell Differentiation by Modulating H2b Monoubiquitylation. *Mol Cell* 46: 662-673.
- Gao, Y., P. Hyttel, and V. J. Hall. 2010. Regulation of H3k27me3 and H3k4me3 During Early Porcine Embryonic Development. *Mol Reprod Dev* 77: 540-549.
- Giordano, A., and M. L. Avantaggiati. 1999. P300 and Cbp: Partners for Life and Death. *J Cell Physiol* 181: 218-230.
- Gregory, G. D., C. R. Vakoc, T. Rozovskaia, X. Zheng, S. Patel, T. Nakamura, E. Canaani, and G. A. Blobel. 2007. Mammalian Ash1l Is a Histone Methyltransferase That Occupies the Transcribed Region of Active Genes. *Mol Cell Biol* 27: 8466-8479.
- Guo, X. W., J. P. Th'ng, R. A. Swank, H. J. Anderson, C. Tudan, E. M. Bradbury, and M. Roberge. 1995. Chromosome Condensation Induced by Fostriecin Does Not Require P34cdc2 Kinase Activity and Histone H1 Hyperphosphorylation, but Is Associated with Enhanced Histone H2a and H3 Phosphorylation. *EMBO J* 14: 976-985.
- Gurdon, J. B. 1962. The Developmental Capacity of Nuclei Taken from Intestinal Epithelium Cells of Feeding Tadpoles. *J Embryol Exp Morphol* 10: 622-640.
- Gurley, L. R., J. A. D'Anna, S. S. Barham, L. L. Deaven, and R. A. Tobey. 1978. Histone Phosphorylation and Chromatin Structure During Mitosis in Chinese Hamster Cells. *Eur J Biochem* 84: 1-15.
- Honda, B. M., P. M. Candido, and G. H. Dixon. 1975a. Histone Methylation. Its Occurrence in Different Cell Types and Relation to Histone H4 Metabolism in Developing Trout Testis. *J Biol Chem* 250: 8686-8689.
- Honda, B. M., G. H. Dixon, and E. P. Candido. 1975b. Sites of in Vivo Histone Methylation in Developing Trout Testis. *J Biol Chem* 250: 8681-8685.
- Humblot, P., P. Holm, P. Lonergan, C. Wrenzycki, A. S. Lequarre, C. G. Joly, D. Herrmann, A. Lopes, D. Rizos, H. Niemann, and H. Callesen. 2005. Effect of Stage of Follicular Growth During Superovulation on Developmental Competence of Bovine Oocytes. *Theriogenology* 63: 1149-1166.
- Kageyama, S., H. Liu, N. Kaneko, M. Ooga, M. Nagata, and F. Aoki. 2007. Alterations in Epigenetic Modifications During Oocyte Growth in Mice. *Reproduction* 133: 85-94.

- Karpiuk, O., Z. Najafova, F. Kramer, M. Hennion, C. Galonska, A. Konig, N. Snaidero, T. Vogel, A. Shchebet, Y. Begus-Nahrmann, M. Kassem, M. Simons, H. Shcherbata, T. Beissbarth, and S. A. Johnsen. 2012. The Histone H2b Monoubiquitination Regulatory Pathway Is Required for Differentiation of Multipotent Stem Cells. *Mol Cell* 46: 705-713.
- Koike, H., R. Ouchi, Y. Ueno, S. Nakata, Y. Obana, K. Sekine, Y. W. Zheng, T. Takebe, K. Isono, H. Koseki, and H. Taniguchi. 2014. Polycomb Group Protein Ezh2 Regulates Hepatic Progenitor Cell Proliferation and Differentiation in Murine Embryonic Liver. *PLoS One* 9: e104776.
- Labrecque, R., and M. A. Sirard. 2014. The Study of Mammalian Oocyte Competence by Transcriptome Analysis: Progress and Challenges. *Mol Hum Reprod* 20: 103-116.
- Lehnertz, B., Y. Ueda, A. A. Derijck, U. Braunschweig, L. Perez-Burgos, S. Kubicek, T. Chen, E. Li, T. Jenuwein, and A. H. Peters. 2003. Suv39h-Mediated Histone H3 Lysine 9 Methylation Directs DNA Methylation to Major Satellite Repeats at Pericentric Heterochromatin. *Curr Biol* 13: 1192-1200.
- Leibfried-Rutledge, M. L., E. S. Critser, W. H. Eyestone, D. L. Northey, and N. L. First. 1987. Development Potential of Bovine Oocytes Matured in Vitro or in Vivo. *Biol Reprod* 36: 376-383.
- Lepikhov, K., and J. Walter. 2004. Differential Dynamics of Histone H3 Methylation at Positions K4 and K9 in the Mouse Zygote. *BMC Dev Biol* 4: 12. <http://www.ncbi.nlm.nih.gov/pmc/articles/PMC521682/pdf/1471-213X-4-12.pdf> (Accessed 15 September 2014)
- Li, E. 2002. Chromatin Modification and Epigenetic Reprogramming in Mammalian Development. *Nat Rev Genet* 3: 662-673.
- Liu, B., Z. Wang, L. Zhang, S. Ghosh, H. Zheng, and Z. Zhou. 2013. Depleting the Methyltransferase Suv39h1 Improves DNA Repair and Extends Lifespan in a Progeria Mouse Model. *Nat Commun* 4: 1868. doi: 10.1038/ncomms2885.
- Liu, H., J. M. Kim, and F. Aoki. 2004. Regulation of Histone H3 Lysine 9 Methylation in Oocytes and Early Pre-Implantation Embryos. *Development* 131: 2269-2280.
- Lo, W. S., R. C. Trievel, J. R. Rojas, L. Duggan, J. Y. Hsu, C. D. Allis, R. Marmorstein, and S. L. Berger. 2000. Phosphorylation of Serine 10 in Histone H3 Is Functionally Linked in Vitro and in Vivo to Gcn5-Mediated Acetylation at Lysine 14. *Mol Cell* 5: 917-926.
- Lodde, V., F. Franciosi, I. Tessaro, S. C. Modina, and A. M. Luciano. 2013. Role of Gap Junction-Mediated Communications in Regulating Large-Scale Chromatin Configuration Remodeling and Embryonic Developmental Competence Acquisition in Fully Grown Bovine Oocyte. *J Assist Reprod Genet* 30: 1219-1226.
- Macaulay, A. D., I. Gilbert, J. Caballero, R. Barreto, E. Fournier, P. Tossou, M. A. Sirard, H. J. Clarke, E. W. Khandjian, F. J. Richard, P. Hyttel, and C. Robert. 2014. The Gametic Synapse; Rna Transfer to the Bovine Oocyte. *Biol Reprod*. 91(4):90. doi: 10.1095/biolreprod.114.119867.

- Mahadevan, L. C., A. C. Willis, and M. J. Barratt. 1991. Rapid Histone H3 Phosphorylation in Response to Growth Factors, Phorbol Esters, Okadaic Acid, and Protein Synthesis Inhibitors. *Cell* 65: 775-783.
- Merton, J. S., A. P. de Roos, E. Mullaart, L. de Ruigh, L. Kaal, P. L. Vos, and S. J. Dieleman. 2003. Factors Affecting Oocyte Quality and Quantity in Commercial Application of Embryo Technologies in the Cattle Breeding Industry. *Theriogenology* 59: 651-674.
- Mowen, K. A., J. Tang, W. Zhu, B. T. Schurter, K. Shuai, H. R. Herschman, and M. David. 2001. Arginine Methylation of Stat1 Modulates Ifnalpha/Beta-Induced Transcription. *Cell* 104: 731-741.
- Niemann, H., and C. Wrenzycki. 2000. Alterations of Expression of Developmentally Important Genes in Preimplantation Bovine Embryos by in Vitro Culture Conditions: Implications for Subsequent Development. *Theriogenology* 53: 21-34.
- Nishioka, K., S. Chuikov, K. Sarma, H. Erdjument-Bromage, C. D. Allis, P. Tempst, and D. Reinberg. 2002. Set9, a Novel Histone H3 Methyltransferase That Facilitates Transcription by Precluding Histone Tail Modifications Required for Heterochromatin Formation. *Genes Dev* 16: 479-489.
- Nowak-Imialek, M., C. Wrenzycki, D. Herrmann, A. Lucas-Hahn, I. Lagutina, E. Lemme, G. Lazzari, C. Galli, and H. Niemann. 2008. Messenger Rna Expression Patterns of Histone-Associated Genes in Bovine Preimplantation Embryos Derived from Different Origins. *Mol Reprod Dev* 75: 731-743.
- Ohsumi, K., C. Katagiri, and T. Kishimoto. 1993. Chromosome Condensation in *Xenopus* Mitotic Extracts without Histone H1. *Science* 262: 2033-2035.
- Park, K. E., C. M. Johnson, X. Wang, and R. A. Cabot. 2011. Differential Developmental Requirements for Individual Histone H3k9 Methyltransferases in Cleavage-Stage Porcine Embryos. *Reprod Fertil Dev* 23: 551-560.
- Park, S. H., S. E. Yu, Y. G. Chai, and Y. K. Jang. 2014. Cdk2-Dependent Phosphorylation of Suv39h1 Is Involved in Control of Heterochromatin Replication During Cell Cycle Progression. *Nucleic Acids Res* 42: 6196-6207.
- Pawlak, M. R., C. A. Scherer, J. Chen, M. J. Roshon, and H. E. Ruley. 2000. Arginine N-Methyltransferase 1 Is Required for Early Postimplantation Mouse Development, but Cells Deficient in the Enzyme Are Viable. *Mol Cell Biol* 20: 4859-4869.
- Peters, A. H., S. Kubicek, K. Mechtler, R. J. O'Sullivan, A. A. Derijck, L. Perez-Burgos, A. Kohlmaier, S. Opravil, M. Tachibana, Y. Shinkai, J. H. Martens, and T. Jenuwein. 2003. Partitioning and Plasticity of Repressive Histone Methylation States in Mammalian Chromatin. *Mol Cell* 12: 1577-1589.
- Qiao, J., Y. Chen, L. Y. Yan, J. Yan, P. Liu, and Q. Y. Sun. 2010. Changes in Histone Methylation During Human Oocyte Maturation and Ivf- or Icsi-Derived Embryo Development. *Fertil Steril* 93: 1628-1636.

- Racedo, S. E., C. Wrenzycki, K. Lepikhov, D. Salamone, J. Walter, and H. Niemann. 2009. Epigenetic Modifications and Related Mrna Expression During Bovine Oocyte in Vitro Maturation. *Reprod Fertil Dev* 21: 738-748.
- Rizos, D., F. Ward, P. Duffy, M. P. Boland, and P. Lonergan. 2002. Consequences of Bovine Oocyte Maturation, Fertilization or Early Embryo Development in Vitro Versus in Vivo: Implications for Blastocyst Yield and Blastocyst Quality. *Mol Reprod Dev* 61: 234-248.
- Ross, P. J., N. P. Ragina, R. M. Rodriguez, A. E. Iager, K. Siripattaraprat, N. Lopez-Corrales, and J. B. Cibelli. 2008. Polycomb Gene Expression and Histone H3 Lysine 27 Trimethylation Changes During Bovine Preimplantation Development. *Reproduction* 136: 777-785.
- Russo, V., N. Bernabo, O. Di Giacinto, A. Martelli, A. Mauro, P. Berardinelli, V. Curini, D. Nardinocchi, M. Mattioli, and B. Barboni. 2013. H3k9 Trimethylation Precedes DNA Methylation During Sheep Oogenesis: Hdac1, Suv39h1, G9a, Hp1, and Dnmts Are Involved in These Epigenetic Events. *J Histochem Cytochem* 61: 75-89.
- Ruthenburg, A. J., C. D. Allis, and J. Wysocka. 2007. Methylation of Lysine 4 on Histone H3: Intricacy of Writing and Reading a Single Epigenetic Mark. *Mol Cell* 25: 15-30.
- Sanchez-Elsner, T., D. Gou, E. Kremmer, and F. Sauer. 2006. Noncoding Rnas of Trithorax Response Elements Recruit Drosophila Ash1 to Ultrabithorax. *Science* 311: 1118-1123.
- Santos-Rosa, H., R. Schneider, A. J. Bannister, J. Sherriff, B. E. Bernstein, N. C. Emre, S. L. Schreiber, J. Mellor, and T. Kouzarides. 2002. Active Genes Are Tri-Methylated at K4 of Histone H3. *Nature* 419: 407-411.
- Santos, F., V. Zakhartchenko, M. Stojkovic, A. Peters, T. Jenuwein, E. Wolf, W. Reik, and W. Dean. 2003. Epigenetic Marking Correlates with Developmental Potential in Cloned Bovine Preimplantation Embryos. *Curr Biol* 13: 1116-1121.
- Sarmiento, O. F., L. C. Digilio, Y. Wang, J. Perlin, J. C. Herr, C. D. Allis, and S. A. Coonrod. 2004. Dynamic Alterations of Specific Histone Modifications During Early Murine Development. *J Cell Sci* 117: 4449-4459.
- Sassone-Corsi, P., C. A. Mizzen, P. Cheung, C. Crosio, L. Monaco, S. Jacquot, A. Hanauer, and C. D. Allis. 1999. Requirement of Rsk-2 for Epidermal Growth Factor-Activated Phosphorylation of Histone H3. *Science* 285: 886-891.
- Sawai, K., S. Kageyama, S. Moriyasu, H. Hirayama, A. Minamihashi, and S. Onoe. 2005. Analysis of Mrna Transcripts for Insulin-Like Growth Factor Receptors and Binding Proteins in Bovine Embryos Derived from Somatic Cell Nuclear Transfer. *Cloning Stem Cells* 7: 189-198.
- Shi, X., T. Hong, K. L. Walter, M. Ewalt, E. Michishita, T. Hung, D. Carney, P. Pena, F. Lan, M. R. Kaadige, N. Lacoste, C. Cayrou, F. Davrazou, A. Saha, B. R. Cairns, D. E. Ayer, T. G. Kutateladze, Y. Shi, J. Cote, K. F. Chua, and O. Gozani. 2006. Ing2 Phd Domain Links Histone H3 Lysine 4 Methylation to Active Gene Repression. *Nature* 442: 96-99.
- Shi, Y., and J. R. Whetstine. 2007. Dynamic Regulation of Histone Lysine Methylation by Demethylases. *Mol Cell* 25: 1-14.

- Sirard, M. A., F. Richard, P. Blondin, and C. Robert. 2006. Contribution of the Oocyte to Embryo Quality. *Theriogenology* 65: 126-136.
- Spencer, T. E., N. Forde, P. Dorniak, T. R. Hansen, J. J. Romero, and P. Lonergan. 2013. Conceptus-Derived Prostaglandins Regulate Gene Expression in the Endometrium Prior to Pregnancy Recognition in Ruminants. *Reproduction* 146: 377-387.
- Strahl, B. D., R. Ohba, R. G. Cook, and C. D. Allis. 1999. Methylation of Histone H3 at Lysine 4 Is Highly Conserved and Correlates with Transcriptionally Active Nuclei in Tetrahymena. *Proc Natl Acad Sci U S A* 96: 14967-14972.
- Sun, Z. W., and C. D. Allis. 2002. Ubiquitination of Histone H2b Regulates H3 Methylation and Gene Silencing in Yeast. *Nature* 418: 104-108.
- Tachibana, M., K. Sugimoto, M. Nozaki, J. Ueda, T. Ohta, M. Ohki, M. Fukuda, N. Takeda, H. Niida, H. Kato, and Y. Shinkai. 2002. G9a Histone Methyltransferase Plays a Dominant Role in Euchromatic Histone H3 Lysine 9 Methylation and Is Essential for Early Embryogenesis. *Genes Dev* 16: 1779-1791.
- Tesfaye, D., N. Ghanem, F. Carter, T. Fair, M. A. Sirard, M. Hoelker, K. Schellander, and P. Lonergan. 2009. Gene Expression Profile of Cumulus Cells Derived from Cumulus-Oocyte Complexes Matured Either in Vivo or in Vitro. *Reprod Fertil Dev* 21: 451-461.
- Trewick, S. C., P. J. McLaughlin, and R. C. Allshire. 2005. Methylation: Lost in Hydroxylation? *EMBO Rep* 6: 315-320.
- Vandel, L., and D. Trouche. 2001. Physical Association between the Histone Acetyl Transferase Cbp and a Histone Methyl Transferase. *EMBO Rep* 2: 21-26.
- Vassena, R., R. J. Mapletoft, S. Allodi, J. Singh, and G. P. Adams. 2003. Morphology and Developmental Competence of Bovine Oocytes Relative to Follicular Status. *Theriogenology* 60: 923-932.
- Veeck, L. L. 1988. Oocyte Assessment and Biological Performance. *Ann N Y Acad Sci* 541: 259-274.
- Vire, E., C. Brenner, R. Deplus, L. Blanchon, M. Fraga, C. Didelot, L. Morey, A. Van Eynde, D. Bernard, J. M. Vanderwinden, M. Bollen, M. Esteller, L. Di Croce, Y. de Launoit, and F. Fuks. 2006. The Polycomb Group Protein Ezh2 Directly Controls DNA Methylation. *Nature* 439: 871-874.
- Wang, D., J. Zhou, X. Liu, D. Lu, C. Shen, Y. Du, F. Z. Wei, B. Song, X. Lu, Y. Yu, L. Wang, Y. Zhao, H. Wang, Y. Yang, Y. Akiyama, H. Zhang, and W. G. Zhu. 2013. Methylation of Suv39h1 by Set7/9 Results in Heterochromatin Relaxation and Genome Instability. *Proc Natl Acad Sci U S A* 110: 5516-5521.
- Wang, H., Z. Q. Huang, L. Xia, Q. Feng, H. Erdjument-Bromage, B. D. Strahl, S. D. Briggs, C. D. Allis, J. Wong, P. Tempst, and Y. Zhang. 2001. Methylation of Histone H4 at Arginine 3 Facilitating Transcriptional Activation by Nuclear Hormone Receptor. *Science* 293: 853-857.

- Weake, V. M., and J. L. Workman. 2008. Histone Ubiquitination: Triggering Gene Activity. *Mol Cell* 29: 653-663.
- Wei, Y., L. Yu, J. Bowen, M. A. Gorovsky, and C. D. Allis. 1999. Phosphorylation of Histone H3 Is Required for Proper Chromosome Condensation and Segregation. *Cell* 97: 99-109.
- Whitworth, K. M., C. Agca, J. G. Kim, R. V. Patel, G. K. Springer, N. J. Bivens, L. J. Forrester, N. Mathialagan, J. A. Green, and R. S. Prather. 2005. Transcriptional Profiling of Pig Embryogenesis by Using a 15-K Member Unigene Set Specific for Pig Reproductive Tissues and Embryos. *Biol Reprod* 72: 1437-1451.
- Wrenzycki, C., D. Herrmann, A. Lucas-Hahn, K. Korsawe, E. Lemme, and H. Niemann. 2005. Messenger Rna Expression Patterns in Bovine Embryos Derived from in Vitro Procedures and Their Implications for Development. *Reprod Fertil Dev* 17: 23-35.
- Zhang, A., B. Xu, Y. Sun, X. Lu, R. Gu, L. Wu, Y. Feng, and C. Xu. 2012. Dynamic Changes of Histone H3 Trimethylated at Positions K4 and K27 in Human Oocytes and Preimplantation Embryos. *Fertil Steril* 98: 1009-1016.
- Zhang, K., L. Li, M. Zhu, G. Wang, J. Xie, Y. Zhao, E. Fan, L. Xu, and E. Li. 2014. Comparative Analysis of Histone H3 and H4 Post-Translational Modifications of Esophageal Squamous Cell Carcinoma with Different Invasive Capabilities. *J Proteomics* 112C: 180-189.
- Zhang, Y., and D. Reinberg. 2001. Transcription Regulation by Histone Methylation: Interplay between Different Covalent Modifications of the Core Histone Tails. *Genes Dev* 15: 2343-2360.

APPENDIX A PROTOCOLS

In vitro Maturation of Cumulus-Oocyte Complexes

1. Prepare bovine maturation media and HEPES-TALP media. Media formulations can be found in Appendix B.
2. Place 35 μL drops of maturation media in 4-well dishes (1 drop per well) and cover them with 570 μL of mineral oil. Carefully place the dishes with the media drops into a 5% CO_2 incubator set at 39°C for at least two hours to equilibrate.
3. Rinse the immature cumulus-oocyte complexes once through HEPES-TALP medium.
4. Rinse the immature cumulus-oocyte complexes four times through maturation medium.
5. Eight to twelve cumulus-oocyte complexes are placed in each maturation media drop for 22 hours. Oocytes are then removed from the incubator and processed for immunocytochemistry.

PCR Amplification

JumpStart™ REDTaq® ReadyMix™ reaction mix

Catalog number P0982, Sigma-Aldrich Inc.

1. Reactions are carried out in PCR tubes in a volume of 50 μL per reaction.
2. 5 μL of calibrator DNA is added to 25 μL of JumpStart™ REDTaq® ReadyMix™, 2 μL of forward primer, 2 μL of reverse primer, and 6 μL of nuclease-free water.
3. PCR tubes were placed in the thermocycler and run with the following protocol:
 - a. 1 cycle
 - i. 2 minutes at 94°C
 - b. 35 cycles
 - i. 30 seconds at 94°C (Denaturation)
 - ii. 30 seconds at 61°C (Annealing)
 - iii. 1 minute at 72°C (Extension)

- c. 1 cycle
 - i. 5 minutes at 72°C (Final extension)
- d. Hold at 4°C until removed from the thermocycler.

RNA Extraction

RNeasy® Plus Micro Kit

Catalog number 74034, QIAGEN®

1. Add 350 µL of buffer RLT Plus directly to the tube containing the sample while still at -80°C (add buffer while tube is still in the freezer).
2. Vortex for two minutes at maximum speed.
3. Transfer lysate to a gDNA Eliminator spin column placed in a 2 mL collection tube.
Centrifuge for 30 seconds at 9,000 X g. Discard the column and save the flow-through.
4. Transfer the sample to an RNeasy MinElute spin column placed in a 2 mL collection tube. Close the lid and centrifuge for 15 seconds at 9,000 X g. Discard flow-through.
5. Add 700 µL of buffer RW1 to the RNeasy MinElute spin column. Close the lid and centrifuge for 15 seconds at 9,000 X g. Discard the flow-through.
6. Add 500 µL of buffer RPE to the RNeasy MinElute spin column. Close the lid and centrifuge for 15 seconds at 9,000 X g. Discard the flow-through.
7. Add 500 µL of 80% ethanol to the RNeasy MinElute spin column. Close the lid and centrifuge for 15 seconds at 9,000 X g. Discard the collection tube with the flow-through.
8. Place the RNeasy MinElute spin column in a new 2 mL collection tube. Leave the lid open and centrifuge at max speed for 5 minutes to dry the membrane. Discard the collection tube with the flow-through.
9. Place the RNeasy MinElute spin column in a new 1.5 mL collection tube. Add 17 µL of RNase-free water directly to the center of the spin column membrane. Close the lid gently and centrifuge for 1 minute at max speed.
10. RNA will be eluted in a volume of approximately 15 µL.

Reverse Transcriptase PCR

iSCRIPT cDNA Synthesis Kit

Catalog number 170-8890, Bio-Rad Laboratories®, Inc.

1. Reactions are carried out in PCR tubes in a volume of 20 μ L per reaction.
2. 15 μ L of mRNA from each sample are added to 1 μ L of reverse transcriptase enzyme and 4 μ L of iSCRIPT reaction mix. If less than 15 μ L of sample is available, nuclease-free water can be added to the reaction to complete the final 20 μ L volume per reaction.
3. PCR tubes are placed in the thermocycler and run for a single cycle with the following protocol:
 - a. 5 minutes at 25°C
 - b. 30 minutes at 42°C
 - c. 5 minutes at 85°C
 - d. Hold at 4°C

Real Time PCR

SsoFast™ EvaGreen® Supermix

Catalog number 172-5200, Sigma-Aldrich Inc.

1. Reactions are carried out in 96-well PCR plates, using a volume of 20 μ L per reaction.
2. Set up plate-template map and upload the template into the computer controlling the thermocycler.
3. Prepare master mixes per gene. Master mixes are prepared to minimize variations due to pipetting small volumes. Negative controls take nuclease-free water instead of a sample and positive controls use a selective dilution of the calibration preparation. Each sample, positive control, and negative control is run in triplicate.
4. 12 μ L of cDNA of each sample is added to 30 μ L of SsoFast™ EvaGreen® Supermix, 3 μ L of forward primer, 3 μ L of reverse primer, and 12 μ L of nuclease-free water. The 60 μ L mix is vortexed and placed in the PCR plates as three replicates of 20 μ L each.

5. Place the PCR plate in the thermocycler and cover it with sealing tape. Run with the following protocol:
 - a. 1 cycle
 - i. 1 minute at 95°C (Activation)
 - b. 40 cycles
 - i. 5 seconds at 95°C (Denaturation)
 - ii. 30 seconds at 61°C (Annealing and extension)
 - c. 68 cycles
 - i. Increase 0.5°C every 10 seconds starting at 61°C and finishing at 95°C (Melting curve)

In vitro Embryo Fertilization and Culture

1. Move two centrifuge carriers into an incubator (39°C).
2. Prepare IVF-TALP. Media formulation can be found in Appendix B.
3. Make fertilization wells:
 - a. 48 µL IVF-TALP drops in each well of a 4-well plate. There will be 8-12 oocytes per drop. Cover with pre-warmed, pre-equilibrated mineral oil.
 - b. Add 500 µL IVF-TALP in each well of a 4-well plate for use as washing dishes.
 - c. Equilibrate everything in the 5% CO₂ incubator for at least 2-3 hours.
4. Place the tube with remaining IVF-TALP medium into the 5% CO₂ incubator (loosened cap) at 39°C to equilibrate.
5. Prepare Percoll Gradient: Fill a 15 mL centrifuge tube with 2 mL of upper layer ISolate®. Use a small syringe with needle to slowly and carefully dispense 2 mL of lower layer ISolate® underneath the upper layer.
6. Transfer the ISolate® gradient to a pre-warmed centrifuge carrier in incubator (39°C).
7. Wash hemocytometer and coverslip with alcohol and place on microscope.
8. Place some extra slides and coverslips on a warmer to use for checking sperm motility.

Semen Thaw and Preparation:

9. After oocyte maturation, thaw two straws of semen in 39°C water for 30 seconds. Be careful not to raise any remaining straws in the liquid nitrogen tank above the frost line.
10. Dry straw and keep it warm and dark. Cut the sealed end off, hold it over the ISolate® gradient, and use a plunger to dispense semen on top of the upper layer.
11. Check viability of the thawed semen by placing a drop of semen remaining in the straw onto a pre-warmed slide. View at 40X magnification to assure that motile sperm are present.
12. Place the Isolate® gradient with semen into the pre-warmed centrifuge carrier and centrifuge at 400g for 20 minutes at 37°C.
13. While the sperm is in the centrifuge, use this time to move the oocytes from maturation medium into IVF-TALP. Wash thoroughly through the IVF-TALP wash dishes which were pre-equilibrated in the 5% CO₂ incubator.
14. Transfer up to 12 oocytes to each 48 µL drop of IVF-TALP located in the 5% CO₂ incubator. Return the 4-well plate back to the incubator when finished.
15. After centrifuge stops, carefully remove carrier with the ISolate® gradient from the centrifuge. There should be a sperm pellet (if not, you must start over with a new gradient and semen).
16. Using a 1 mL pipette, place the tip on the edge of the tube at the top of the ISolate® and slowly pull up the gradient until it is down to the sperm pellet.
17. Wash with 5 mL IVF-TALP. Centrifuge in a second pre-warmed carrier at 400g for 10 minutes. There will be another pellet. Aspirate excess IVF-TALP.
18. Wash a second time with 2 mL IVF-TALP. Centrifuge in a third pre-warmed carrier at 400 X g for 5 minutes. When the centrifuge stops, aspirate the IVF-TALP down to the sperm pellet.
19. Determine sperm pellet concentration:

- a. Add 95 μL of water into a small centrifuge tube.
- b. Gently swirl the sperm pellet to resuspend the sperm with any remaining medium. Transfer 5 μL of sperm suspension into the 95 μL of water in the small tube. Pipette gently to mix.
- c. Place the 15 mL tube with the rest of the sperm suspension into the 5% CO_2 incubator. Sperm must be kept warm.
- d. Add 10 μL of the sperm/water dilution to each side of the hemocytometer and wait a minute to allow sperm to settle to the bottom before counting.
- e. Count the sperm heads within five double-ruled squares on each side of the hemocytometer. One side should not vary more than 10% from the other side (if so, clean the hemocytometer and count again).

20. Dilute the sample in IVF-TALP:

- a. Average the counts from both counting fields. This number, "X", will be divided into 7500 to get the number of μL of sperm needed for the dilution. Subtract the amount of sperm from 300 μL to obtain the amount of IVF-TALP to use.
Example: $7500/X = \mu\text{L of sperm}$; $300 - \mu\text{L sperm} = \text{amount of IVF-TALP}$
- b. Add the appropriate amount of IVF-TALP medium to a microcentrifuge tube and then add the appropriate volume from the sperm pellet. Mix gently by pipetting.

Fertilization:

21. Add 2 μL of the final sperm suspension (to make a final concentration of 1×10^6 sperm/mL) to each drop. Record the time and date on the dish.
22. Incubate sperm and oocytes for 18 hours in a humidified incubator with 5% CO_2 at 39°C .

Culture:

23. Prepare culture media. Media formulations can be found in Appendix B.
24. Prepare dishes with HEPES-TALP for washing.
25. Prepare dishes or 4-well plates with culture media for washing.

26. Make 35 μ L drops of culture media in dishes. Cover the drops with 570 μ L of mineral oil that has been pre-warmed. Equilibrate dishes in the incubator for at least two hours.
27. Strip off the cumulus cells:
 - a. Thaw one vial of hyaluronidase (1 mg/mL). See Appendix B for solution formulations.
 - b. Place in a 15 mL conical tube and incubate in the water bath for 2 minutes.
 - c. Place the oocytes in the tube containing the hyaluronidase solution.
 - d. Vortex at max speed for 5 minutes (or until the majority of cumulus cells are removed).
28. Transfer the oocytes to a wash dish containing HEPES-TALP.
29. After washing through HEPES-TALP, wash oocytes four times through culture media.
30. Place 10 oocytes in each 35 μ L drop of culture media.
31. Incubate in 5% CO₂ for 7 days (or change media at Day 3 if using a sequential media).

Immunocytochemistry

1. Place the embryos in a well containing PBST-BSA for 1 minute.
2. Pre-fix embryos with 0.25% paraformaldehyde for 10 minutes at 37°C.
3. Wash the embryos with PBS-PVA. Incubate for 10 minutes at 4°C.
4. Place the embryos in 88% methanol for 1 minute.
5. Transfer the embryos into 88% methanol and incubate for 30 minutes at -20°C.
6. Wash embryos with PBST-BSA.
7. Transfer the embryos into MAXblock™ blocking medium (15252, Active Motif®) and incubate for: 1 hour at 37°C, or 2 hours at 25°C, or overnight at 4°C.
8. Aspirate the blocking media and add 1 mL of MAXwash™ washing medium (15254, Active motif®). Rock the plate for 10 minutes at room temperature on a rotating platform.
9. Prepare the primary antibody dilution.

10. Aspirate the MAXwash and add 1 mL of primary antibody solution. Incubate for 1 hour at 37°C.
11. Aspirate the primary antibody solution and add 1 mL of MAXwash™ washing medium (15254, Active motif®). Rock the plate for 10 minutes at room temperature on a rotating platform. Repeat the wash two more times.
12. Prepare the secondary antibody dilution.
13. Aspirate the MAXwash and add 1 mL of secondary antibody solution. Incubate for 1 hour at 37°C.
14. Aspirate the secondary antibody solution and add 1 mL of MAXwash™ washing medium (15254, Active motif®). Rock the plate for 10 minutes at room temperature on a rotating platform. Repeat the wash three more times.
15. Prepare the Hoechst 33342 dilution.
16. Aspirate the Hoechst solution and add 1 mL of MAXwash™ washing medium (15254, Active motif®). Rock the plate for 10 minutes at room temperature on a rotating platform. Repeat the wash one more time.
17. Put the embryos on a clean microscope slide with a drop of commercial antifade. Post with silicone on a coverslip. Seal the edges of the coverslip with nail polish. Keep the slide in a dark, humid, and cool environment until microscopic analysis.

APPENDIX B

STOCK SOLUTIONS AND MEDIA FORMULATIONS

Stock Solutions

1. Oocyte Collection Medium: Add 100 mL of 10X D-PBS solution (Sigma D-1283) to 900 mL of autoclaved H₂O to make 1 L of D-PBS. Add 10 mL of Bovine Calf Serum (HyClone) and 1 mL of Heparin (Sagent Pharmaceuticals, Schaumburg, IL, USA) to make the D-PBS oocyte collection medium.
2. Pen/Strep: Gibco 15140. Aliquot ≈500 µL of new pen/strep solution into sterile centrifuge tubes. Store at -20°C until use.
3. Na Pyruvate: Sigma P-4562. Dissolve 22 mg of sodium pyruvate in 10 mL of sterile Millipore-Q water. Sterile filter into an aluminum foil-wrapped 15 mL conical tube and store at 4°C for up to a month.
4. L-Glutamine: Sigma G-8540. Make a 100X stock solution with a concentration of 200 mM by dissolving 2.92 g of glutamine in 100 mL of water. Aliquot 1.0 mL into sterile centrifuge tubes and store at -20°C.
5. FSH: Folltropin-V (Bioniche). Make a 1000X stock solution (5 mg/mL) by diluting a 400 mg vial of folltropin in 80 mL of water. Store at -20°C in 100 µL aliquots.
6. PH: First, make a 1 mM hypotaurine stock by dissolving 1.09 mg hypotaurine (H-1384) in 10 mL 0.9% saline solution. Then make a 2 mM penicillamine (P-4875) stock by adding 3 mg penicillamine to 10 mL 0.9% saline solution. Combine 2.5 mL hypotaurine stock, 2.5 mL penicillamine stock, and 4 mL 0.9% saline solution. Sterile filter. Store at -20°C in aliquots.
7. Heparin: Add 2 mg of heparin (H-3149) to 8 mL IVF-TALP. Store at -20°C in 1 mL aliquots.
8. Hyaluronidase: Sigma H-3506. Prepare a 1 mg/mL solution by dissolving 10 mg hyaluronidase into 10 mL of HEPES-TALP. Aliquot 1 mL into 1.5 mL sterile centrifuge tubes. Store at -80°C indefinitely.

Media Formulations

HEPES-TALP Medium

Component	Source	Product Number	Amount
BSA, Fraction V	Sigma	A-4503	60 mg
HEPES-TL	Caisson	IVL01	20 mL
Na Pyruvate	stock solution	P-4562	200 µL
Pen/Strep	Gibco	15140	200 µL

Sterile filter. Date, label, and store at 4°C for no more than one week.

Maturation Medium

Component	Source	Product Number	Amount
Medium-199	Sigma	M-4530	8.68 mL
Fetal Bovine Serum	cellgro	35-010-CV	1 mL
Pen/Strep	Gibco	15140	100 µL
Na Pyruvate	stock solution	P-4562	100 µL
Glutamine	100x stock solution	G-8540	100 µL
FSH (Folltropin)	1000x stock solution	Bioniche	10 µL

Sterile filter. Date, label, and store at 4°C for up to one week.

IVF-TALP Medium

Component	Source	Product Number	Amount
TL-FERT	Caisson	IVL02	22.5 mL
PH	stock solution	P-4875 / H-1384	1 mL
Heparin	stock solution	H-3149	1 mL
Pen/Strep	Gibco	15140	100 µL
Na Pyruvate	stock solution	P-4562	100 µL
BSA	Sigma	A-6003	150 mg

Sterile filter. Date, label, and store at 4°C for up to one week.

SOFaa Culture Medium

Component	Source	Product Number	Amount
SOF stock media	Caisson	IVL05	14.4 mL
BME	Sigma	B-6766	300 µL
MEM	Sigma	M-7145	150 µL
Pen/Strep	Gibco	15140	150 µL
BSA	Sigma	A-4503	75 mg

Sterile filter. Date, label, and store at 4°C for up to one week.

APPENDIX C EQUIPMENT AND MATERIALS USED

Transvaginal Ultrasound guided aspiration of cumulus-oocyte complexes (TUGA)

- SonoSite® MicroMaxx® ultrasound system
- 7.5 MHz convex transducer (model C11e, SonoSite®)
- Hard plastic probe handle equipped with accessories to accommodate short-needle collection systems
- Plastic probe covers used to protect the transducer probe (273028-3436, Reproductive Resources™)
- Sterilized non-spermicidal lubricating jelly (Priority care®, VetOne®)
- Non-radiopaque polyethylene tubing (1.67 mm inner diameter and 2.42 mm outside diameter, Intramedic®)
- Ureteral catheter connectors (050010, Cook Urological®)
- EZ Way® Embryo collection filters (362829, Santa Cruz Animal Health™)
- 18 gauge X 1.5 inches Polypropylene hypodermic disposable needles (8881, Kendall®)
- 18 gauge X 3.0 inches disposable needles (8300015026, Air-Tite Products Co., Inc.)
- Lidocaine 2% (130954, VetOne®)
- Regulated vacuum pump (VMAR-5000, Cook Veterinary Products®)

APPENDIX D

ADDITIONAL DATA TABLES

Table D.1. Geometric mean of housekeeping genes in Experiment One.

Treatment	Immature COCs			In vitro Matured COCs			In vivo Matured COCs		
Gene	PolyA	GADPH	GeoMean	PolyA	GADPH	GeoMean	PolyA	GADPH	GeoMean
Calibrator	26.560	28.950	27.729	26.560	28.950	27.729	26.560	28.950	27.729
Sample 1	29.170	25.770	27.417	29.470	28.520	28.991	27.200	27.980	27.587
Sample 2	30.780	29.570	30.169	29.247	28.787	29.016	26.400	25.250	25.819
Sample 3	28.760	28.640	28.700	29.350	26.559	27.919	26.880	26.590	26.735
Sample 4	30.860	27.320	29.036	30.122	29.723	29.922	27.130	26.600	26.864
Sample 5	30.420	30.670	30.545	30.096	29.352	29.722	27.000	28.010	27.500
Sample 6	30.950	27.150	28.988	30.321	28.886	29.595	26.100	24.210	25.137
Sample 7	30.840	28.920	29.865	29.265	28.856	29.060	26.980	27.540	27.259
Sample 8	30.500	30.870	30.684	26.916	26.740	26.828	27.000	25.880	26.434
Sample 9	31.320	27.100	29.134	31.395	31.183	31.289	32.150	30.660	31.396
Sample 10	32.060	29.620	30.816	31.820	31.472	31.646	28.470	27.060	27.756
Sample 11	29.750	28.410	29.072	31.257	32.422	31.834	29.880	27.500	28.665
Sample 12	28.850	25.580	27.166	30.969	30.506	30.736	30.770	27.960	29.331
Sample 13	31.100	30.530	30.814	33.530	31.289	32.390	30.080	28.200	29.125
Sample 14	31.020	26.720	28.790	35.550	29.950	32.630	27.460	25.230	26.321
Sample 15	31.200	30.030	30.609	34.169	32.916	33.536	29.370	28.200	28.779
Sample 16	31.620	30.490	31.050	20.671	20.796	20.733	30.390	26.510	28.384

The geometrical mean between the CT values of housekeeping genes Poly A polymerase (PolyA) and Gliceraldehyde 3 phosphate dehydrogenase (GADPH) were calculated for use as a reference value to normalize the expression of the genes of interest in Experiment One.

Table D.2. QPCR values in Experiment One.

Treatment	Immature COCs				In vitro Matured COCs				In vivo Matured COCs			
Gene	ASH1L	EHMT2	SUV39H1	KDM6B	ASH1L	EHMT2	SUV39H1	KDM6B	ASH1L	EHMT2	SUV39H1	KDM6B
Calibrator	25.337	25.040	27.072	28.248	25.337	25.040	27.072	28.248	25.337	25.040	27.072	28.248
Sample 1	30.562	32.390	27.314	28.826	29.720	29.636	30.074	31.256	31.710	30.733	30.649	31.390
Sample 2	32.651	34.025	25.793	29.156	27.504	26.096	27.535	25.837	20.193	28.937	27.975	27.393
Sample 3	32.730	32.460	29.664	27.643	30.410	27.922	29.157	26.819	30.966	32.036	29.886	30.048
Sample 4	30.973	28.333	27.972	27.426	31.292	27.803	31.160	30.513	29.173	32.562	29.634	31.088
Sample 5	29.681	31.987	28.070	28.877	32.078	26.783	29.360	29.610	29.962	31.973	29.987	30.812
Sample 6	32.922	33.294	29.416	28.293	28.709	26.279	28.237	28.472	26.260	28.883	27.891	27.770
Sample 7	30.620	29.769	31.221	30.890	30.733	25.821	26.972	29.185	29.012	30.733	29.779	26.315
Sample 8	34.423	33.790	28.394	28.939	30.606	24.904	28.274	28.113	29.535	32.412	29.530	28.681
Sample 9	30.768	29.761	32.833	32.318	33.707	27.555	30.401	32.516	29.914	29.749	28.009	32.968
Sample 10	33.246	30.079	35.208	32.349	33.540	30.789	30.109	31.890	28.577	27.221	28.305	28.656
Sample 11	31.789	29.178	32.523	30.269	31.817	32.585	31.810	31.202	31.285	28.926	28.813	32.037
Sample 12	30.484	26.506	29.891	30.525	30.354	32.235	31.389	31.915	33.350	29.810	29.505	32.572
Sample 13	29.468	28.479	31.305	32.639	30.413	34.665	30.846	24.123	31.467	29.053	28.265	31.978
Sample 14	32.900	29.522	33.313	31.471	30.179	32.832	35.236	31.919	26.365	27.520	27.713	28.878
Sample 15	25.132	28.529	31.191	31.058	32.576	28.631	28.783	27.036	30.449	29.279	29.476	27.286
Sample 16	34.293	30.056	31.159	31.383	17.473	22.986	20.933	21.226	33.742	29.799	29.857	32.773

The QPCR values (Ct values) of each sample in each treatment in Experiment One. Four genes of interest: ¹ASH1L: *Bos taurus* absent, small, or homeotic-like *Drosophila*, mRNA; EHMT2: *Bos taurus* euchromatic histone-lysine N-methyltransferase 2, mRNA; SUV31: *Bos taurus* suppressor of variegation 3-9 homologue 1, mRNA; KDM6B: PREDICTED: *Bos taurus* lysine (K)-Specific Demethylase 6B, mRNA.

Table D.3. Geometric mean of housekeeping genes in Experiment Two.

Treatment	Immature Oocytes			In vitro Matured Oocytes			In vivo Matured Oocytes		
Gene	PolyA	GADPH	GeoMean	PolyA	GADPH	GeoMean	PolyA	GADPH	GeoMean
Calibrator	26.592	29.187	27.859	29.187	28.516	28.849	29.187	29.018	29.102
Sample 1	32.175	29.883	31.008	29.012	28.114	28.560	31.939	32.175	32.057
Sample 2	29.160	29.459	29.309	29.857	30.078	29.968	30.945	30.927	30.936
Sample 3	29.418	27.103	28.237	29.505	29.665	29.585	31.490	28.913	30.174
Sample 4	29.565	29.602	29.583	30.005	28.199	29.088	31.569	28.481	29.985
Sample 5	29.974	29.675	29.824	32.810	34.314	33.554	30.858	31.499	31.177
Sample 6	29.795	28.160	28.966	31.575	30.499	31.032	32.225	31.596	31.909
Sample 7	29.405	27.955	28.670	27.824	28.540	28.179	31.730	31.319	31.524

The geometrical mean between the CT values of housekeeping genes Poly A polymerase (PolyA) and Glicereraldehyde 3 phosphate dehydrogenase (GADPH) were calculated for use as a reference value to normalize the expression of the genes of interest in Experiment Two.

Table D.4. QPCR values in Experiment Two.

Treatment	Immature Oocytes				In vitro Matured Oocytes				In vivo Matured Oocytes			
Gene	ASH1L	EHMT2	SUV39H1	KDM6B	ASH1L	EHMT2	SUV39H1	KDM6B	ASH1L	EHMT2	SUV39H1	KDM6B
Calibrator	25.476	26.832	26.613	24.346	25.476	26.832	26.613	24.346	25.476	26.832	26.613	24.346
Sample 1	35.024	33.048	31.411	33.140	32.744	31.373	30.900	30.719	35.473	36.143	33.765	32.892
Sample 2	28.771	30.389	30.760	30.774	34.322	32.330	32.424	31.943	36.562	32.915	32.199	34.222
Sample 3	32.293	30.802	30.629	29.189	34.372	32.678	31.304	32.740	33.339	33.589	30.527	35.119
Sample 4	33.874	31.134	30.453	31.155	32.666	31.155	30.570	30.729	35.147	33.623	32.793	31.170
Sample 5	33.819	31.487	29.874	31.605	33.266	33.285	30.305	32.340	35.746	33.196	31.945	-----
Sample 6	33.672	29.785	30.354	30.295	33.423	31.225	29.270	31.725	33.966	31.409	32.399	33.167
Sample 7	25.503	32.204	31.180	31.600	27.250	28.164	27.825	25.664	34.424	31.365	29.690	34.308

The QPCR values (Ct values) of each sample in each treatment in Experiment Two. Four genes of interest: ¹ASH1L: Bos taurus absent, small, or homeotic-like Drosophila, mRNA; EHMT2: Bos taurus euchromatic histone-lysine N-methyltransferase 2, mRNA; SUV31: Bos taurus suppressor of variegation 3-9 homologue 1, mRNA; KDM6B: PREDICTED: Bos taurus lysine (K)-Specific Demethylase 6B, mRNA.

Table D.5. Geometric mean of housekeeping genes in Experiment Three.

Treatment	Immature Cumulus Cells			In vitro Matured Cumulus Cells			In vivo Matured Cumulus Cells		
Gene	PolyA	GADPH	GeoMean	PolyA	GADPH	GeoMean	PolyA	GADPH	GeoMean
Calibrator	26.592	29.187	27.859	26.592	29.187	27.859	26.592	29.187	27.859
Sample 1	29.215	24.771	26.901	26.964	24.941	25.933	30.829	25.784	28.194
Sample 2	27.364	21.655	24.343	26.474	25.055	25.755	27.384	21.839	24.455
Sample 3	30.400	27.060	28.681	26.947	25.129	26.022	26.895	21.650	24.130
Sample 4	29.458	23.980	26.578	26.940	25.128	26.018	29.345	23.787	26.420
Sample 5	31.032	25.251	27.993	27.500	26.055	26.768	26.139	20.889	23.367
Sample 6	30.015	25.118	27.458	28.700	27.963	28.329	25.398	20.903	23.041
Sample 7	30.410	24.949	27.544	27.129	25.370	26.235	28.155	21.870	24.814

The geometrical mean between the CT values of housekeeping genes Poly A polymerase (PolyA) and Gliceraldehyde 3 mphosphate dehydrogenase (GADPH) were calculated for use as a reference value to normalize the expression of the genes of interest in Experiment Three.

Table D.6. QPCR values in Experiment Three.

Treatment	Immature Cumulus Cells				In vitro Matured Cumulus Cells				In vivo Matured Cumulus Cells			
Gene	ASH1L	EHMT2	SUV39H1	KDM6B	ASH1L	EHMT2	SUV39H1	KDM6B	ASH1L	EHMT2	SUV39H1	KDM6B
Calibrator	25.476	26.832	26.613	24.346	25.476	26.832	26.613	24.346	25.476	26.832	26.613	24.346
Sample 1	32.580	32.105	31.747	30.800	31.122	29.563	33.220	28.740	33.062	33.224	34.219	33.119
Sample 2	31.348	29.570	29.790	31.146	27.626	31.572	31.120	29.874	30.548	30.084	32.533	28.536
Sample 3	33.875	33.770	34.565	32.659	30.745	30.815	30.465	29.715	29.702	29.030	29.562	30.178
Sample 4	33.028	31.750	31.900	31.829	30.693	30.402	31.751	28.744	31.082	32.227	32.798	32.543
Sample 5	33.558	32.795	33.060	33.075	31.683	31.525	30.763	29.744	30.253	29.432	29.558	28.240
Sample 6	32.240	33.123	28.340	31.654	27.104	30.127	28.978	28.656	30.145	31.513	31.194	29.245
Sample 7	32.925	31.700	32.183	33.085	31.008	29.806	31.209	30.435	31.131	29.965	29.885	32.342

The QPCR values (Ct values) of each sample in each treatment in Experiment Three. Four genes of interest: ¹ASH1L: Bos taurus absent, small, or homeotic-like Drosophila, mRNA; EHMT2: Bos taurus euchromatic histone-lysine N-methyltransferase 2, mRNA; SUV31: Bos taurus suppressor of variegation 3-9 homologue 1, mRNA; KDM6B: PREDICTED: Bos taurus lysine (K)-Specific Demethylase 6B, mRNA

Table D.7. Fluorescent intensity data for Experiment Four.

Treatment	Oocyte	Non-normalized Intensity	Background Intensity	Normalized Intensity
1	1	1,111,376	104,633	1,006,743
1	2	551,381	115,026	436,355
1	3	1,264,551	140,665	1,123,886
1	4	167,211	108,968	58,243
1	5	236,036	69,799	166,237
1	6	166,387	144,201	22,186
2	7	2,352,915	59,326	2,293,589
2	8	1,986,862	366,063	1,620,799
2	9	9,082,480	57,455	9,025,025
2	10	8,295,104	198,619	8,096,485
2	11	2,702,502	255,354	2,447,148
2	12	2,989,271	274,459	2,714,812
2	13	8,926,342	283,338	8,643,004
2	14	5,015,970	312,455	4,703,515
2	15	468,357	234,127	234,230
2	16	3,939,362	81,171	3,858,191
2	17	2,380,149	312,026	2,068,123
2	18	6,921,490	80,207	6,841,283
2	19	5,610,019	305,336	5,304,683
2	20	12,874,420	341,950	12,532,470
2	21	1,391,339	55,125	1,336,214
2	22	6,071,813	338,505	5,733,308
2	23	6,865,661	214,161	6,651,500
2	24	5,471,721	221,860	5,249,861
2	25	6,060,546	327,728	5,732,818
2	26	5,943,178	128,974	5,814,204
2	27	6,174,976	211,425	5,963,551
2	28	7,054,145	295,985	6,758,160
2	29	2,791,172	257,710	2,533,462
2	30	6,763,926	285,565	6,478,361

Table D.8. Fluorescent intensity data for Experiment Five.

Treatment	Embryo	Blastomere	Fluorescent Intensity: Regions of Interest	Fluorescent Intensity: Background	Fluorescent Intensity: Sample
1	1	1	396591	5316	391275
1	1	2	140803	5316	135487
1	1	3	176298	5316	170982
1	1	4	108005	5316	102689
1	2	5	91385	2346	89039
1	2	6	133704	2346	131358
1	2	7	78007	2346	75661
1	2	8	198910	2346	196564
1	2	9	289810	2346	287464
1	3	10	60397	2792	57605
1	3	11	65847	2792	63055
1	3	12	71259	2792	68467
1	3	13	73785	2792	70993
1	3	14	106132	2792	103340
1	3	15	129518	2792	126726
1	4	16	132662	3986	128676
1	4	17	140640	3986	136654
1	4	18	73782	3986	69796
1	4	19	79420	3986	75434
1	5	20	308157	2345	305812
1	5	21	139687	2345	137342
1	6	22	295707	4963	290744
1	6	23	257329	4963	252366
1	6	24	202985	4963	198022
1	6	25	124906	4963	119943
1	7	26	211560	3954	207606
1	7	27	187462	3954	183508
1	7	28	240731	3954	236777
1	8	29	72045	1965	70080

(Table D.8 continued)

Treatment	Embryo	Blastomere	Fluorescent Intensity: Regions of Interest	Fluorescent Intensity: Background	Fluorescent Intensity: Sample
1	8	30	139093	1965	137128
1	8	31	136540	1965	134575
1	9	32	115054	3467	111587
1	9	33	131282	3467	127815
1	9	34	114423	3467	110956
1	9	35	221551	3467	218084
1	10	36	110841	2335	108506
1	10	37	188236	2335	185901
1	10	38	205737	2335	203402
1	11	39	245923	4322	241601
1	11	40	186170	4322	181848
1	11	41	132319	4322	127997
1	11	42	76260	4322	71938
1	12	43	127755	2960	124795
1	12	44	150050	2960	147090
1	12	45	108572	2960	105612
1	12	46	129536	2960	126576
1	13	47	262503	3998	258505
1	13	48	85442	3998	81444
1	14	49	56153	1868	54285
1	14	50	98669	1868	96801
1	14	51	166421	1868	164553
1	14	52	68002	1868	66134
1	15	53	114755	2625	112130
1	15	54	58465	2625	55840
1	15	55	71131	2625	68506
1	15	56	63344	2625	60719
1	16	57	237874	3345	234529
1	16	58	115074	3345	111729
1	16	59	87417	3345	84072

(Table D.8 continued)

Treatment	Embryo	Blastomere	Fluorescent Intensity: Regions of Interest	Fluorescent Intensity: Background	Fluorescent Intensity: Sample
1	16	60	16599	3345	13254
1	17	61	173015	3103	169912
1	17	62	81184	3103	78081
1	17	63	153555	3103	150452
1	17	64	140724	3103	137621
1	18	65	31078	1320	29758
1	18	66	45265	1320	43945
1	18	67	45316	1320	43996
1	18	68	25342	1320	24022
1	18	69	43984	1320	42664
1	18	70	4530	1320	3210
1	18	71	38990	1320	37670
1	18	72	242690	1320	241370
1	19	73	128832	2556	126276
1	19	74	94276	2556	91720
1	19	75	128349	2556	125793
1	19	76	129143	2556	126587
1	20	77	162410	3145	159265
1	20	78	194417	3145	191272
1	20	79	178399	3145	175254
1	20	80	88110	3145	84965
1	21	81	198322	4648	193674
1	21	82	180658	4648	176010
1	21	83	104984	4648	100336
1	21	84	320375	4648	315727
1	21	85	83773	4648	79125
1	22	86	238039	5412	232627
1	22	87	89060	5412	83648
1	22	88	243346	5412	237934
1	22	89	228552	5412	223140

(Table D.8 continued)

Treatment	Embryo	Blastomere	Fluorescent Intensity: Regions of Interest	Fluorescent Intensity: Background	Fluorescent Intensity: Sample
2	23	90	320681	3966	316715
2	23	91	307291	3966	303325
2	23	92	204435	3966	200469
2	24	93	392751	6745	386006
2	24	94	301726	6745	294981
2	25	95	70457	1336	69121
2	25	96	166056	1336	164720
2	25	97	112709	1336	111373
2	26	98	297061	2546	294515
2	26	99	109370	2546	106824
2	26	100	83105	2546	80559
2	26	101	115812	2546	113266
2	26	102	259442	2546	256896
2	26	103	112607	2546	110061
2	26	104	103344	2546	100798
2	26	105	135027	2546	132481
2	27	106	585289	6539	578750
2	27	107	288730	6539	282191
2	27	108	113611	6539	107072
2	27	109	68253	6539	61714
2	28	110	280447	1978	278469
2	28	111	193172	1978	191194
2	28	112	138532	1978	136554
2	28	113	228289	1978	226311

VITA

Jairo Alberto Sarmiento Guzmán Rozo Rojas Laguna Flórez Barrero was born in Villavicencio, Colombia to Jairo Sarmiento Rozo and Piedad Guzmán de Sarmiento. He has an older sister, Maria Piedad Sarmiento, who is a Doctor of Medicine and specializes in pediatric intensive care. He also has a younger brother, Andrés Ricardo Sarmiento, who is a Doctor of Law. Jairo attended the Claustro Moderno School in Bogotá, Colombia during his elementary, middle, and high school years.

Jairo attended the National University of Colombia from 1997 to 2001 to obtain a Doctoral degree in Veterinary Medicine and Surgery. During his time as a vet student Jairo had the opportunity to learn large animal internal medicine from Dr. Olimpo Oliver Espinoza and Theriogenology from Dr. Claudia Jimenez Escobar. They became his mentors and a most influential force in the development of his professional interests.

Upon graduation, Jairo started a private practice in Barranquilla, Colombia where he worked as a large animal practitioner. During this time he combined the practice of his three favorite activities: working with horses, practicing volleyball, and teaching vet students large animal internal medicine and reproduction.

Jairo moved to the United States in January 2008. He first attended the University of California at Davis for one semester and the University of Massachusetts at Boston during the following two semesters. Jairo moved to Baton Rouge, Louisiana in January 2009 to attend graduate school at the Louisiana State University School of Animal Sciences under the direction of Dr. Kenneth Bondioli. He is now a candidate for the degree of Doctor of Philosophy in Animal and Dairy Sciences at Louisiana State University, Baton Rouge, Louisiana.